NINA BERBERICH

DISSERTATION

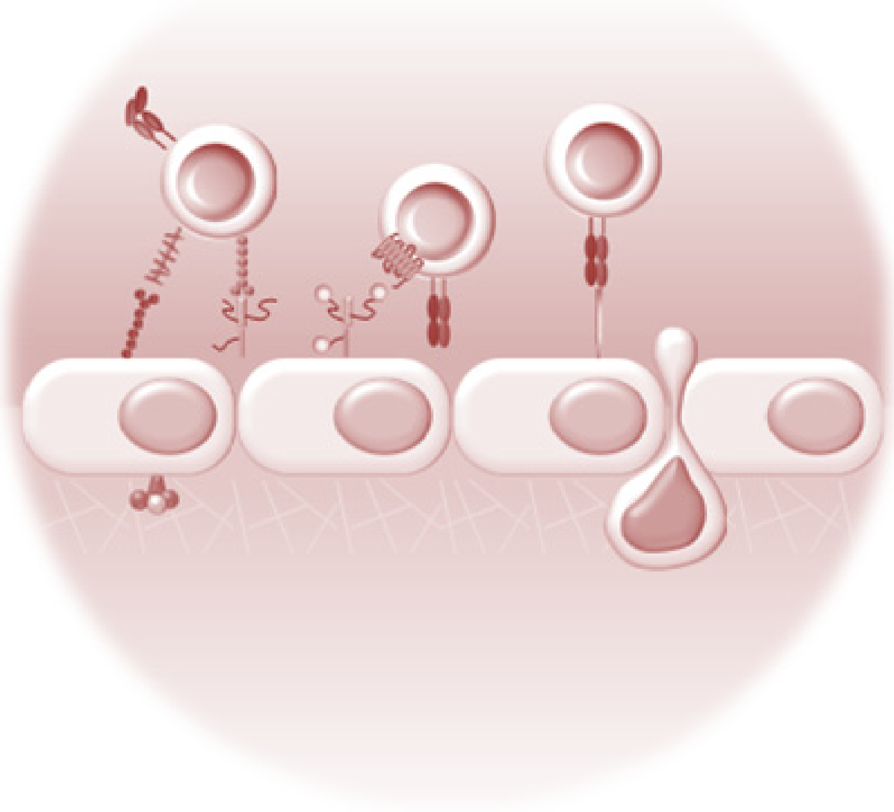

ELUCIDATION OF A NOVEL MODE OF ACTION UNDERLYING THE ANTI -INFLAMMATORY EFFECT OF THE CDK INHIBITOR ROSCOVITINE

Dissertation zur Erlangung des Doktorgrades
der Fakultät für Chemie und Pharmazie
der Ludwig-Maximilians-Universität München

ELUCIDATION OF A NOVEL MODE OF ACTION UNDERLYING THE ANTI-INFLAMMATORY EFFECT OF THE CDK INHIBITOR ROSCOVITINE

Nina Berberich

aus Zweibrücken

2010

Erklärung:

Diese Dissertation wurde im Sinne von §13 Abs. 3 bzw. 4 der Promotionsordnung vom 29. Januar 1998 von Frau Prof. Dr. Angelika M. Vollmar betreut.

Ehrenwörtliche Versicherung:

Diese Dissertation wurde selbstständig, ohne unerlaubte Hilfe erarbeitet.

München, 20. Mai 2010

Nina Berberich

Dissertation eingereicht am:	20. Mai 2010
1. Gutachter:	Prof. Dr. Angelika M. Vollmar
2. Gutachter:	Prof. Dr. Carsten Culmsee
Mündliche Prüfung am:	21. Juni 2010

dedicated to my mother

CONTENTS

CONTENTS

I. INTRODUCTION 1

1. INFLAMMATION 1
   1.1. THE ENDOTHELIUM 2
   1.2. LEUKOCYTES 2
   1.3. LEUKOCYTE-ENDOTHELIAL CELL INTERACTION 3
   1.4. STEPS OF LEUKOCYTE EXTRAVASATION 5
2. REGULATION OF ICAM-1 6
3. THE TRANSCRIPTION FACTOR NF-κB 7
   3.1. GENERAL ASPECTS 7
   3.2. SIGNALING 7
4. CYCLIN-DEPENDENT KINASES 9
   4.1. CELL CYCLE RELATED CDKs 10
   4.2. TRANSCRIPTIONAL CDKs 11
   4.3. CDK5 13
5. CYCLIN DEPENDENT KINASE INHIBITORS 15
   5.1. GENERAL ASPECTS 15
   5.2. ROSCOVITINE 15
6. AIM OF THE STUDY 17

II. MATERIALS AND METHODS 21

1. MATERIAL 21
   1.1. ROSCOVITINE 21
   1.2. REAGENTS 21
   1.3. TECHNICAL EQUIPMENT 23
2. CELL CULTURE 24
   2.1. HUVECs – HUMAN UMBILICAL VEIN ENDOTHELIAL CELLS 24
   2.2. GRANULOCYTES 25
3. ANIMALS 25
4. WESTERN BLOT ANALYSIS 26
   4.1. SAMPLE PREPARATION 26
   4.2. SDS-PAGE 27

4.3. ELECTROBLOTTING 28
4.4. PROTEIN DETECTION 29
4.5. STAINING OF GELS AND MEMBRANES 31
4.6. PROTEIN QUANTIFICATION 32
5. WHOLE MOUNT CREMASTER MUSCLE PREPARATION AND INTRAVITAL MICROSCOPY 32
5.1. SURGICAL PROCEDURE 32
5.2. EXPERIMENTAL PROTOCOL 33
5.3. INTRAVITAL MICROSCOPY AND DETERMINATION OF MICROHEMODYNAMIC PARAMETERS 33
6. GRANULOCYTE ADHESION ASSAY 34
7. FLOW CYTOMETRY 34
7.1. QUANTIFICATION OF DNA FRAGMENTATION 35
7.2. EXPRESSION OF ENDOTHELIAL CELL ADHESION MOLECULES 36
7.3. EXPRESSION OF CD11B 36
7.4. DHR OXIDATION (OXIDATIVE BURST) 36
8. TRANSFECTION AND GENE TRANSFER 37
8.1. TRANSFECTION WITH siRNA 37
8.2. VIRAL-MEDIATED GENE TRANSFER (TRANSDUCTION) 38
9. NF-kB PROMOTER ACTIVITY ASSAY (REPORTERGENE ASSAY) 38
10. IMMUNOCYTOCHEMISTRY AND CLSM 39
10.1. IMMUNOCYTOCHEMISTRY 39
10.2. CONFOCAL LASER SCANNING MICROSCOPY 40
11. ELECTROPHORETIC MOBILITY SHIFT ASSAY 40
11.1. EXTRACTION OF NUCLEAR PROTEINS 40
11.2. ELECTROPHORETIC MOBILITY SHIFT ASSAY (EMSA) 41
12. IKKβ ACTIVITY ASSAY 42
13. QUANTITATIVE REAL-TIME PCR 42
13.1. RNA ISOLATION 42
13.2. REVERSE TRANSCRIPTION 43
13.3. QUANTITATIVE REAL-TIME PCR 43
14. KINOME ARRAY (PEPCHIP) 44

15. STATISTICAL ANALYSIS 44

III. RESULTS 47

1. THE ANTI-INFLAMMATORY POTENTIAL OF ROSCOVITINE 47
   1.1. IN VIVO 47
   1.2. IN VITRO 49
2. EFFECTS OF ROSCOVITINE ON THE NF-κB PATHWAY 53
   2.1. CYTOTOXICITY OF ROSCOVITINE ON ENDOTHELIAL CELLS 53
   2.2. ROSCOVITINE REDUCES TNF-α-EVOKED NF-κB PROMOTER ACTIVITY 54
   2.3. ROSCOVITINE DOES NOT ALTER TNF-α-INDUCED NF-κB DNA-BINDING CAPACITY 54
   2.4. ROSCOVITINE HAS NO INFLUENCE ON THE TNF-α-INDUCED TRANSLOCATION OF p65 55
   2.5. ROSCOVITINE HAS NO EFFECTS ON IKK AND IκBα 56
3. THE INFLUENCE OF ROSCOVITINE ON KINASES 58
   3.1. PEPCHIP ASSAY / KINASE PANEL 58
   3.2. EC50 PROFILING OF ROSCOVITINE 58
4. INVOLVEMENT OF PKA, RS6K AND CDKs ON THE EXPRESSION OF ICAM-1 59
   4.1. INHIBITION OF PKA OR RS6K HAS NO INFLUENCE OF ICAM-1 EXPRESSION 59
   4.2. THE IMPACT OF CDKs ON THE EXPRESSION OF ICAM-1 61

IV. DISCUSSION 65

1. INFLAMMATION AND CDK INHIBITORS 65
   1.1. IN GENERAL 65
   1.2. THE IMPACT OF ROSCOVITINE ON LEUKOCYTE-ENDOTHELIUM INTERACTION *IN VIVO* AND *IN VITRO* 65
2. IMPACT OF ROSCOVITINE ON THE NF-κB SIGNALING 67
3. ROSCOVITINE INHIBITS RS6K, PKA, AND DIVERSE CDKs 68
4. IMPACT OF THE IDENTIFIED KINASES ON THE TNF-α-INDUCED ICAM-1 EXPRESSION 68
   4.1. PKA 68
   4.2. CDK5 and RS6K 69
   4.3. CDK9 69
5. CONCLUSION 70

V. SUMMARY **73**
VI. REFERENCES **77**
VII. ATRIAL NATRIURETIC PEPTID (ANP) **87**
1. SURVIVAL EXPERIMENTS 87
1.1. DETERMINATION OF THE APPROPRIATE LPS (*E.coli* and *Salmonella enterica*) DOSIS FOR SURVIVAL EXPERIMENTS 87
1.2. ANP PRE-TREATMENT HAS NO INFLUENCE ON THE SURVIVAL OF LPS (*E.coli*)-CHALLENGED MICE 88
1.3. ANP PRE-TREATMENT HAS NO INFLUENCE ON THE SURVIVAL OF LPS (*Salmonella enterica*)-CHALLENGED MICE 89
2. CYTOKINE MEASUREMENT 89
VIII. APPENDIX **93**
1. PUBLICATIONS 93
2. CURRICULUM VITAE 94
3. ACKNOWLEDGEMENTS 95

INTRODUCTION

I INTRODUCTION

1 INFLAMMATION

Inflammation is a protective response of the body to harmful stimuli like pathogens and toxins. Ideally, following prompt detection of a microorganism by immune mechanisms, an inflammatory reaction should contain and destroy intruding pathogens (acute inflammation) before they multiply, spread, become established or cause harm. After successful immune responses, resolution of inflammation occurs by safe removal of inflammatory cells, tissue debris and dissipated mediators to restore tissue homeostasis. Failure of this self-regulation as well as ineffective or excessive immune responses result in tissue injury and elicit chronic inflammatory diseases or even systemic inflammation (sepsis).[1-2] Occurring immune response against the body's own cells and tissues is a failure of the organism. Such aberrant immune response also initiates inflammatory reactions (e.g. lupus erythematodes) and is termed auto-immune disease (Figure I-1).

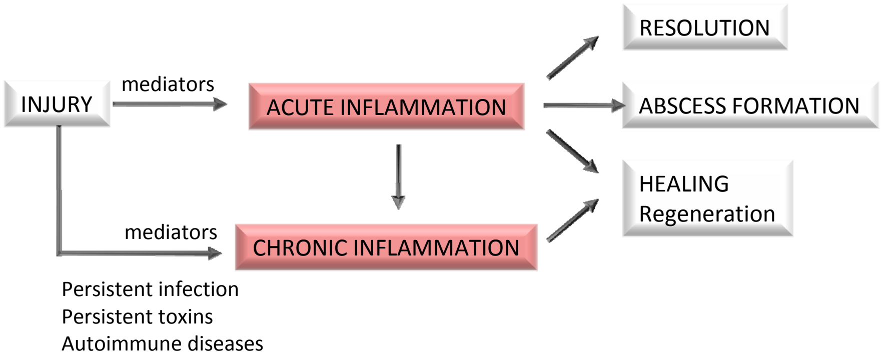

Figure I-1 Outcome of acute inflammation.
Inflammation can be classified as either *acute* or *chronic*. *Acute inflammation* is the initial response of the body to harmful stimuli and is achieved by the increased movement of plasma and leukocytes from the blood into the injured tissue. Prolonged inflammation, known as *chronic inflammation*, leads to a progressive shift in the type of cells which are present at the site of inflammation and is characterized by simultaneous destruction and healing of the tissue from the inflammatory process. Acute inflammation can lead to chronic inflammation, if the immune response is not successful or the resolution of inflammation not efficient.

Acute inflammatory reactions are attended by symptoms such as heat, redness, swelling and pain – traditionally defined by the four Latin words, *calor, rubor, dolor* and *tumor*[3] – all of these reflect changes of the vascular system, especially alterations of the endothelium, as well as the achievement of emigrated acting leukocytes in the inflammatory site.

1.1 THE ENDOTHELIUM

The endothelium, a single layer of cells, lines the interior surface of all blood vessels, thereby forming an interface between circulating blood in the lumen and the vessel wall. In the past, the endothelium was considered to be inert, described as a "cellophane-like membrane" with only non-reactive barrier properties. However, over the years it became clear that the endothelium is rather a dynamic, heterogeneous, disseminated organ with vital secretory, synthetic, metabolic and immunologic properties.[4-5]

Especially during inflammatory processes, the endothelium plays a major role. By pro-inflammatory mediators it becomes activated which, in turn, leads to phenotypical changes resulting in dilation of the blood vessel, rise of endothelial permeability and expression of important adhesion molecules on the surface of the endothelial cells. By these three parameters, the four cardinal signs of inflammation are to explain: The consequence of the vessel dilation is an increased local blood flow accounting for the red color (*rubor*) and warmth (*calor*) of inflamed tissue. The increased endothelial permeability results in emission of fluid and macromolecules that runs from the blood into the tissue, and this causes edema (*tumor*).

Since major defense components such as leukocytes and macrophages are normally carried in the bloodstream, they are recruited to the inflamed tissue to dilute and destroy the "enemy" (which causes pain [*dolor]*). This recruitment of immune cells is supported by endothelial surface proteins, whose expression is upregulated as soon as pro-inflammatory mediators have activated the endothelium.

1.2 LEUKOCYTES

Leukocytes are also referred to as white blood cells that build a group of cells, deriving from hematopoietic stem cells in the bone marrow, whose common feature is their involvement in the immune response. The major players during the innate immune response are granulocytes and macrophages. Granulocytes are "foot soldiers" of the inflammatory response, they migrate from the circulation across post-capillary venule endothelial cells[6] and employ a formidable armamentarium to overcome their adversaries. They are attracted by, and are believed to follow a concentration gradient of, chemotactic stimuli released by invading pathogens or tissues under challenge.

Granulocytes are divided into neutrophils, eosinophils and basophils. Their names result from the characteristic staining patterns of their prominent granules. Neutrophils and eosinophils are key players in the immune response to bacteria, fungi and parasites, while basophils are involved in allergic reactions. The elimination of the invaders is achieved by secreting cytotoxic and pro-inflammatory compounds and by phagocytosis.

Macrophages are phagocytes, which are distributed widely in the body tissues. Their immature progenitor cells, so called monocytes, circulate in the blood and differentiate continuously into macrophages upon migration into the tissue. There, they act as guardians and eliminate invaders by phagocytosis and release of pro-inflammatory mediators, which recruit additional inflammatory cells.

Also lymphocytes, mast cells and dentritic cells belong to the group of leukocytes. Lymphocytes, divided into the three types, B-cells, T-cells and natural killer cells are involved in the adaptive immune response, whereas mast cells affect the vascular permeability by releasing vasodilating mediators such as histamine.

1.3 LEUKOCYTE-ENDOTHELIAL CELL INTERACTION

Leukocytes, circulating in the blood flow, are recruited to the tissue in events like immune surveillance, wound repair and acute and chronic inflammation.[7] However, endothelial cells represent a physical barrier between blood and tissue, which must be crossed by the leukocytes to exert their function in the previous listed events. Especially, the rapid recruitment of leukocytes to the site of inflammation is essential. To accomplish a rapid cross of the leukocytes through the endothelial barrier, endothelial cells interact with leukocytes after their respective activation by cytokines or other pro-inflammatory stimuli. This activation is accompanied by an increased expression of diverse endothelial adhesion molecules and leukocyte integrins, by which endothelial cells and leukocytes interact which each other.

1.3.1 Endothelial adhesion molecules and integrins

A. Selectins

Selectins are a family of cell adhesion molecules and include L-(leukocyte), P-(platelet) and E-(endothelial) selectins. There is a striking homology between the cDNA sequences of these lectin-like molecules, suggesting a common functional purpose within the vasculature. In fact, all three members are involved in leukocyte-endothelium interaction by facilitating leukocyte tethering and rolling on the endothelium.[8] The counterreceptors are not clearly defined, but sialyl-Lewis x and other fucosylated carbohydrates (e.g. PSGL-1) appear to play a role. L-selectin is constitutively expressed by leukocytes and functional on all leukocytes.[9] P-selectin is stored preformed in the α granules of platelets and Weibel-Palade bodies,[10] while E-selectin is synthesized and expressed exclusively by endothelial cells. The expression of both is initiated by cytokines (e.g. TNF-α, IL-1) or other pro-inflammatory stimuli (e.g. LPS).[11]

B. Integrins

Integrins are required for firm leukocyte adherence on the endothelium. Furthermore, they also act as cell surface receptors that mediate cell-cell interaction and attachment to the extracellular matrix. Structurally, they are glycoprotein heterodimers composed of α- and β-subunits, whose different combinations result in a wide variety of adherence specificity. The different subfamilies that can be defined by their β-subunit on leukocyte include β_1 through β_8 integrins.

Relevant for the leukocyte-endothelium interaction is the β_2 integrin-family, particularly Leukocyte function associated antigen 1 (LFA-1, [CD11a/CD18] and Macrophage 1 antigen (Mac-1, [CD11b/CD18]). These are responsible for the firm adherence on the endothelium after they have achieved the high-affinity state by conformation change.

C. Immunoglobulin superfamily of cell adhesion molecules

The immunoglobulin superfamily of cell adhesion molecules (CAMs) encompasses ICAMs (Intercellular cell adhesion molecules), VCAM-1 (Vascular cell adhesion molecule 1) and PECAM-1 (Platelet endothelial cell adhesion molecule 1), whereas the ICAMs form an own subgroup. CAMs are large glycoproteins and crucial players of leukocyte-endothelial cell interactions.

ICAM-1 is an 80-115 kD glycoprotein constitutively expressed by various cells (e.g. endothelial cells, leukocytes,[12] Schwann-cells,[13] epithelial cells), whereas VCAM-1 is not constitutively expressed in most tissues. By pro-inflammatory stimuli such as TNF-α or LPS,[12,14] the expression of ICAM-1 and VCAM-1 on the luminal site of the endothelium is upregulated through *de novo* synthesis and remains on high level for about 20 h. By interaction with integrins on circulating leukocytes, CAMs are responsible for the firm adherence on the endothelium. Hereby, ICAM-1 binds to LFA-1 or MAC-1[15], while Very late antigen-4 (VLA4, $\alpha_4\beta_1$ integrin) is the binding partner of VCAM-1.[16]

PECAM-1 is a 130 kD transmembrane glycoprotein, which is highly expressed at the intercellular junction of endothelial cells and on leukocytes. Homologue interaction of PECAM-1 on endothelial cells with PECAM-1 on leukocytes facilitates the extravasation of leukocytes from the blood into the inflamed tissue.[17]

1.4 STEPS OF LEUKOCYTE EXTRAVASATION

An essential feature of any inflammatory response is the rapid recruitment of leukocytes from the blood to the site of inflammation, usually through post-capillary venules.[18-19] This recruitment process requires leukocytes to migrate through the blood-vessel wall and enter tissues by a multistep mechanism known as extravasation or diapedesis (Figure I-2). Key steps during extravasation include initial attachment and rolling of leukocytes on the activated endothelium, chemokine-mediated activation of integrins on leukocyte surfaces, stable adherence of the activated leukocytes to the endothelium, degradation of the subendothelial basement membrane and migration of leukocytes, possibly along chemokine gradients, into the inflamed tissue.[20]

Leukocyte extravasation is a complex process, a dynamic interplay between molecules expressed on leukocytes as well as by endothelial cells.

Initially, the tethering to and rolling of leukocytes on the inflamed endothelium involves three selectins and their counter ligands. P- and E-selectin (on the endothelium) mediate initial attachment to the endothelium while L-selectin (on leukocytes) subsequently reduces the rolling velocity of leukocytes and allows the cells to interact, through G protein-coupled receptors, with chemokines that are bound to the surface of the activated endothelium.[21] Chemokine binding causes activation of leukocytes. This is on the one hand associated with a rapid activation of β_2 integrins (LFA-1 [CD11a/CD18] and Mac-1 [CD11b/CD18]) by conformational changes in order to achieve a high-avidity state.[18] On the other hand it is linked with a mobilization of preformed Mac-1 from intracellular pools.[22] Thereby, integrin surface expression increases severalfold. In this active state, leukocytes arrest on the vessel wall via the binding of their integrins with immunoglobulin superfamily members such as ICAM-1 and VCAM-1, expressed by endothelial cells.[23-24]

With the support of endothelial junction proteins, such as PECAM and JAM (Junctional adhesion molecule), activated leukocytes can now cross the endothelial barrier, usually between the endothelial cells.[25] The leukocytes passage through the subendothelial basement membrane by deploying various degradative enzymes (metalloproteinases and heparanase)[19,26] and enter the inflamed tissue to exert their function.

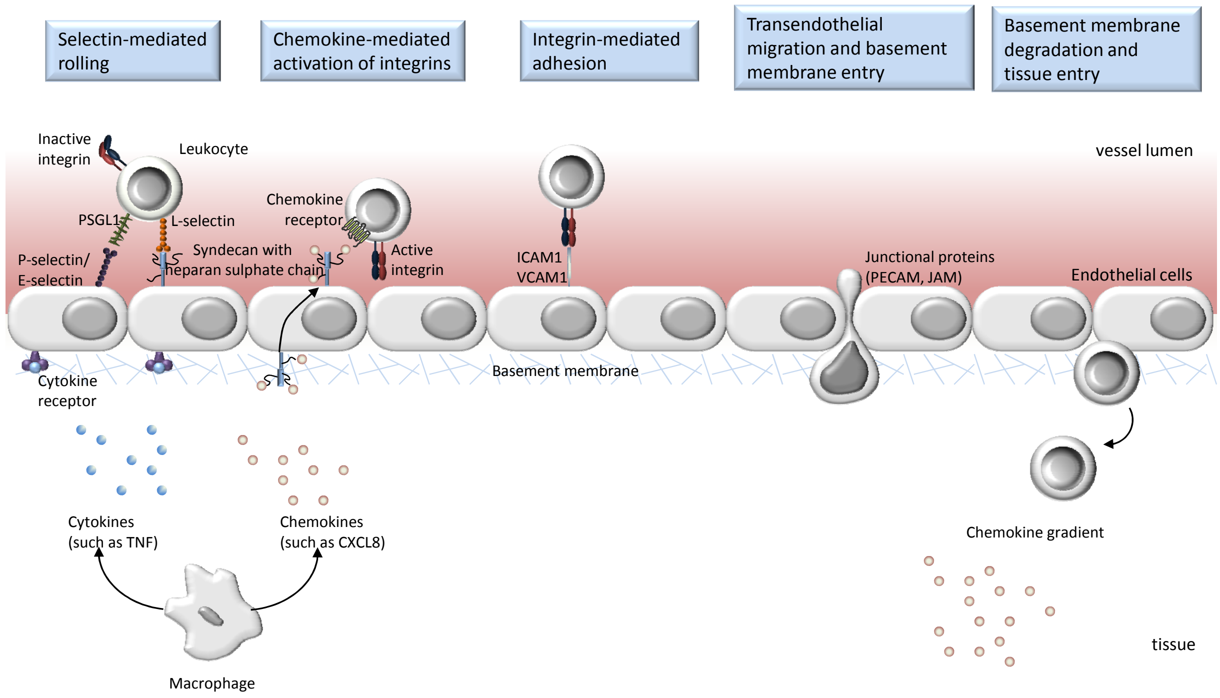
Selectin-mediated rolling
Chemokine-mediated activation of integrins
Integrin-mediated adhesion
Transendothelial migration and basement membrane entry
Basement membrane degradation and tissue entry
Inactive integrin
Leukocyte
vessel lumen
Chemokine receptor
PSGL1
L-selectin
P-selectin/ E-selectin
Syndecan with heparan sulphate chain
Active integrin
ICAM1
VCAM1
Junctional proteins (PECAM, JAM)
Endothelial cells
Cytokine receptor
Basement membrane
Cytokines (such as TNF)
Chemokines (such as CXCL8)
Macrophage
Chemokine gradient
tissue

Figure I-2 The steps of the leukocyte extravasation.
If the immune system is activated by an inflammatory stimulus, macrophages produce chemokines, such as IL8, and cytokines, such as TNF-α. These induce the rapid expression of P-and E-selectin on the surface of endothelial cells. The interaction between the selectins and their ligands, such as P-selectin glycoprotein ligand 1 (PSGL1), on leukocytes probably initiates rolling on the endothelium. Rolling is further stabilized by L-selectin binding to endothelial cell heparan sulphate. Heparan sulphate also presents chemokines to chemokine receptors on leukocytes. This process activates leukocyte integrins and results in more stable leukocyte adhesion by binding to ICAM-1 and VCAM-1. With the support of PECAM and other molecules the leucocytes migrate through the endothelium and follow the chemokine gradient to the inflammation, where they exert their functions. The image is adapted from *Parish*.[20]

2 REGULATION OF ICAM-1

The level of ICAM-1 expression on the surface of any given cell type depends on the concentration of pro- and anti-inflammatory mediators and on the availability of specific receptor-mediated signal transduction pathways and their nuclear transcription factor target on the ICAM-1 promoter.[27]

The architecture of the ICAM-1 promoter has been shown to be very complex, containing a large number of binding sites for inducible transcription factors (Figure I-3). Besides binding sites for the transcriptions factors STAT and AP1, both relevant in inflammatory processes,[28] the ICAM-1 promotor contains a recognition site for NF-κB (nuclear factor κB), the most important transcription factor for the induction of ICAM-1 transcription.[29] Activation of the NF-κB pathway by cytokines (e.g. TNF-α) or other pro-inflammatory stimuli (e.g. LPS), releases NF-κB from its inhibitory complex (IκBα) and allows it to translocate into the nucleus, where it can bind to its recognition site on the ICAM-1 promotor and consequently initiate, with the support of co-activators, the transcription of ICAM-1.

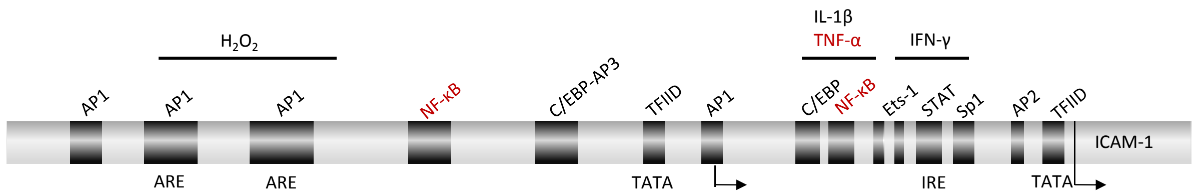

Figure I-3 Structure and regulation of the ICAM-1 promoter.
The ICAM-1 promoter contains multiple transcription initiation sites (the two major ones at -41 and -319 relative to translation start site are indicated by right angle arrows). Upstream of each initiation site is a consensus TATA element that binds the general transcription factor IID (TFIID). The ICAM-1 promoter contains a number of binding sites for inducible transcription factors (indicated by solid rectangles) that mediate various activation signals elicited at the cell surface. The TNF-α- and IL-1β-responses are mediated by cooperativity between the transcription factors C/EBP and NF-κB. The IFN-γ (Interferon-γ) response is mediated by STAT binding to the IFN-γ response element (IRE). The H_2O_2 response is mediated by the antioxidant response elements (ARE), which bind the transcription factors AP-1 and Ets.

3 THE TRANSCRIPTION FACTOR NF-κB

3.1 GENERAL ASPECTS

NF-κB is a dimeric transcription factor and is composed of various members of the NF-κB/REL family, which includes Rel-A (also known as p65), c-Rel, Rel-B, p50 and p52.[30] NF-κB proteins exist in the cytoplasma in an inactive form, as a result of their association with IκB proteins – IκBα, IκBβ, IκBε[31] – or the precursor proteins p100 and p105, which can function as IκB-like proteins. The degradation of IκB allows NF-κB proteins to translocate to the nucleus and bind their cognate DNA-binding sites to regulate the transcription of a large number of genes that control diverse physiological functions such as apoptosis, proliferation, inflammation and innate and adaptive immune response.[32-33] In inflammatory processes, NF-κB is one of the pivotal regulators of pro-inflammatory cytokines, chemokines, adhesion molecules matrix metalloproteases (MMPs), cyclooxygenase 2 (COX 2) and inducible nitric oxide synthase (iNOS).[34-35]

3.2 SIGNALING

NF-κB is controlled by two distinct regulatory pathways, termed the “canonical” and “non-canonical” pathways. The “non-canonical” pathway is activated during the development of lymphoid organs responsible for the generation of B and T lymphocytes, and only a small number of stimuli (lymphotoxin B and BAFF [B cell activating factor]) are known to activate NF-κB via this pathway.

The “canonical” or classical pathway (Figure I-4) is activated rapidly in response to a wide range of stimuli, including pathogens, stress signals and pro-inflammatory cytokines such as TNF-α or IL-1. These stimuli are recognized by different receptors (e.g. LPS via LBP and CD14 by the Toll-like receptor; TNF-α via TNF-receptor [TNFR]) and this leads to transduction of distinct intracellular signals and to the recruitment of effector molecules (TRADD, TRAF & RIP recruitment is mediated via TNFR). Ultimately, their cascades converge in the activation of the IKK complex, which consists of the two catalytic subunits IKKα and IKKβ as well as the regulatory subunit IKKγ (also known as NEMO). If the IKK complex is activated by phophorylation of the upstream kinases, IκBα, the inhibitory unit of NF-κB, is phosphorylated on specific serine residues, ubiquitylated and degradated by the ATP-dependent 26S proteasom. This leads to NF-κB (in inflammatory processes the heterodimer p50/p65) release and in the following to its translocation into the nucleus. In the nucleus costimulating processes like acetylation by histone acetyltransferases (HAT) and phosphorylation are needed to enable NF-κB transcriptional activity.

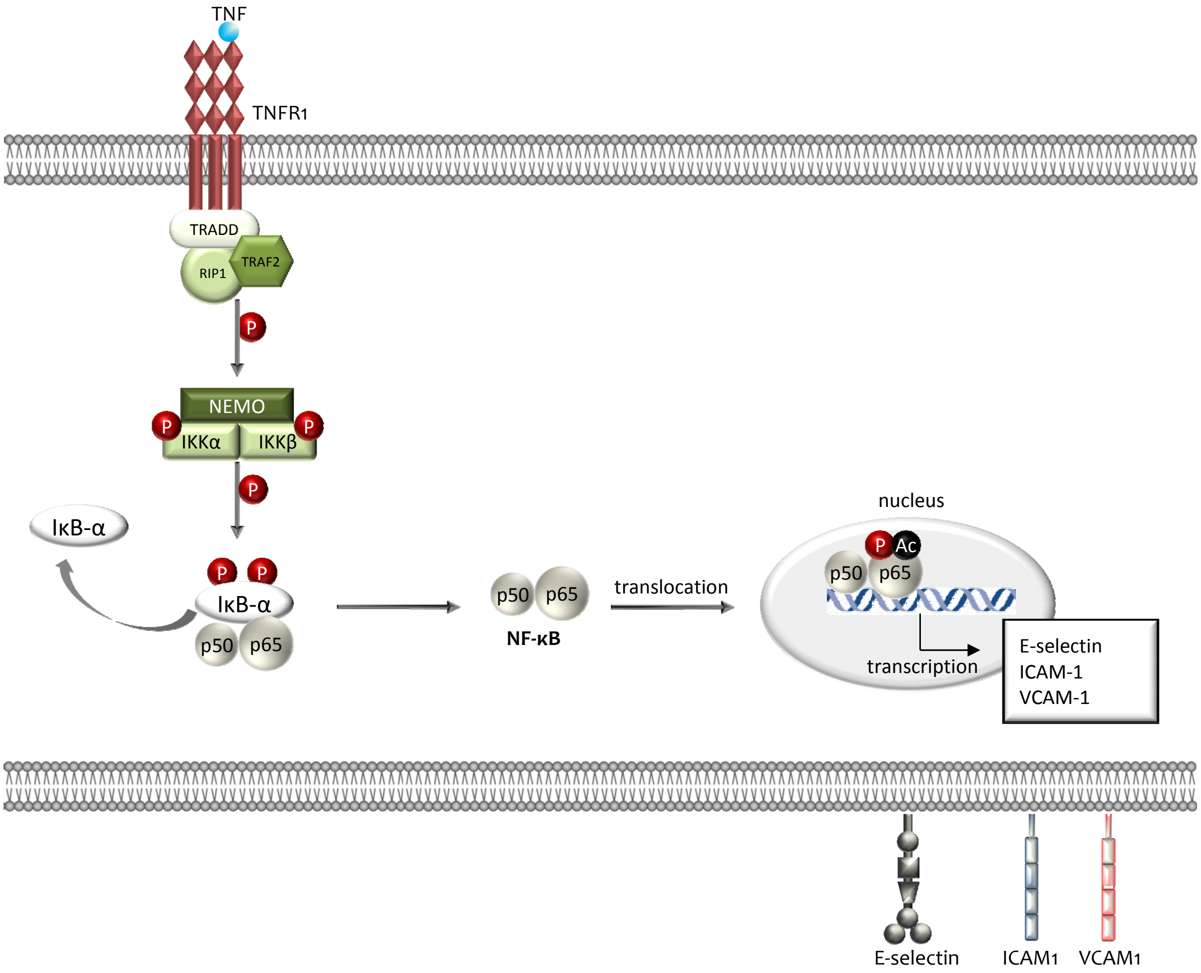

Figure I-4 The canonical NF-κB pathway using the example of TNF-α stimulation.
The canonical pathway is induced by inflammatory stimuli, such as TNF-α, which initially leads to the recruitment of effector molecules (TRADD, TRAF2, RIP1) and subsequently converges in the activation of the IKK complex (NEMO, IKKα, IKKβ). This activation results in the phosphorylation (P) of IκBα at Ser^{32} and Ser^{36}. The phosphorylated IκBα is then ubiquitylated at Lys^{21} and Lys^{22}, which targets it for degradation by the 26S proteasome, thereby releasing NF-κB dimers from the cytoplasmic NF-κB–IκB complex and allowing them to translocate to the nucleus. There it binds to its recognition site and enables gene transcription with the support of co-stimulators (Ac= acetylation).

4 CYCLIN-DEPENDENT KINASES

About 30 years ago, cyclin-dependent kinases (CDKs) were discovered by different researches independently. *Nurse et al.* identified a gene (CDC2) in fission yeast, regulating the entry into mitosis,[36] while Masui and Smith characterized a complex, called “maturating-promoting factor” (MPF) in amphibian oocytes.[37-38] Following these fundamental findings, extensive studies on the cell division cycle revealed that the progression through the G1, S, G2 and M phases of the cell division cycle is directly controlled by the transient activation of various CDKs.[39]

CDKs are a family of small kinases, which induce cellular processes by phosphorylation of target proteins on serine and threonine residues immediately upstream of a proline-residue. CDKs can be activated by phosphorylation by the CDK-activating kinase (CAK),[40] but only when bound to their corresponding cyclin. In addition, CDKs are regulated by various post-translational modifications (phosphorylation by Wee 1/Myt 1, dephosphorylation by cdc25, ubiquitin-dependent degradation), transient association with a natural inhibitory protein (Cip1, Kip1/2 or Ink4A-D), and their intracellular localization (Figure I-5).[41]

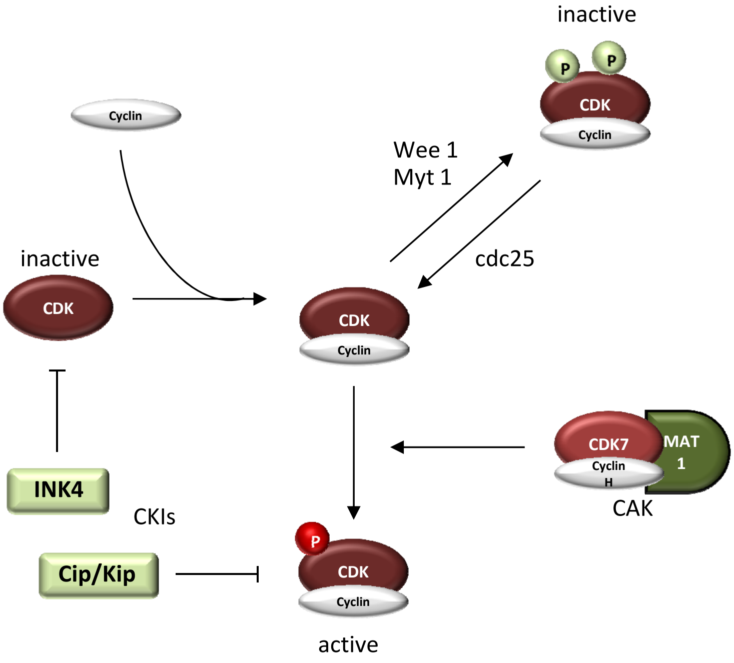

Figure I-5 Regulation of CDKs.
Activation of CDKs requires association with a cyclin regulatory subunit and phosphorylation of CAK. CDKs are inactivated by Wee1/Myt1-mediated phosphorylation and by association with endogenous CDK-inhibitors (Cip/Kip- or INK4-family members).

Cyclins were originally classified as proteins, the levels of which oscillate during the cell cycle, but they are now more accurately defined as members of a family of structurally related proteins that bind to and activate CDKs. Today 13 CDKs and 25 cyclins are known. CDKs act not only as key regulators of cell cycle progression,[42] but are also involved in apoptosis,[43-44] neuronal physiology,[45] pain signaling,[46] insulin release by pancreatic cells[47], transcription[48-49] and mRNA slicing.[49]

Regarding their physiological functions CDKs are divided into 2 groups:

1.) Cell cycle related CDKs (also called mitotic CDKs) including CDK1, CDK2, CDK3, CDK4 and CDK7, whereas CDK7 plays a dual role (described in I-4.2.2., CDK 7 (CAK, TFIIH)]).[50]

2.) CDKs that are not involved in the cell cycle. These play a role in diverse processes like neuronal migration and development (CDK5),[51] gene transcription control (CDK7, 8, and 9)[52] or RNA splicing (CDK10, 11, 12 and 13)[42].

4.1 CELL CYCLE RELATED CDKs

The cell cycle is the series of events that takes place in a cell leading to its division and duplication (replication). The cell cycle consists of four distinct phases: G_1 phase, S phase (synthesis), G_2 phase (collectively known as interphase) and M phase (mitosis). M phase is itself composed of two tightly coupled processes: mitosis, in which the cell's chromosomes are divided between the two daughter cells, and cytokinesis, in which the cell's cytoplasm divides in half forming distinct cells. Cells that have temporarily or reversibly stopped dividing have entered a state of quiescence called G_0 phase.[53]

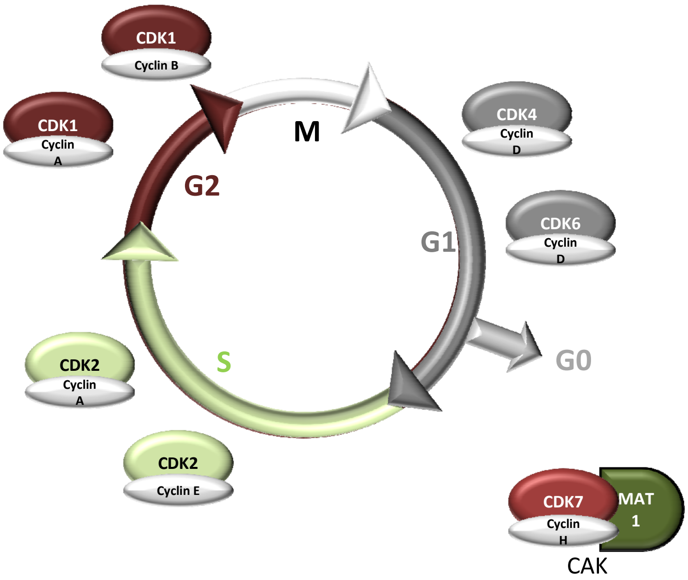

Figure I-6 The cell cycle and its regulation by cell cycle related CDKs.
CDK4 and CDK6 associate with cyclin D during G_1 phase. CDK2 is activated by cyclin E during DNA synthesis and by cyclin A during S/G_2 transition. CDK1 associates with cyclin A during G_2 phase and with cyclin B at G_2/M transition, respectively.

To diminish all risks of aberrant chromosome segregation and to remain the stability of genomic DNA over generations, the cell cycle is based on orchestrated coordination of enzymatic reactions, in which the CDKs are strongly involved.[54-56] Each phase of the cell cycle is characterized by the presence of phase-specific CDK/cyclin complexes (Figure I-6). The transient existence of the cyclins achieved by *de novo* synthesis and degradation presents the temporal regulation of the cell cycle.[57]

4.2 TRANSCRIPTIONAL CDKs

4.2.1 Transcription and its regulation

The gene transcription represents the process by which the genetic information encoded in the DNA is transcribed into RNA. This process may be divided into the three major steps, “initiation”, “pausing” and “elongation”. Initially, the promoter region of the respective gene has to be cleared from nucleasomes to allow its accessibility for the pre-initiation complex TFIIH (Transcription factor II H). After binding to the promoter, TFIIH phosphorylates the Ser^5 residue of the C-terminal domain of RNA polymerase II.[58] Subsequently, the RNA polymerase II is paused on the 5’ end of promoter by the factors NELF (negative elongation factor) and DSIF (DRB-sensitivity initiation factor), which complex the RNA polymerase II for some time.[59] To enter processive mode inactivation of the transcriptional repressors NELF and DSIF, as well as the phosphorylation of the Ser^2 position of the C-terminal domain of RNA polymerase II is indispensable.[60-61] That is accomplished by activated p-TEFb (positive transcription elongation factor b), which is composed of CDK9 and cyclinT (as described in I-4.2.3. in detail).

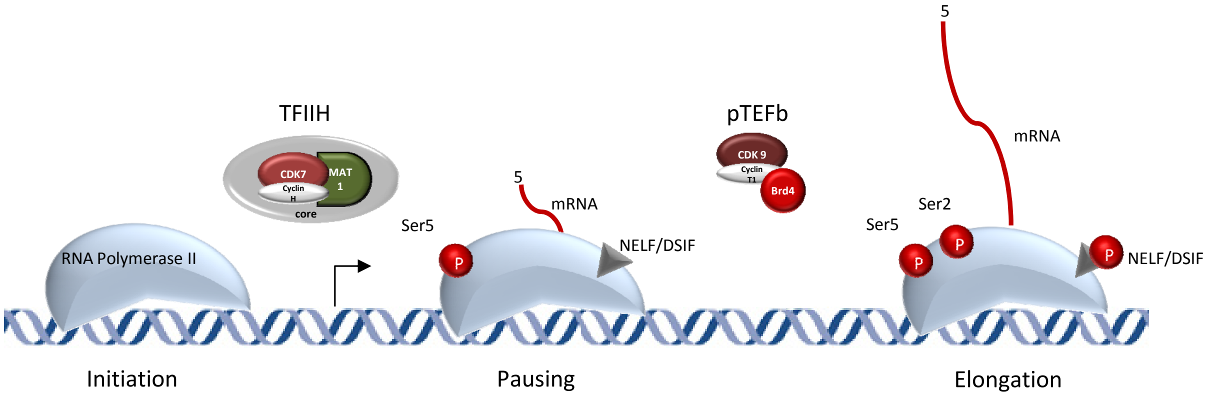

Figure I-7 The multistep process of the transcription cycle.
TFIIH, a general transcription factor, initiates the transcription by phosphorylation of the RNA polymerase II and elongation begins. In the following, pausing of the RNA-polymerase II is caused by repression of the NELF and DSIF. pTEFb phosphorylates repression factors and RNA polymerase II to continue elongation.

4.2.2 CDK 7 (CAK, TFIIH)

CDK7 plays a dual role because it is a component of CAK, which represents a constituent of the general transcription factor II H (TFIIH). CAK is a trimeric complex composed of the catalytic component CDK7, the regulatory cyclin H and MAT1 ("menage a trois-1"), a RING finger assembly factor.[58,62] As constituent of CAK, CDK7 phosphorylates other CDKs which leads to their activation after binding their respective cyclin. This phosphorylation on a conserved threonine residues leads by a conformational change to the uncovering of the active site (Figure I-8).

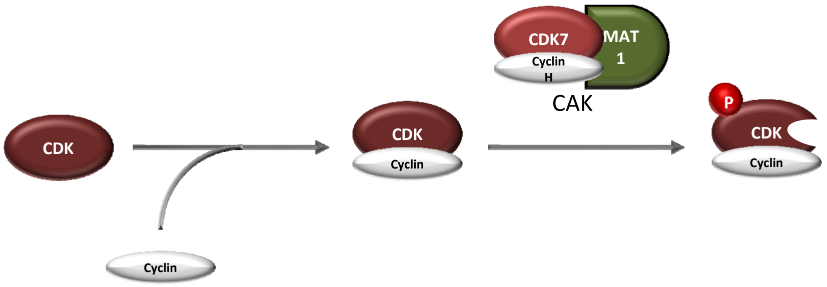

Figure I-8 Activation of CDKs by cyclin binding and phosphorylation by CAK.
Activation of CDKs depends on binding to cyclins followed by phosphorylation of conserved threonine residues by CAK, which leads to uncovering of the active site.

The general transcription factor TFIIH, composed of CAK (CDK7/cyclin H/MAT1) and a core consisting of 7 subunits (Figure I-9),[63] makes up the RNA polymerase II pre-initiation complex and consequently activates transcriptional initiation as CDK7, its catalytic component, phosphorylates the RNA polymerase II.

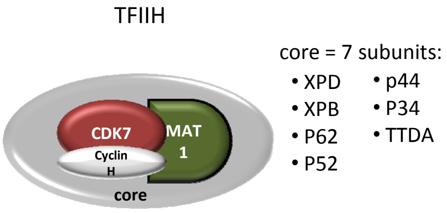

Figure I-9 Structure of the transcription factor II H (TFIIH).
The general transcription factor is composed of a core of 7 subunits and CAK that includes CDK7, cyclin H and MAT1. Initiation of the transcription is caused by phosphorylation of RNA polymerase II by CDK7, the catalytic component of TFIIH.

4.2.3 CDK9 (pTEFb)

CDK9 is not involved in the cell cycle, but plays an important role in the regulation of transcription. Like other CDKs, it associates with cyclins, namely cyclin T, K and E, in order to achieve its kinase activity. Most of the CDK9 in the cell is associated with nuclear cyclin T, found distributed primarily in the nucleus and associated with nuclear speckles. This CDK9/cyclin complex represents the positive elongation factor pTEFb, which regulates the transcriptional elongation via phosphorylation of the carboxy-terminal domain of RNA-polymerase II on serines at both the 2 and 5 positions. Furthermore, proteins like NELF and DSIF, that are responsible for transcriptional pausing, are phosphorylated by pTEFb which allows their release from the RNA polymerase II and the elongation process can be continued.

While pTEFb is bound by HEXIM1/7SKsnRNA in its inactive state, it associates with bromodomain containing protein 4 (Brd4) in order to be activated (Figure I-10).[64] It is thought that Brd4 might be required for p-TEFb activity through its ability to associate with acetylated lysines and thereby facilitates its chromatin contact or binding. [65]

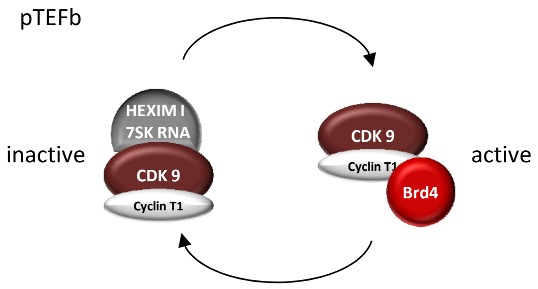

Figure I-10 States of pTEFb.
pTEFb is associated with HEXIM I and 7SKRNA in its inactive state, while Brd4 is bound to be activated.

4.3 CDK5

In 1992, the small cyclin-dependent kinase family was joined by CDK5 as an atypical member. Unlike the mitotic CDKs, it plays no apparent role in cell cycle regulation. Instead, CDK5 is involved in physiological functions of the central nervous system, such as regulating of the cytoarchitecture during brain development, neuronal migration, adhesion, axon guidance, membrane transport, neuronal survival, dopaminergic signaling, drug addiction and synaptic function (Figure I-11).[51] Apparently, abnormal regulation of CDK5 leads to neurodegenerative diseases including Alzheimer`s diseases (AD) or amyotrophic lateral sclerosis (ALS), caused by hyperphosphorylation of the microtubule binding protein tau by the CDK5/p25 complex.[51]

Despite its prominent role in the central nervous system, CDK5 is ubiquitously expressed in humans. Unpublished data of our lab indicate a crucial role of CDK5 in angiogenesis, as inhibition of CDK5 (by siRNA and small molecule inhibitors) severely reduced migration of endothelial cells. According to its anti-angiogenic effects, inhibition of CDK5 might present a promising approach in cancer therapy.

CDK5 is also expressed in insulin-secreting pancreatic cells. Inhibition of CDK5 in these cells leads to reduction of insulin secretion, indicating that CDK5 might be a positive regulator of insulin exocytosis.[47]

Like other CDKs, monomeric CDK5 shows no enzymatic activity and requires association with a regulatory partner for activation. But instead of a classic cyclin, CDK5 associates with its own activator p35 or p39. Both share about 57% amino acid identity and are themselves regulated by transcription and ubiquitin-mediated degradation. A myristolation motif targets p35 and p39 to cell membranes and cell periphery, dicating the subcellular distribution of CDK5.[51]

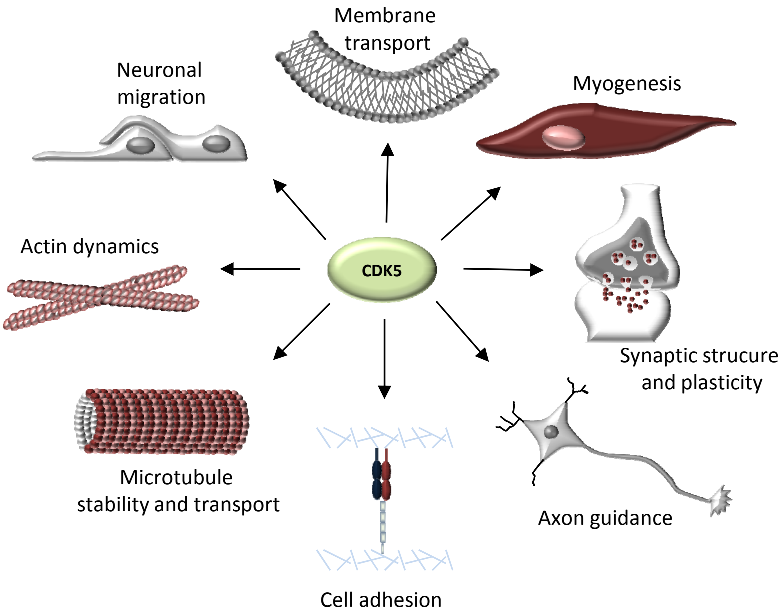

Figure I-11 Cellular processes regulated by CDK5.
The pleiotropic nature of CDK5 is evident in its involvement in several cellular processes. **Neuronal migration**: Defects in neuronal positioning in the *Cdk5*- and *p35*-deficient mice show that CDK5 is crucial for neuronal migration. **Actin dynamics**: Phosphorylation of the Rac effector, Pak1, by CDK5 can regulate actin dynamics, and CDK5 activity promotes neurite outgrowth. **Microtubule stability and transport**: Several microtubule-associated proteins (MAPs) are substrates of CDK5, and regulate microtubule polymerization. Inhibition of CDK5 decreases anterograde transport, and nudel and neurofilament proteins are substrates of CDK5. Cell adhesion: CDK5 phosphorylates β-catenin, disrupts the N-cadherin–β-catenin complex and inhibits adhesion. Axon guidance: *p35*-mutant mice have defects in fasciculation of several axon tracts, and, in *Drosophila*, increase or decrease of CDK5 activity results in errors in axon pathfinding. **Synaptic structure and plasticity**: CDK5 phosphorylates several synaptic proteins, modulates dopaminergic signalling and development of the neuromuscular junction. **Myogenesis**: CDK5 kinase activity induces expression of MyoD and Mrf4, master regulators of myogenesis. **Membrane transport**: CDK5 phosphorylates the Munc18–syntaxin1 complex and amphyphysin, indicating a possible role in membrane fusion, neurosecretion and endocytosis. The image is adapted from *Dhavan*.[51]

5 CYCLIN DEPENDENT KINASE INHIBITORS

5.1 GENERAL ASPECTS

CDKs are involved in various physiological functions, therefore it may not be surprising that deregulations of CDKs and their regulators are observed, involved and causative in numerous and diverse human diseases. Due to their regulatory function in the progression of the cell cycle, it has been shown that deregulation of CDKs leads to malignancies. Furthermore, abnormal activities of CDKs in the brain cause chronic degenerative disease such as AD. Also there is evidence that deregulated CDKs play a role in kidney diseases,[66] type II diabetes[67] and viral infections.[68]
Deregulation of CDKs occurs if just one of the different regulatory ways is deficient (Figure I-5).

In the beginning, CDK inhibitors were designed as promising anti-proliferative agents for cancer therapy. However, due to the many links between CDKs and other human diseases, an intensive search for potent and selective pharmacological inhibitors of these kinases has been encouraged. During recent years, a large variety of small molecule weight inhibitors have been identified and characterized and although they all act by competing with ATP for the binding on the catalytic site of the kinase, their kinase selectivity varies greatly. Some CDK inhibitors are currently undergoing clinical trials, including classic and well-established compounds like flavopiridol, 7-hydroxystaurosporine and roscovitine.

5.2 ROSCOVITINE

Roscovitine belongs to the family of 2,6,9-trisubstituted purines (see chemical structure in Figure I-12) which encompasses some of the first described CDK inhibitors. Among these purines, the R-stereoisomer of roscovitine is one of the most frequently studied and used CDK inhibitors. It shows improved potency and selectivity when compared to previous described CDK inhibitors such as olomoucine. This improved selectivity of roscovitine is reflected by exclusive inhibition of CDK1, CDK2, CDK5, CDK7 and CDK9.

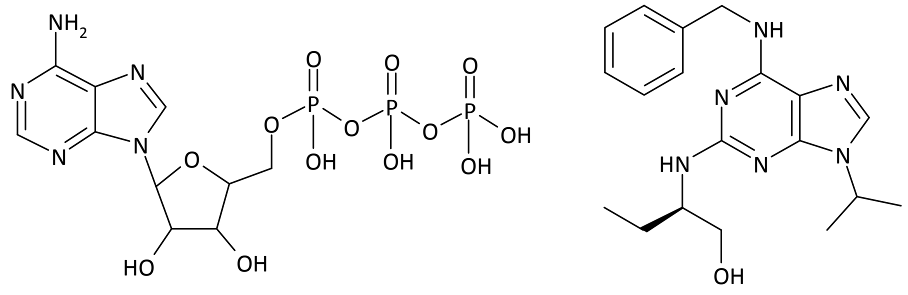

Adenosin-triphosphat (ATP)

(R)-Roscovitine
(Seliciclib, CYC202)

Figure I-12 Chemical structure of ATP and roscovitine.
Due to its structure similarity to ATP, roscovitine competes with it for binding to the catalytic site of CDKs. Thus, the purine portion binds to the adenine binding pocket of CDKs. The benzyl function enables the inhibitor to connect with the enzyme. The insertion of isopropyl on position 9 improved the potency and selectivity of roscovitine compared to olomoucine.

Roscovitine, also referred to as CYC202 or Seliciclib, (R)-roscovitine, has been evaluated for its effects on a wide variety of cultured cell lines. Thereby, it has been shown that roscovitine arrests the cell cycle in G_1, S or in G_2/M phase depending on the cell line used, its concentration and the length of treatment. Moreover, a pro-apoptotic profile of roscovitine was described. Roscovitine induces cell death in myeloma cells by inhibition of RNA polymerase II–dependent transcription and down-regulation of Mcl-1 via inhibition of CDK7 and CDK9.[69] Also, its pro-apoptotic effects result from the activation of p53, a tumor suppressor protein, by blocking p53 degradation by the E3 ubiquitin ligase MDM2.[70] Further, activation of p53-dependent transcription was maintained when roscovitine was combined with NF-κB-activating stimuli (e.g. TNF-α), which can be explained by roscovitine-evoked inhibition of the NF-κB activation[71], caused by inhibition of IKK involved in the NF- κB activation cascade.

According to these effects, roscovitine has now reached phase 2 clinical trials for nasopharyngeal cancer, B cell malignancies and breast cancer, and phase 2b against non small cell lung cancer.[72]

Further, roscovitine has been found to exert anti-inflammatory effects in different *in vivo* models of inflammatory diseases. In these models roscovitine enhanced the apoptosis of immune cells (e.g. neutrophils and eosinophils) by Mcl-1 inhibition (like in myeloma cells). Thus, the resolution of inflammation is promoted by roscovitine.

Roscovitine has also been found to be beneficial in neurodegenerative diseases by inhibition of CDK5. Therefore, it is undergoing pre-clinical animal evaluation against Alzheimer's disease, Parkinson's disease, stroke and Niemann-Pick's disease type III.

6 AIM OF THE STUDY

Roscovitine is a selective inhibitor of cyclin-dependent kinases, which plays a crucial role in the regulation of the cell cycle. Therefore, its use as anti-proliferative drug in cancer treatment was obvious. Currently, roscovitine is evaluated in clinical trials against diverse cancers. Beside its potential application in cancer therapy roscovitine has been found to exert anti-inflammatory properties in different inflammatory diseases. However, in these models, roscovitine was only shown to exert its anti-inflammatory effects by promoting apoptosis in inflammatory cells and thereby enhancing the clearing of inflammation. Also, research in the field of inflammation in general has been focusing on identification and determination of functions of tissue-infiltrating leukocytes for a very long time, whereas the role of vascular endothelial cells in this process has been disregarded for a long time. Endothelial cells represent the physical barrier between blood and tissue and thus regulates blood cell trafficking. An essential feature of inflammation is the transmigration of leukocytes from the blood to the inflamed tissue and therefore inhibiting the interaction of endothelial cells and leukocytes might represent a promising approach in the treatment of acute and chronic inflammatory (e.g. chronic obstructive pulmonary disease, rheumatoid arthritis) as well as auto-immune diseases (e.g. Lupus erythematosus, Crohn`s diseases).

In the recent years, beside their anti-proliferative function, CDK inhibitors have been found to exert pro-apoptotic effects, to inhibit the gene transcription and to affect signaling pathways. According to these physiological functions, CDK inhibitors have an enormous potential for new approaches in diverse diseases.

The aim of the present study was to analyze the influence of the CDK inhibitor roscovitine on the leukocyte-endothelial cell interaction during inflammation *in vitro* as well as *in vivo* and to decipher the underlying molecular mechanism.

MATERIALS AND METHODS

II MATERIALS AND METHODS

1 MATERIAL

1.1 ROSCOVITINE

“Roscovitine” refers to (R)-roscovitine, as the (R)-stereoisomer was used. Roscovitine was from Sigma-Aldrich, Munich, Germany.

Roscovitine was dissolved in DMSO at 100 mM. 10 µl aliquots were stored at -20°C for long time storage, and at 4°C for direct laboratory use.

For experiments, the compounds were freshly diluted in growth medium to 100 µM and further diluted to the indicated concentrations.

1.2 REAGENTS

Reagent	**Company**
Accustain® formaldehyde	Sigma-Aldrich, Taufkrichen, Germany
BC Assay reagent	Interdim, Montulocon, France
Bradford Reagent™	Bio-Rad, Munich, Germany
Calyculin	Millipore, Schwabach/Ts., Germany
cAMPS-Rp	Biotrend, Cologne, Germany
CellTiter Blue™	Promega, Madison, WI, USA
Collagen A	Biochrom AG, Berlin, Germany
Collagen G	Biochrom AG, Berlin, Germany
Complete®	Roche, Mannheim, Germany
Dianisidinehydrochlorid	Sigma-Aldrich, Taufkirchen, Germany
Dihydrorhodamine-123 (DHR)	Invitrogen, Karlsruhe, Germany
Endothelial Cell Growth Medium (ECGM)	Provitro, Berlin, Germany
FCS gold	PAA Biotech, Aidenbach, Germany
FluorSave aqueous mounting medium	VWR, Darmstadt, Germany
N-formylmethionine leucyl phenylalanine (fMLP)	Sigma-Aldrich, Taufkirchen, Germany
Formaldehyde, 16% ultrapure	Polysciences Europe GmbH, Eppelheim, Germany
M199 Medium	PAA Biotech, Aidenbach, Germany
NaF	Merck, Darmstadt, Germany

Na_3VO_4	ICN Biomedicals, Aurora, Ohio, USA
Page Ruler™ Prestained Protein Ladder	Fermentas, St. Leon-Rot, Germany
Penicillin	PAA Biotech, Aidenbach, Germany
Phenylmethylsulfonylfluorid (PMSF)	Sigma-Aldrich, Munich, Germany
PKI (PKA-inhibitor fragment [6-22])	Biotrend, Cologne, Germany
Propidium iodide	Sigma-Aldrich, Taufkirchen, Germany
Rapamycin	Sigma-Aldrich, Taufkirchen, Germany
RNAlater	Ambion, Austin, TX, USA
Staurosporine	NEB GmbH, Frankfurt a.M., Germany
Streptomycin	PAA Biotech, Aidenbach, Germany
Triton X-100	Merck, Darmstadt, Germany
Tumor Necrosis Factor (TNF)-α	TebuBio, Offenbach, Germany

For heat inactivation, FCS was partially thawed for 30 min at room temperature. Subsequently, it was totally thawed at 37°C using a water bath. Finally, FCS was inactivated at 56°C for 30 min. Thereafter, 50 ml aliquots of heat inactivated FCS were stored at -20°C.

Trypsin/EDTA (T/E) (pH 7.4)		**PBS (+) (pH 7.4)**	
Trypsin	0.50 g	NaCl	7.20 g
EDTA	0.20 g	Na_2HPO_4	1.48 g
PBS	ad 1.0 l	KH_2PO_4	0.43 g
H_2O	ad 1.0 l	($MgCl_2$ x 6 H_2O	0.10 g)
		($CaCl_2$ x 2 H_2O	0.10 g)
		H_2O	ad 1.0 l

HEPES buffer (pH 7.4)	
NaCl	125 mM
KCl	3 mM
NaH_2PO_4	1.25 mM

$CaCl_2$	2.5 mM
$MgCl_2$	1.5 mM
Glucose	10 mM
Hepes	10 mM
H_2O	

1.3 TECHNICAL EQUIPMENT

Name	Device	Producer
AB 7300 RT-PCR	Real-time PCR system	Applied Biosystems, Fosterer City, CA, USA
Curix 60	Tabletop film processor	Agfa, Cologne, Germany
Cyclone	Storage Phosphor Screens	Canberra-Packard, Schwadorf, Austria
FACSCalibur	Flow cytometer	Becton Dickinson, Heidelberg, Germany
LSM 510 Meta	Confocal laser scanning microscope	Zeiss, Jena, Germany
Mikro 22R	Table centrifuge	Hettich
Nanodrop ND-1000	Spectrophotometer	Peqlab, Wilmington, DE, USA
Odyssey 2.1	Infrared Imaging System	LI-COR Biosciences, Lincoln, NE, USA
Orion II Microplate Luminometer	Luminescence	Berthold Detection Systems, Pforzheim, Germany
Polytron PT1200	Ultrax homogenizer	Kinematica AG, Lucerne, Switzerland
Nucleofector® II	Electroporation device	Lonza Cologne AG, Cologne, Germany
SpectraFluor Plus™	Microplate multifunction reader	Tecan, Crailsheim, Germany
Sunrise™	Microplate absorbance reader	Tecan, Crailsheim, Germany
Vi-CELL™	Cell viability analyser	Beckman Coulter, Krefeld, Germany

2 CELL CULTURE

2.1 HUVECs – HUMAN UMBILICAL VEIN ENDOTHELIAL CELLS

2.1.1 Isolation and cultivation

Human umbilical cords were kindly provided by Klinikum München Pasing, Frauenklinik Dr. Wilhelm Krüsmann and Rotkreuzklinikum München. After childbirth, umbilical cords were placed in PBS+Ca^{2+}/Mg^{2+} containing Penicillin (100 U/ml) and Streptomycin (100 µg/ml) and stored at 4°C. Cells were isolated within one week. The umbilical vein was washed with PBS+Ca^{2+}/Mg^{2+}, filled with 0.1 g/l collagenase A and incubated for 45 min at 37°C. To isolate endothelial cells, the vein was flushed with stopping medium and the eluate was centrifuged (1,000 rpm, 5 min). Afterwards, cells were resolved in growth medium and plated in a 25 cm^2 flask. After reaching confluency, cells were trypsinized and plated in a 75 cm^2 flask. Experiments were performed using cells at passage 3. HUVECs were used for all assays.

Endothelial cells (ECs) were cultured under constant humidity at 37°C and with 5% CO_2 in an incubator (Heraeus, Hanau, Germany). Cells were routinely tested for contamination with mycoplasms using the PCR detection kit VenorGeM (Minerva Biolabs, Berlin, Germany).

2.1.2 Passaging

After reaching confluency, cells were either sub-cultured 1:3 in 75 cm^2 culture flasks or seeded either in multiwell-plates or dishes for experiments. For passaging, cells were washed twice with pre-warmed PBS, which was removed completely with a sterile pipette. 3 ml T/E was added (75 cm^2 flask), and cells were incubated for 1-2 min at 37°C. The digest was terminated by adding approximately 20 ml stopping medium. Next, cells were centrifuged for 5 min at 1,000 rpm to remove the T/E. The supernatant was discarded, the cell-pellet was resuspended in pre-warmed ECGM, and the cells were seeded into flasks or well plates (coated with Collagen G)

Growth medium		**Stopping medium**	
ECGM	500 ml	M199	500 ml
Supplement	23.5 ml	FCS	50 ml
FCS	50 ml		
Antibiotics	3.5 ml		

2.2 GRANULOCYTES

2.2.1 Isolation

Peripheral blood was obtained from healthy volunteers. For each donor, approximately 20 ml blood was collected into 25 ml syringe filled with 400 µl EDTA (50 mg/ml), portioned in 2 x 15 ml polypropylene conical tubes (Falcon; Becton Dickinson) and centrifuged at 1,400 rpm for 20 min at room temperature (without brake). The received buffy coat (Figure II-1) was completely removed and transferred into a fresh 50 ml polypropylene conical tube.

The isolated buffy coat was incubated with human CD15 microbeads (Miltenyi Biotec) (15 µl/ml buffy coat) at 4°C for 20 min. Granulocytes were purified from the buffy coat by magnetic cell sorting positive selection using MiniMACS™ (MACS, Miltenyi Biotec). The used MS columns were firstly rinsed with separation buffer (Table 1) before cell sorting started. The received granulocytes were washed with separation buffer, centrifuged and resuspended in HEPES (II-1.2, Reagents) or granulocyte medium (Table 1) obtaining a cell-concentration of 1 x 10^6 granulocytes/ml.

Table 1 Buffer and medium for granulocyte isolation

Granulocyte medium		**Separation buffer**	
M199	500 ml	PBS	500 ml
FCS	10 ml	BSA	2.5 ml
Antibiotics	3.5 ml	EDTA	2 mM

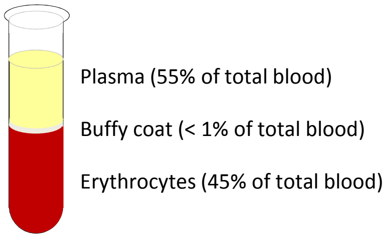
Plasma (55% of total blood)
Buffy coat (< 1% of total blood)
Erythrocytes (45% of total blood)

Figure II-1 Total blood seperated by centrifugation into plasma, buffy coat and erythrocytes

3 ANIMALS

Male C57BL/6 mice were purchased from Charles River (Sulzfeld, Germany). All experiments were performed with male mice at the age of 10-12 weeks. Animals were housed under conventional conditions with free access to food and water. All experiments were performed according to German legislation for the protection of animals and approved by the local government authorities.

4 WESTERN BLOT ANALYSIS

Western blot analysis is an extensively used technique to identify specific proteins in various protein mixtures, e.g. cell lysates or tissue homogenates. It includes the electrophoretic separation of proteins according to their molecular weights, their transfer to a membrane ("blotting") and their visualization by immunodetection.

4.1 SAMPLE PREPARATION

For Western blot analysis, cells were washed with ice-cold PBS. PBS was removed completely and cells were lysed by adding RIPA buffer or modified RIPA buffer and freezed at -80°C. Cells were thawed on ice, scratched from the plate/dish and transferred to 1.5 ml reaction tubes. Cellular debris was removed by centrifugation for 10 min at 10,000 g and 4°C. Supernatants were transferred to a new reaction tube and aliquots were taken for protein quantification (II-4.6, Protein quantification). 5x SDS-sample buffer was added to the lysates, and lysates were boiled for 5 min at 95°C for inactivation. Protein samples were stored at -20°C until use.

RIPA Buffer		**Modified RIPA Buffer**	
Tris/HCl	0.79 g ≙ 50 mM	Tris/HCl	0.79 g ≙ 50 mM
NaCl	0.87 g ≙ 150 mM	NaCl	0.87 g ≙ 150 mM
Nonidet NP 40	1.0 ml	Nonidet NP 40	1.0 ml
Deoxycholic acid	0.25 g	Deoxycholic acid	0.25 g
SDS	0.10 g	SDS	0.10 g
H_2O	ad 100 ml	H_2O	ad 100 ml
		Na_3VO_4	300 µM
		NaF	1 mM
		pyrophosphate	10 mM
		β-gylcerophosphate	3 mM
add before use:		**add before use:**	
Complete®	1:25	Complete®	1:25
PMSF	1mM	PMSF	1 mM
Na_3VO_4	1 mM	H_2O_2	600 µM
NaF	1 mM		

For the detection of phosphorylated proteins the modified RIPA buffer was used.

5x SDS-Sample Buffer (store at -20° C)	
Tris/HCl	3.125 M, pH 6.8
Glycerol	10 ml
SDS	5%
DTT	2%
Pyronin Y	0.025%
H_2O	ad 20 ml

4.2 SDS-PAGE

SDS-PAGE according to Laemmli[73] was performed by using the Mini Protean III system from Bio-Rad (Munich, Germany). Prior to loading the samples, the apparatus was assembled as described by the producer, and the chamber was filled with ice-cold electrophoresis buffer.

Protein concentrations of the probes were unified by adding the required volume of 1x SDS-sample buffer. Then, probes were boiled for 5 min at 95°C before loading the samples on the SDS-gel. Empty slots were filled with an appropriate volume of 1x SDS-sample buffer. To estimate the molecular weights of the separated proteins, 2 µl of the marker Page Ruler™ Prestained Protein Ladder were additionally loaded on the gel.

Proteins were separated in a discontinuous electrophoresis: proteins were focused by running the samples through the stacking gel, pH 6.8, (100 V, 20 min) and then separated in the separating gel, pH 8.8 (200 V, 45 min).

Stacking Gel		**Separating Gel (10%)**	
PAA solution 30%	1.275 ml	PAA solution 30%	5.0 ml
1.25 M Tris/HCl, pH 6.8	0.75 ml	1.5 M Tris/HCl, pH 8.8	3.75 ml
10% SDS	75 µl	10% SDS	150 µl
H_2O	5.25 ml	H_2O	6.1 ml
APS	75 µl	APS	75 µl
TEMED	20 µl	TEMED	20 µl

Electrophoresis Buffer	
Tris base	3.0 g
Glycine	14.4 g
SDS	1.0 g
H_2O	ad 1.0 l

4.3 ELECTROBLOTTING

After protein separation, proteins were transferred onto nitrocellulose membranes by electroblotting, the most commonly used method to transfer proteins from a gel to a membrane.[74] The protein transfer can be achieved either by placing the gel-membrane sandwich between absorbent paper soaked in transfer buffer (semi-dry transfer) or by complete immersion of the gel-membrane sandwich in a buffer (wet transfer). In the present work, semi-dry transfer has been used.

Semi-dry transfer:
Using a Transblot SD semidry transfer cell (Bio-Rad, Hercules, USA), the separated proteins were electrophoretically transferred to a nitrocelluose membrane (Hybond ECl, GE Healthcare, Munich, Germany). Prior to blotting, the membrane was incubated for at least 30 min in Anode buffer on a shaking platform. For semi-dry transfer, the gel-membrane sandwich is placed between carbon plate electrodes. Therefore, one sheet of thick blotting paper (Whatman, Schleicher & Schüll, Dassel, Germany) was soaked with Anode buffer and rolled onto the anode. Subsequently, the membrane and the gels were added. Finally, the stack was covered with another sheet of thick blotting paper soaked with Cathode buffer. The transfer cell was closed and transfer was carried out at 15 V for 1 h.

Anode buffer		Cathode buffer	
Tris	12 mM	Tris	12 mM
CAPS	8 mM	CAPS	8 mM
Methanol	15 %	SDS	0.1%
H_2O		H_2O	

4.4 PROTEIN DETECTION

4.4.1 Specific protein staining with antibodies

Prior to the immunological detection of the relevant proteins, unspecific protein binding sites were blocked. Therefore, the membrane was incubated in non-fat dry milk powder (Blotto 5%) or bovine serum albumin (BSA 5%) for 2 h at room temperature. Afterwards, detection of the proteins was performed by incubating the membrane with the respective primary antibody at 4°C overnight. After four washing steps (each 5 min) with PBS containing 0.1% Tween20 (PBS-T), the membrane was incubated with the secondary antibody, followed by 4 additional washing steps. All steps regarding the incubation of the membrane were performed under gentle agitation.

In order to visualize the proteins, two different methods were used depending on the labels of secondary antibodies.

A. Antibodies directly labeled with infrared (IR) fluorophores:

Secondary antibodies coupled to IRDye™800 or IRDye™688 with emission at 800 and 688 nm, respectively, were used. Membranes were incubated for 1 h. Protein bands of interest were detected using the Odyssey imaging system (LI-COR Biosciences, Lincoln, NE, USA). After scanning the membrane with two-color detection, bands could be quantified using Odyssey software.

B. Antibodies coupled to horseradish peroxidase (HRP):

Membranes were incubated for 2 h with HRP-conjugated secondary antibodies. For detection, luminol was used as a substrate. The membrane was incubated in a 1:0.025 mixture of ECL solution A and B for 1 minute (ECL Plus Western Blotting Detection Reagent RPN 2132, GE Healthcare, Munich, Germany). The enzyme HRP catalyzes the oxidation of luminol in the presence of H_2O_2 (Figure II-2). The appearing luminescence was detected by exposure of the membrane to an X-ray film (Super RX, Fuji, Düsseldorf, Germany) and subsequently developed with a Curix 60 Developing system (Agfa-Gevaert AG, Cologne, Germany).

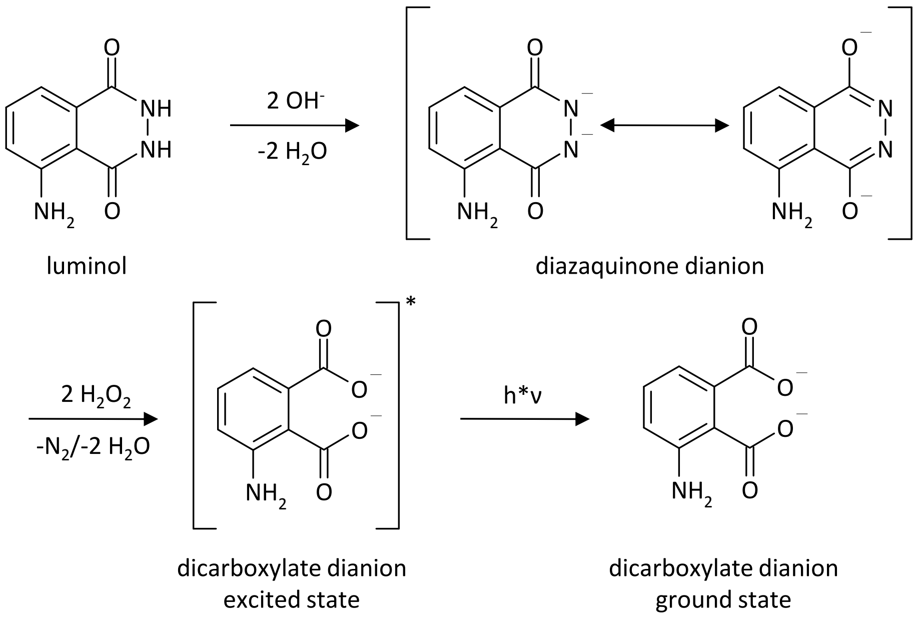
2 OH-
-2 H2O
luminol
diazaquinone dianion
2 H2O2
-N2/-2 H2O
h*v
dicarboxylate dianion excited state
dicarboxylate dianion ground state

Figure II-2 HRP-Luminol reaction

Primary antibodies used for protein detection are listed in Table 2; secondary antibodies are displayed in Table 3.

Table 2 Primary antibodies

Antigen	Isotype	Dilution	Provider	Detection
β-actin	mouse monoclonal	1:1,000	Chemicon	LI-COR/ECL
β-tubulin	mouse monoclonal	1:500	Santa Cruz	LI-COR/ECL
CDK2	rabbit polyclonal	1:1,000	Santa Cruz	LI-COR
CDK5	mouse monoclonal	1:1,000	Santa Cruz	LI-COR
CDK7	mouse monoclonal	1:1,000	Cell Signaling/NEB	LI-COR
CDK9	mouse monoclonal	1:1,000	Santa Cruz	ECL
IκBα	rabbit polyclonal	1:1,000	Santa Cruz	LI-COR
IKKα/β phospho	rabbit polyclonal	1:500	Cell Signaling/NEB	LI-COR
RS6K phospho	rabbit polyclonal	1:1,000	Cell Signaling/NEB	ECL

Table 3 Secondary antibodies

Antigen	Conjugate	Dilution	Provider
Goat anti-rabbit	HRP	1:1,000	Dianova
Goat anti-mouse	HRP	1:1,000	Santa Cruz
Goat anti-rabbit	IR-Dye 688	1:10,000	LI-COR Bioscience
Goat anti-rabbit	IR-Dye 800	1:10,000	LI-COR Bioscience
Goat anti-mouse	IR-Dye 688	1:10,000	LI-COR Bioscience
Goat anti-mouse	IR-Dye 800	1:10,000	LI-COR Bioscience

4.5 STAINING OF GELS AND MEMBRANES

In order to ensure equal protein loading and blotting efficiency, gels as well as membranes were stained with Coomassie and Ponceau staining solution, respectively.

Staining of gels with Commassie staining solution:

After transfer, gels were incubated with Coomassie staining solution for 20 min. The dye penetrates the gel and stains all proteins. Afterwards, gels were extensively washed with Coomassie destaining solution for 60 min (6x 10 min) until proteins appeared as blue bands.

Coomassie staining solution		Coomassie destaining solution	
Coomassie blue G	0.3%	Glacial acetic acid	10%
Glacial acetic acid	10%	Ethanol	33%
Ethanol	45%	H_2O	
H_2O			

Staining of membranes with Ponceau solution:

Membranes were incubated with Ponceau solution on a shaking platform for 5 min and were washed with water until the background disappeared.

Ponceau solution	
Ponceau S	0.1%
Glacial acetic acid	0.1%
H_2O	

4.6 PROTEIN QUANTIFICATION

In order to employ equal amounts of proteins in all samples for Western blot analysis, protein concentrations were determined using either Bicinchoninic protein assay or Bradford assay. After measurement, protein concentration was adjusted by adding SDS-sample buffer (1x).

4.6.1 Bicinchoninic protein assay (BCA assay)

Bicinchoninic acid (BCA) Protein Assay (BC Assay reagents, Interdim, Montulocon, France) was performed as described previously.[75] 10 µl protein samples were incubated with 200 µl BC Assay reagent for 30 min at 37°C. Absorbance of the blue complex was measured photometrically at 550 nm. Protein standards were obtained by diluting a stock solution of Bovine Serum Albumin (BSA, 2 mg/ml). Linear regression was used to determine the actual protein concentration of each sample.

4.6.2 Bradford assay

Bradford assay (Bradford solution, Bio-Rad, Munich, Germany) was performed as described previously.[76] It employes Coomassie Brillant Blue as a dye, which binds to proteins. 10 µl protein samples were incubated with 190 µl Bradford solution (1:5 dilution in water) for 5 min. Thereafter, absorbance was measured photometrically at 592 nm. Protein standards were achieved as described above (BCA assay).

5 WHOLE MOUNT CREMASTER MUSCLE PREPARATION AND INTRAVITAL MICROSCOPY

The whole mount cremaster muscle preparation and intravital microscopy was performed in collaboration with Dr. Christoph Reichel and Bernd Uhl from the group of Prof. Dr. Fritz Krombach (Walter Brendel Centre of Experimental Medicine, Munich, Germany).

5.1 SURGICAL PROCEDURE

The surgical preparation was performed as originally described by Baez with minor modifications.[77] Mice were anesthetized using a ketamine/xylazine mixture (100 mg/kg ketamine and 10 mg/kg xylazine), administered by intra-peritoneal injection. The left femoral artery was cannulated in a retrograde manner for administration of microspheres and drugs (see below). Surgical preparation of cremaster muscles and intravital microscopy were performed as described previously.[78] One cremaster muscle was used to investigate the leukocyte-endothelium interaction by intravital microscopy and the other cremaster muscle was incubated in RNAlater to later quantify the ICAM-1 mRNA level.

5.2 EXPERIMENTAL PROTOCOL

Leukocyte recruitment to the cremaster muscle was induced by intra-scrotal injection of recombinant murine TNF-α (500 ng in 0.4 ml PBS, R&D Systems Europe Ltd., Wiesbaden, Germany). After 240 min, five vessel segments were randomly chosen in a central area of the spread-out cremaster muscle among those that were at least 150 µm away from neighboring postcapillary venules and did not branch over a distance of at least 150 µm. After having obtained recordings of migration parameters, blood flow velocity was determined as prior described. Blood samples were collected by cardiac puncture for the determination of systemic leukocyte counts using a Coulter ACT Counter (Coulter Corp., Miami, FL, USA). Anesthetized animals were then killed by bleeding to death.

5.3 INTRAVITAL MICROSCOPY AND DETERMINATION OF MICROHEMODYNAMIC PARAMETERS

For off-line analysis of parameters describing the sequential steps of leukocyte extravasation, we used the Cap-Image image analysis software (Dr. Zeintl, Heidelberg, Germany). Rolling leukocytes were defined as those moving slower than the associated blood flow and quantified for 30 s. Firmly adherent cells were determined as those resting in the associated blood flow for more than 30 s and related to the luminal surface per 100 µm vessel length. Transmigrated cells were counted in regions of interest, covering 75 µm on both sides of a vessel over 100 µm vessel length. By measuring the distance between several images of one fluorescent bead under stroboscopic illumination, centerline blood flow velocity was determined. From measured vessel diameters and centerline blood flow velocity, apparent wall shear stress was calculated, assuming a parabolic flow velocity profile over the vessel cross section.

6 GRANULOCYTE ADHESION ASSAY

Confluent monolayers of HUVECs, seeded in 24-well plates, were exposed to different concentrations of roscovitine in presence or absence of TNF-α for 24 h. After treatment, endothelial growth medium was replaced by medium 199 containing 2% FCS (Table 1) and granulocytes were then added at a concentration of exactly 1×10^5 cells/well. To distribute the granulocytes on the monolayer, the 24-well plates were centrifuged for 3 min at 800 rpm. After centrifugation, the granulocytes were allowed to adhere for 30 min at 37°C. Then, the monolayers were gently washed three times with warmed PBS containing magnesium and calcium, and non-adhered granulocytes were then rinsed out. After washout, 100 µl of lysis buffer (Table 4) per well was added and the plates were incubated for 30 min at 37°C. Afterwards, adhered granulocytes were quantified by a myeloperoxidase (MPO) assay. The activity of MPO was analyzed by spectrometric measurement. 100 µl of MPO substrate (Table 4) was added to 100 µl of each lysate. The conversion of the substrate was determined at 540 nm using SPECTRAFluor Plus plate reader. The number of adhered granulocytes was calculated from the gradient of the conversion curve of dianisidine.

Table 4 Buffer and medium for granulocyte adhesion assay

Phosphate buffer (pH 6.0)		**Lysis buffer**	
KH_2PO_4	9.08 g/l	HTAB (Hexadecyltrimethyl-ammoniumbromide	1%
Na_2HPO_4	11.88 g/l	Phosphate buffer (pH 6.0)	
H_2O			

MPO substrate	
Dianisidine	0,06%
H_2O_2	0,0009%

7 FLOW CYTOMETRY

Flow cytometry (FACS) allows counting, sorting and analysis of various parameters of single cells or particles suspended in a fluid. Each cell passes a focused laser beam and scatters the illuminating light. If particles have previously been stained with a fluorescent dye, fluorescence emission occurs and can be detected.

Flow cytometry has been used for quantification of DNA fragmentation, the analysis of endothelial cell adhesion molecule expression (ICAM-1, VCAM-1 and E-selectin), the expression of CD11b and the fluorescence intensity of oxidated DHR. All measurements were performed on a FACSCalibur (Becton Dickinson, Heidelberg, Germany). Cells are illuminated by a blue argon laser (488nm). Scattered light and emitted fluorescence are filtered and the last is measured with several detectors: FL-1 (530 nm), FL-2 (585 nm), FL-3 (650 nm) or FL-4 (optional, in this case FL-3 detects >670 nm).

Table 5 Buffers for FACS measurement and PI staining (Nicoletti method)

FACS Buffer		Buffer	
NaCl	8.12 g	Propidium iodide	75 nM
KH_2PO_4	0.26 g	Na_3-citrate	0.1%
Na_2HPO_4	2.35 g	Triton-X 100	0.1%
KCl	0.28 g	PBS	ad 1 ml
Na_2EDTA	0.36 g		
LiCl	0.43 g		
Na-azide	0.20 g		
H_2O	ad 1.0 l, pH 7.37		

7.1 QUANTIFICATION OF DNA FRAGMENTATION

During the apoptotic process endogenous endonucleases become activated and cause the fragmentation of nuclear DNA into oligonucleosomal-size fragments. A widely used assay to quantify apoptotic cell death is the counting of nuclei with subdiploid DNA content after staining with propidium iodide (PI). Quantification of apoptosis was carried out according to Nicoletti et al [79].

HUVECs were seeded into 12-well-plates until confluence and left untreated or treated with various concentrations of roscovitine for 24 and 48 h. After treatment, cells were washed, trypsinized, resuspended in the supernatant and centrifuged (10 min, 600 g at 4°C).

Afterwards, cells were incubated in a buffer (Table 5) containing Triton X-100 for permeabilization and propidium iodide (PI) for staining. PI is a red fluorescent dye that intercalates with doublestranded DNA, detecting the DNA content of the cell. After incubation at 4°C overnight, cells were analyzed by flow cytometry. The respective fluorescence intensity gives information about the DNA content of a cell, and thus, about rate of apoptosis and cell cycle phases. Low fluorescence indicates DNA fragmentation characterized for apoptotic cells. They appear “left” to the G1/G0 peak in the histogram plot (“sub-G1 peak”).

The fluorescence intensity was measured in the logarithmic mode of the fluorescence channel 2 (FL-2, λ_{em} 585 nm) using a flow cytometer.

7.2 EXPRESSION OF ENDOTHELIAL CELL ADHESION MOLECULES

HUVECs (24-well plates, 200 µl) were grown until confluence and were left either untreated or treated with TNF-α (10 ng/ml, Sigma, Taufkirchen, Germany). The effect of roscovitine on the surface expression of endothelial cell adhesion molecules was determined. Roscovitine was added to the cells 30 min before TNF-α. After 6 h (E-selectin) or 24 h (ICAM-1, VCAM-1), surface expression of adhesion molecules was measured by flow cytometry using FITC-labeled antibodies against ICAM-1, VCAM-1 and E-selectin (Biosource, Nivelles, Belgium).

After treatment, cells were washed with warm PBS and trypsinized. Then the detached cells were transferred into FACS tubes, filled with 100 µl PBS/4% paraformaldehyde to fix the cells. After centrifugation, the received cell pellet was washed and incubated with the respective antibody for 45 min in the dark at room temperature. The cells were again washed with PBS and resuspended in PBS for flow cytometric analysis. 10,000 events were measured in the FL-1 channel (509 nm) to detect the changes in expression of surface proteins as evidenced by a median shift in fluorescence intensity.

7.3 EXPRESSION OF CD11B

Freshly isolated granulocytes (10^6/ml, 100 µl) were either left untreated or treated with the indicated concentration of roscovitine before activation with fMLP (10^{-7}M) for 15 min. Then, cells were fixed with 4% formaldehyde and washed with PBS followed by incubation with saturating concentrations of FITC-labeled antibody against CD11b for 45 min at room temperature. Cells were washed once with PBS, resuspended in PBS and analyzed by flow cytometry. At least, 5,000 events were acquired.

7.4 DHR OXIDATION (OXIDATIVE BURST)

Oxidative burst in granulocytes was assessed by measuring the intracellular oxidation of DHR to rhodamine. Granulocytes (10^6/ml, 100 µl) in suspension were primed with DHR (1 µM) for 10 min at 37°C. Cells were pretreated for 30 min with 10 µM or 20 µM roscovitine and activated with fMLP (10^{-7}M) for 15 min. The reaction was stopped on ice and the cells were analyzed by flow cytometry. At least, 5,000 events were acquired.

8 TRANSFECTION AND GENE TRANSFER

8.1 TRANSFECTION WITH siRNA

Transfection refers to the introduction of genetic material into cultured mammalian cells. Genetic material (i.e. plasmid DNA or siRNA constructs) can be transfected using calcium phosphate, electroporation, lipofection, or magnetofection. For transient transfection with siRNA, HUVECs were electroporated using the Nucleofector® II device in combination with the HUVEC Nucleofector®Kit (both from Amaxa, Cologne, Germany).

In order to silence Cdk2 and Cdk7, respectively, HUVECs were transiently transfected with Cdk2 as well as Cdk7 siRNA. Two On-TARGETplus individual duplexes were used for CDK2 and On-TARGETplus SMARTpool was used for CDK7 (Dharmacon, Lafayette, CO, USA). On-TARGETplus siCONTROL Non-targeting (nt) siRNA was used as a control. siRNAs were suspended in Dharmacon 1x siRNA buffer, aliquoted and stored at -80°C. The concentration of siRNA was verified using a NanoDrop (Wilmington, DE, USA). For each transfection, 2 x 10^6 HUVECs were suspended in 100 µl HUVEC Nucleofector® Solution and added to 3 µg of the respective siRNA:

Cdk2 siRNA:
1.5 µg siRNA Duplex J-003236-11 (sequence: 5’-PUAUUAGGAUGGUUAAGCUCUU-3’)
1.5 µg siRNA Duplex J-003236-12 (sequence: 5’-PUCUCCCGUCAACUUGUUUCUU-3’)

Cdk7 siRNA:
0.75 µg siRNA Duplex J-003241-09 (sequence: 5’-CAUACAAGGCUUAUUCUUA-3’)
0.75 µg siRNA Duplex J-003241-10 (sequence: 5’-AAACUGAUCUAGAGGUUAU-3’)
0.75 µg siRNA Duplex J-003241-11 (sequence: 5’-CAACAUUGGAUCCUACAUA-3’)
0.75 µg siRNA Duplex J-003241-12 (sequence: 5’-GAUGACUCUUCAAGGAUUA-3’)

nt siRNA (transfection control):
ON-TARGETplus siCONTROL nt siRNA D-001810-01
(sequence: 5’-UGGUUUACAUGUCGACUAA-3’)

The mixture of cells and siRNA was transferred to an Amaxa-certified cuvette and transfection was performed (program A-034). Immediately after electroporation, 900 µl of pre-warmed culture medium was added to the cuvette. Afterwards, cells were seeded into 24-well plates (250,000 cells per well) for flow cytometry measurements and in 6-well plates (1,000,000 cells per well) for Western Blot analysis.

Flow cytometry measurements were performed 48 h after transfection. Efficiency of downregulation of the respective protein was checked 24 and 48 h after transfection by Western Blot analysis.

8.2 VIRAL-MEDIATED GENE TRANSFER (TRANSDUCTION)

Viral-mediated gene transfer provides a convenient and efficient means to introduce genetic material into recipient cells. Hereby, adenoviral vectors are well-established gene transfer tools for quantitative gene transfer into mammalian cells. Adenoviral vectors enter cells after binding to cellular receptors by using the cell's endocytosis pathway.[80] This approach allows for high efficient knock-down even in hard-to-transfect cell types, including primary cells.

The introduction of target specific shRNA was utilized to knock down the gene expression of CDK5 and CDK9 using adenoviral vectors. This adenovirus technology was performed by SIRION BIOTECH GmbH (Martinsried, Germany). 72 h after transduction, HUVECs were left untreated or treated with roscovitine for 30 min in the indicated concentration, followed by TNF-α treatment. After 24 h, the ICAM-1 expression was determined using flow cytometric analysis.

9 NF-kB PROMOTER ACTIVITY ASSAY (REPORTERGENE ASSAY)

Reporter gene assays are powerful tools to study the regulation of a gene of interest. As reporter, firefly luciferase is widely used to study gene expression. Light is produced by converting the chemical energy of luciferin oxidation through an electron transition, forming the product molecule oxyluciferin (Figure II-3). The enzyme catalyzes the luciferin oxidation using ATP and Mg^{2+} as co-substrates. The generated flash of light can be conveniently measured on a luminometer.

HUVECs were transiently cotransfected with 4 µg of pGL4.32[luc2P/NFκB-RE/Hygro] and 0.4 µg of pGL4.74[hRluc/TK] using Amaxa® HUVEC Nucleofector® Kit (Lonza Cologne AG, Cologne, Germany). All plasmid vectors (Promega GmbH, Mannheim Germany) were purified using an EndoFree Plasmid Maxi Kit (QIAGEN Sciences, Germantown, MD). 6 h after transfection, the culture medium was replaced with fresh medium and the transfected cells were incubated in a humidified atmosphere for 24 h. Then the cells were pre-incubated with different concentrations of roscovitine and subsequently treated with TNF-α for 5.5 h. After 6 h, cells were washed with PBS including magnesium and calcium and harvested with passive lysis puffer (Promega GmbH, Mannheim, Germany).

NF-κB reporter gene activity assays were performed using a Dual-Luciferase™ Reporter Assay System according to the manufacturer`s instructions (Promega GmbH, Mannheim, Germany). The luciferase activities were measured using luminometer (Berthold Orion II, Berthold Detection Systems, Pforzheim, Germany). The NF-κB-dependent firefly luciferase activity was normalized to the activity of the internal control (*Renilla* luciferase).

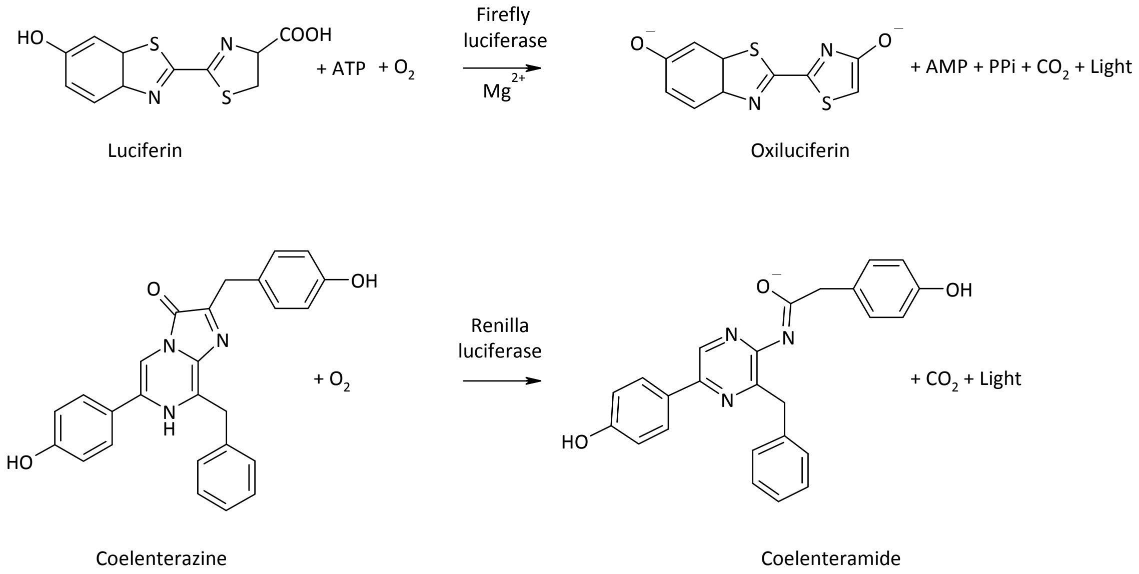

Figure II-3 Bioluminescent reactions catalyzed by the firefly and *Renilla* luciferases

10 IMMUNOCYTOCHEMISTRY AND CLSM

10.1 IMMUNOCYTOCHEMISTRY

Cells were seeded on ibi-Treat µ-slides (IBIDI, Martinsried, Germany). After stimulation, cells were washed once with ice-cold PBS$^+$ and fixed in 4% formaldehyde (Accustain®, Sigma-Aldrich, Taufkrichen, Germany) for 10-15 min. After one PBS washing step, cells were permeabilized by incubating cells in 0.2% Triton X-100 in PBS for exactly 2 min. Then, cells were washed three times for 5 min with PBS, blocked for 15 minutes in 0.2% BSA in PBS and incubated with the primary antibody against p65 (Santa-Cruz Biotechnology Inc., 1:100 in 250 µl 0.2% BSA/PBS) for 45-60 min. After three washes with PBS for 5 min, cells were incubated with light-protection for 30-60 min with the Alexa Fluor 488-conjugated secondary antibody (Molecular Probes, 1:400 in 0.2% BSA/PBS). Afterwards, cells were washed again three times with PBS and covered with FluorSave aqueous mounting medium for confocal microscopy.

10.2 CONFOCAL LASER SCANNING MICROSCOPY

Confocal laser scanning microscopy is an extensively used method in life sciences due to its great advantages. The key feature of the confocal microscopy is that it only captures light reflected or emitted by a single plane of a specimen. Out of focus light is filtered out so that only light coming from in-focus objects can reach the detector. A laser beam scans the specimen pixel by pixel and line by line. Afterwards, data are assembled, resulting in an image that represents an optical section through the specimen. This results in high-quality images with high contrast and maximum resolution, gives information about co-localization of signals from different fluorochromes and allows three-dimensional reconstructions of thick specimens.[81]

11 ELECTROPHORETIC MOBILITY SHIFT ASSAY

11.1 EXTRACTION OF NUCLEAR PROTEINS

For nuclear preparation, HUVECs were treated as indicated and washed twice with ice-cold PBS. The PBS was removed completely and cells were lysed by adding 400 µl nuclear extraction buffer A. Cells were scraped off the plate/dish and transferred to 1.5 ml reaction tubes. Cells were allowed to swell on ice for 15 min. Nonidet P-40 (0.625 %) was added, followed by 10 s of vigorous vortexing. Probes were centrifuged (14,000 rpm, 1 min, 4 °C), supernatants removed, and pellets incubated for 30 min under agitation at 4°C in 40 µl nuclear extraction buffer B. After centrifugation (14,000 rpm, 5 min, 4°C), supernatants were collected and frozen at -80 °C. Protein concentrations were determined by Bradford assay (II-4.6., PROTEIN QUANTIFICATION).

Table 6 Buffer for the extraction of nuclear proteind

Extraction Buffer A		**Extraction Buffer B**	
HEPES, pH 7.9	10 mM	HEPES, pH 7.9	20 mM
KCl 10	10 mM	NaCl	0.4 mM
EDTA	0.1 mM	EDTA	0.1 mM
EGTA	0.1 mM	EGTA	0.1 mM
DTT	1.0 mM	DTT	1.0 mM
PMSF	0.5 mM	PMSF	0.5 mM
Glycerol	25%		

11.2 ELECTROPHORETIC MOBILITY SHIFT ASSAY (EMSA)

Transcription factor-specific oligonucleotides were 5’ end-labeled with [γ^{32}P]-ATP using the T4 polynucleotide kinase. Oligonucleotides for NF-κB with the consensus sequence 5’-AGT TGA GGG GAC TTT CCC AGG C-3’ were purchased from Promega. Equal amounts of protein were incubated with 2 µg poly(dIdC) and 3 µl of freshly prepared reaction buffer for 10 min at room temperature. The reaction buffer consisted of 450 µl 5x binding buffer, 50 µl Gel loading buffer and 1 mM DTT. The binding-reaction was started by adding 1 µl of the radioactive oligonucleotide and carried out for 30 min at roomtemperature. The protein-oligonucleotide complexes were separated by gel electrophoresis (Mini-Protean III, BioRad) with 0.25 x TBE buffer at 100 V for 70 min using non-denaturating polyacrylamide gels (5% PAA, 20% glycerol). After electrophoresis, gels were exposed to Cyclone Storage Phosphor Screens (Canberra-Packard, Schwadorf, Austria) for 24 h, followed by analysis with a phosphor imager station (Cyclone Storage Phosphor System, Canberra-Packard).

Table 7 Buffers for EMSA

5x Binding Buffer		**Loading Buffer**	
Tris/HCl	50 mM	Tris/HCl	250 mM
NaCl	250 mM	Glycerol	40%
$MgCl_2$	5.0 mM	Bromphenolblue	0.2%
EDTA	2.5 mM		
Glycerol	20%		

Reaction buffer		**10 x TBE**	
5x Binding buffer	90%	Tris	890 mM
Loading buffer	10%	Boric acid	890 mM
DTT	2.6 mM	EDTA	20 mM
		H_2O	

12 IKKβ ACTIVITY ASSAY

The effect of roscovitine on purified IκB kinase (IKK) activity was determined with a highly sensitive HTScan® IKKβ Kinase Assay Kit according to the instructions of the manufacturer (Cell Signaling Technology). The kit provides a means of performing kinase activity assays with recombinant human IKKβ kinase. It includes active IKKβ kinase (supplied as GST fusion protein), a biotinylated peptide substrate and a phospho-serine antibody for detection of the phosphorylated form of the substrate peptide. Purified IKKβ kinase was pre-treated with different doses of roscovitine (3 µM to 30 µM) 5 min prior to the treatment of substrate peptide. The assay was performed on a 96-well high-binding streptavidin-coated plate, and the absorbance of each well was read at 450 nm using the absorbance Reader (TECAN Sunrise™). Each kinase assay was performed in triplicates.

The percentage inhibition of IKKβ kinase activity was calculated using the formula:
$\textit{Percentage inhibition} = 1-[(\Delta \textit{inhibited}-\Delta \textit{blank})/(\Delta \textit{uninhibited} -\Delta \textit{blank})]\times 100$

13 QUANTITATIVE REAL-TIME PCR

13.1 RNA ISOLATION

13.1.1 RNA isolation from cremaster muscle

RNA was isolated from RNAlater-stored cremaster muscles using the RNeasy Mini Kit (Qiagen, Hilden, Germany). The tissues were homogenized, each about 25 mg in 600 µl RLT buffer (provided with the RNeasy Mini Kit) using the ultraturax homogenizer. Then, procedures were followed as default by the RNeasy Mini Kit protocol. Finally, RNA was eluted with RNase-free water, amounts were quantified with the NanoDrop, and integrity of the RNA was controlled on an agarose-gel (18S and 28S rRNA subunits).

13.1.2 RNA isolation from HUVECs

HUVECs were cultured in 6-well plates and pre-treated with the indicated concentration of roscovitine for 30 min prior TNF-α treatment for 4 h. Afterwards, cells were lysed and homogenized in the presence of a highly denaturating buffer (RLT buffer), a component of the RNeasy Mini Kit (Qiagen, Hilden, Germany). In the following, we continued with RNA isolation using the manufacturers' protocol. RNA quantification and integrity was proofed as described above.

13.2 REVERSE TRANSCRIPTION

2 µg of total RNA were re-transcribed with random primers and the high capacity cDNA Reverse Transcription Kit (Applied Biosystems, Foster City, CA, USA) for 2 h at 37°C. The cDNA was stored at -20° C until qRT-PCR.

13.3 QUANTITATIVE REAL-TIME PCR

Quantitative real-time PCR was performed on AB 7300 RealTime PCR system, using TaqMan Universal PCR Mastermix (Applied Biosystems). ICAM-1 and GAPDH primers were designed using the Primer Express® 2.0 software program (Applied Biosystems) The used probes and primers are depicted in Table 8. PCR on GAPDH was used as reference, and serial dilution of cDNA served as standard curves. Fluorescence-development was analyzed using the AB 7300 system software, and calculation of relative mRNA amount was done according to Pfaffl et al.[82]

Table 8 Used primers and probes

mouse	ICAM-1 (5'-3')	GAPDH (5'-3')
forward	ctg ctg ctt ttg aac aga atg g	tgc agt ggc aaa gtg gag at
reverse	tct gtg aca gcc aga gga agt g	tgc cgt gag tgg agt cat act
probe	FAM-aga cag cat tta ccc tca g-BHQ	FAM-cca tca acg acc cct tca ttg acc tc- BHQ
company	Biomers, Ulm, Germany	Biomers, Ulm, Germany

human	ICAM-1 (5'-3')	GAPDH (5'-3')
forward	gca gac agt gac cat cta cag ctt	ggg aag gtg aag gtc gga gt
reverse	ctt ct gaga cct ctg gct tvg t	tcc act tta cca gag tta aaa gca g
probe	FAM-ccg gcg ccc aac gtg att ct-BHQ	FAM-acc agg cgc cca ata cga cca a- TAMRA
company	Invitrogen, Ulm, Germany	Invitrogen, Ulm, Germany

14 KINOME ARRAY (PEPCHIP)

To address the question which effects roscovitine have on overall signaling in endothelial cell, a kinome array (PepChip) was performed. The array was done by Dr. Jos Joore from Pepscan System BV, Lelystad, The Netherlands.

HUVECs in 4x 100 mm dishes for each treatment group were grown to confluence. Untreated cells and cells treated with TNF-α (10 ng/ml, 4 h) in the absence or presence of roscovitine (10 µM) were washed twice with ice-cold PBS and lysed with M-PER Mammalian Protein Extraction Reagent (Pierce, Rockford, IL), containing 2.5 mM Na_4-pyrophosphate, 2 mM Na_2-β-glycerophosphate, 1 mM Na_3VO_4 and 1mM NaF. Lysates were centrifuged for 10 min at 13,000 rpm, 4°C, and supernatants were frozen immediately in liquid nitrogen. PepChip performance and analysis of the results were done by Pepscan Presto BV (Lelystad, The Netherlands). On the chip 1,152 different peptides with best possible specific phosphorylation motifs for upstream kinases were spotted in triplicates. Native protein lysates of HUVECs incubated on PepChip with [γ-^{33}P] ATP. A radiosensitive screen determined and quantified the phosphorylation status of peptides ($\triangleq$ kinase substrates), which gave information about the activity of the associated upstream kinase.

15 STATISTICAL ANALYSIS

All experiments were performed at least three times unless otherwise indicated in the figure legend. Data are expressed as mean ± SEM. Statistical analysis was performed with GraphPad Prism^{TM} version 3.03 for Windows (GraphPad Software, San Diego, CA). Unpaired *t* test was used to compare two groups. To compare three or more groups, ANOVA one-way analysis of variance followed by Newman-Keuls post-hoc test was used. P values ≤ 0.05 were considered significant.

RESULTS

III RESULTS

1 THE ANTI-INFLAMMATORY POTENTIAL OF ROSCOVITINE

1.1 IN VIVO

1.1.1 Effect of roscovitine on the leukocyte-endothelial cells interaction in vivo

As proof of principle, the leukocyte-endothelial cell interaction was investigated *in vivo* to test the anti-inflammatory properties of roscovitine. Therefore, intravital microscopy of the mouse cremaster muscle dissected from roscovitine/TNF-α-treated mice and drug vehicle/TNF-α-treated mice, respectively was performed. As readout parameters, leukocyte adherence and leukocyte transmigration were monitored. Inhibition of both leukocyte adherence (decreased by 40%) and transmigration (decreased by 26%) in post-capillary venules of the cremaster muscle was achieved by pre-treatment of mice with roscovitine (Figure III-1).

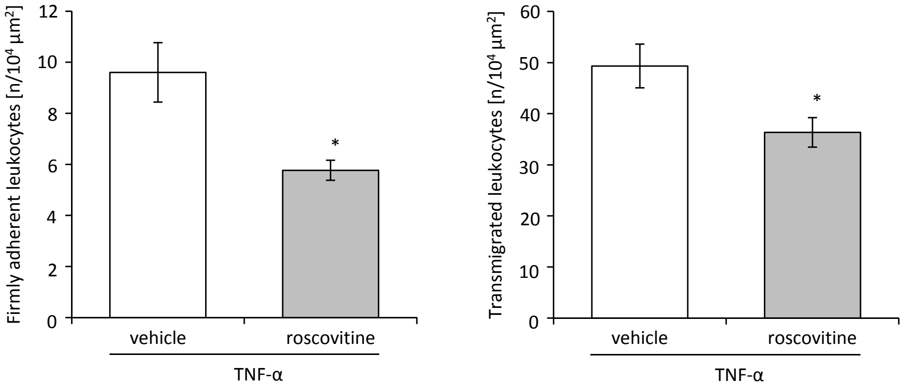

Figure III-1 Roscovitine inhibits leukocyte adherence and transmigration *in vivo*.
The number of firmly adherent leukocytes in postcapillary venules (left) and the number of transmigrated leukocytes (right) were quantitatively analyzed using intravital video fluorescence microscopy. Mice were treated with roscovitine/TNF-α or drug vehicle/TNF-α for 240 min before intravital microscopy was performed. A bolus injection (3.5 µg) sufficient to reach approximately 10 µM plasma concentration was applied. Leukocytes firmly attached to the endothelium for more than 30 s were counted as permanently adherent cells and expressed as number of cells per square millimeter endothelial surface. Transmigrated cells were counted in regions of interest, covering 75 µm on both sides of a vessel over 100 µm vessel length. n = 6 animals each group; data show mean ± SEM. *, $p<0.05$, compared with drug vehicle/TNF-α-treated group.

1.1.2 Microhemodynamic parameters and systemic leukocyte count

To investigate differences between the roscovitine-treated group and the drug vehicle-treated group, microhemodynamic parameters including systemic leukocyte count were measured. While blood flow (Vmean) and shear rate in the postcapillary venules were increased by roscovitine, the inner vessel diameter remained unchanged (Table 9). A possible reason for the increased hemodynamic parameters blood flow velocity (Vmean) and shear stress might be an effect of roscovitine on NO, which acts in blood vessels upstream of the venules in the vascular bed, however we could not show an altered release of this crucial vasodilator (data not shown).

A further reason for the increased parameters might be a change in blood viscosity by roscovitine.

The total count of systemic leukocytes has not changed in the observed mouse cremasters by co-treatment of roscovitine and TNF-α compared to drug vehicle and TNF-α (6.4 × 10^3/µl ± 1.4× 10^3/µl in drug vehicle/TNF-α-treated mice to 5.0 × 10^3/µl ± 1.1× 10^3/µl in roscovitine/TNF-α-treated mice), suggesting that roscovitine is not harmful to leukocytes.

Table 9 Microhemodynamic parameters and systemic leukocyte count.
Mice were intravenously injected with roscovitine or drug vehicle (Co) before TNF-α administration (intrascrotal). After 4 hours, intravital microscopy was performed and at least five unbranched postcapillary venules were analyzed per animal. n = 6 animals each group; data show mean ± SEM. *, $p<0.05$, compared with drug vehicle/TNF-α treated group.

parameters	**drug vehicle**	**roscovitine**
Systemic leukocyte count [x 10^3 μl^{-1}]	6.4 ± 1.4	5.0 ± 1.1
Vmean [mm/s]	1.2 ± 0.1	1.8 ± 0.1*
Inner diameter [µm]	25.4 ± 0.4	24.8 ± 0.4
Shear rate [s^{-1}]	1896.7 ± 74.1	2833.0 ± 199.8*

1.1.3 Roscovitine inhibits the ICAM-1 expression in the cremaster muscle

Next, mRNA level of ICAM-1 in cremaster muscles of roscovitine- and drug vehicle-treated mice were determined. It could be shown that the ICAM-1 mRNA expression in roscovitine/TNF-α-treated mice is slightly decreased by about 12% (Figure III-2).

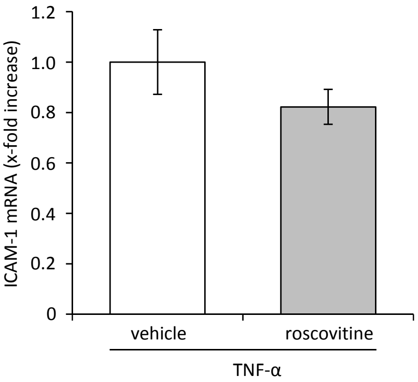

Figure III-2 Roscovitine slightly reduces the ICAM-1 mRNA expression in cremaster muscle of TNF-α-treated mice.
Mice were intravenously injected with roscovitine or drug vehicle before TNF-α administration (intra-scrotal). After 4 hours, the cremaster muscle was dissected and stored in RNA-later. Total RNA of the muscle was isolated for real-time PCR on ICAM-1. The mRNA level of ICAM-1 in drug vehicle/TNF-α treated mice was set as 1. (Mice per group = 6, data show mean ± SEM; non-significant, p>0.05, compared with drug vehicle/TNF-α treated mice)

1.2 IN VITRO

1.2.1 Leukocytes

1.2.1.1 Granulocyte adhesion is inhibited by roscovitine

The adherence of granulocytes on TNF-α-activated HUVECs was determined in the absence and in the presence of roscovitine. Also *in vitro*, it could be shown that roscovitine concentration-dependently inhibits the granulocyte adherence on the endothelium. At a roscovitine concentration of 10 µM, the TNF-α-induced granulocyte adherence was inhibited by about 40% (Figure III-3).

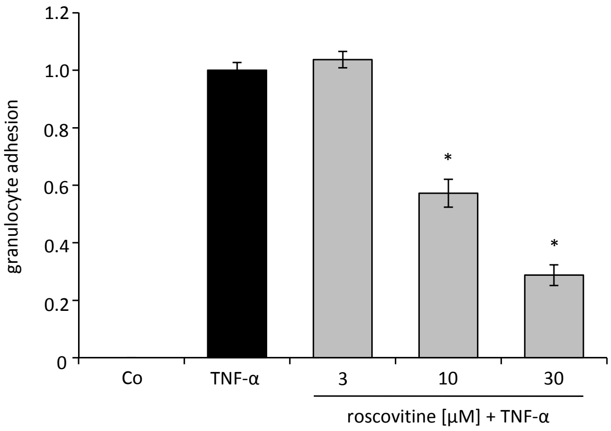

Figure III-3 Roscovitine attenuates the adherence of granulocytes on the endothelium in vitro.
Granulocyte adherence is concentration-dependently inhibited *in vitro* by roscovitine. HUVECs were seeded in 24-well plates. Confluent cells were pre-treated with different concentrations of roscovitine (3, 10, 30 µM) for 30 min before TNF-α treatment. After 24 h, isolated human granulocytes were added to the HUVECs for 30

min. The adherent granulocytes were quantified via assessing MPO activity. Results are expressed as the average of three independent experiments performed in triplicates ± SEM, *, $p<0.05$, compared TNF-α-treated HUVECs with TNF-α/roscovitine treated HUVECs.

1.2.1.2 The influence of roscovitine on the leukocyte activation

A. CD11b

An increased expression of the leukocyte integrin Mac1, composed of CD11b and CD18, is a marker for leukocyte activation, resulting in increased adherence on the endothelium. To clarify if the activation of leukocytes is affected by roscovitine, the amount of CD11b on the surface of leukocytes was measured.

Leukocytes that were treated with the chemoattractant fMLP showed a 2.5 fold increase in CD11b expression compared to untreated cells. This fMLP-induced CD11b expression is inhibited by roscovitine at the indicated concentrations (Figure III-4).

B. Oxidative burst

Rapid release of reactive oxygen species is referred to as oxidative burst. The oxidative burst, which can be quantified by oxidation of DHR due to the release of reactive oxygen species (ROS), is another marker for leukocyte activation. As positive control, leukocytes were treated with fMLP, resulting in increased ROS levels and correspondingly increased DHR oxidation. fMLP-treated cells that were pre-treated with roscovitine showed no significant decrease in oxidative burst (Figure III-4).

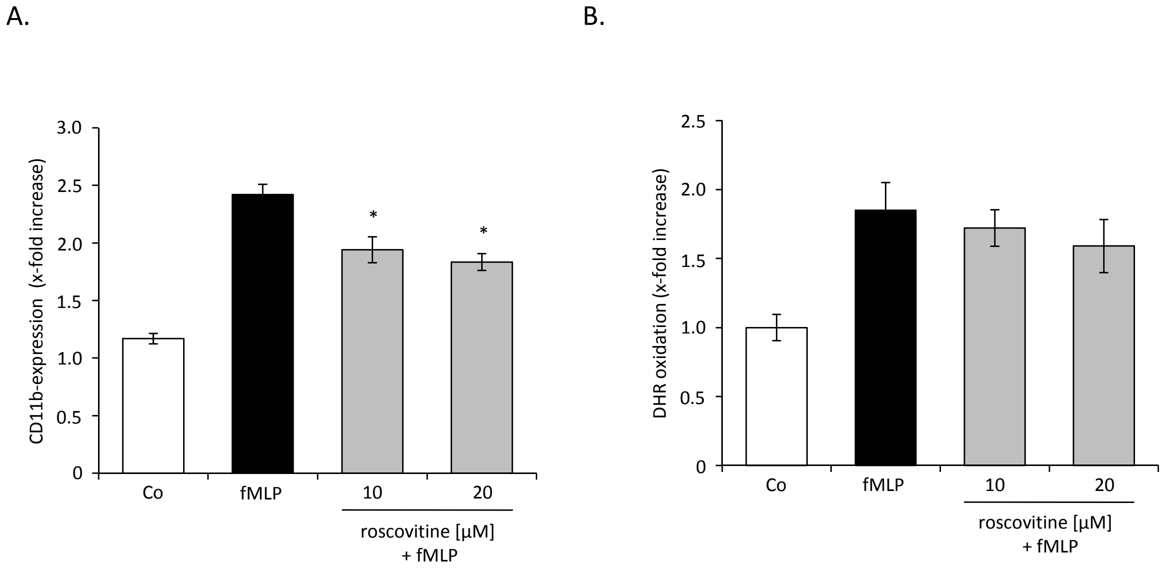

Figure III-4 The influence of roscovitine on the leukocyte activation
A. Roscovitine inhibits the fMLP-induced CD11b expression. The activation of leukocytes was detected by measurement of the surface marker CD11b. Human granulocytes were isolated and left untreated or treated with fMLP for 15 min. Some of the cells were pre-treated with roscovitine (10 µM and 20 µM) 30 min before

fMLP. Granulocytes were incubated with CD11b antibody and the CD11b expression was measured by flow cytometric analysis. (n = 3 independent experiments; mean ± SEM. *, $p<0.05$, compared with fMLP-treated cells).
B. Roscovitine showed no significant effect on the oxidative bust. The activation of leukocytes was detected by measurement of oxidated DHR. Human granulocytes were isolated and left untreated or treated with fMLP for 15 min. Some of the cells were pre-treated with roscovitine (10 µM and 20 µM) 30 minutes before fMLP treatment. To determine the oxidative burst by FACS analysis, the granulocytes were pre-incubated with 10 µM DHR before treated with roscovitine and fMLP. (n = 3 independent experiments; mean ± SEM. *, $p<0.05$, compared with fMLP treated cells).

We proposed that the effect of roscovitine on CD11b expression and the oxidative burst does not sufficiently explain the strong effect on granulocyte adhesion. Thus, we proceed with the analysis of roscovitine on endothelial cells.

1.2.2 ENDOTHELIUM

1.2.2.1 Roscovitine reduces the TNF-α-induced expression of cell adhesion molecules

To investigate whether roscovitine influences endothelial cells, in particular endothelial adhesion molecules, the surface expression of E-selectin, ICAM-1 and VCAM-1 was determined.

TNF-α, a major pro-inflammatory cytokine, was used to trigger the expression of endothelial adhesion molecules. Roscovitine concentration-dependently reduced the expression of these adhesion molecules – almost to control level (Figure III-5, A: ICAM-1, B: VCAM-1, C: E-selectin)

A.

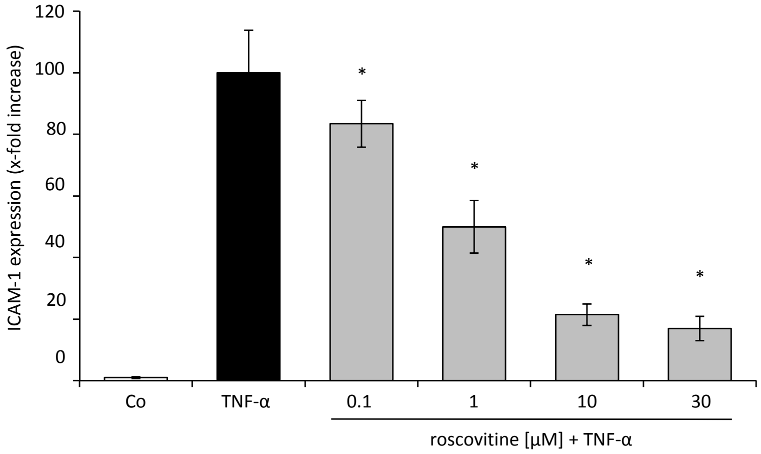

B.

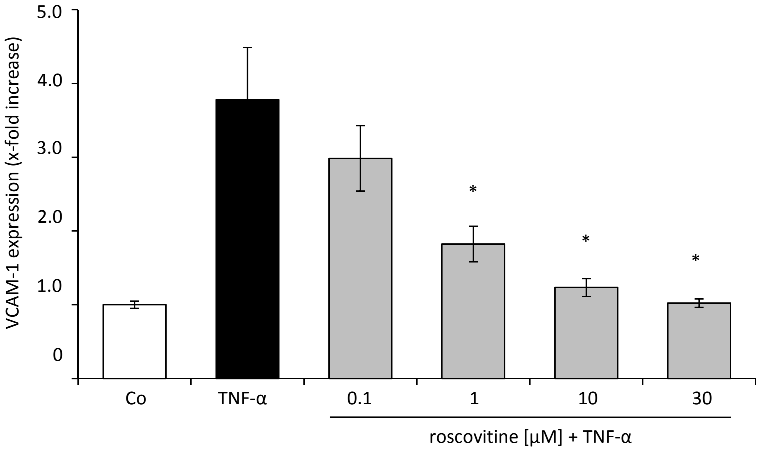

C.

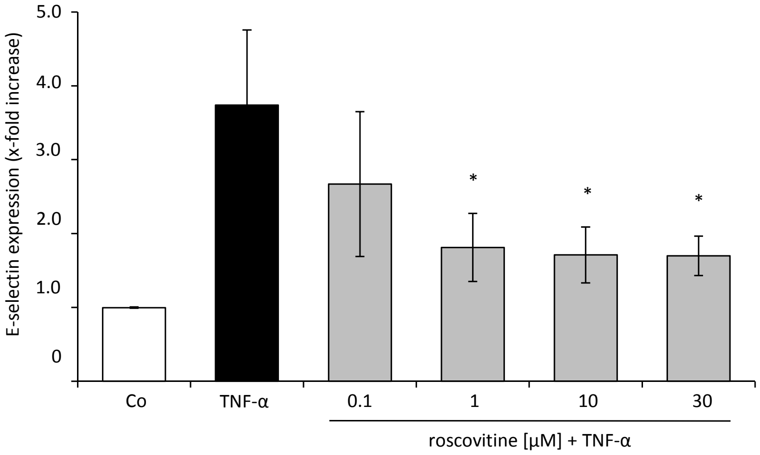

Figure III-5 The Expression of endothelial adhesion molecules is decreased by roscovitine.
HUVECs were cultured in either medium alone (Co) or in medium containing TNF-α (10 ng/ml) with or without pre-treatment (30 min) of roscovitine at various concentration (0.1 - 30 µM). The influence of roscovitine on TNF-α-induced CAM and selectin expression was measured by flow cytometric analysis. ICAM-1 and VCAM-1 expression were determined 24 h after TNF-α treatment, E-Selectin expression after 6 h. Results are shown as bar graphs showing on the y-axes the x-fold increase in expression of the respective cell adhesion molecule. (n = 3 independent experiments; mean ± SEM. *, $p<0.05$, compared with TNF-α-treated cells).

1.2.2.2 Roscovitine reduces the mRNA level of ICAM-1

To investigate whether roscovitine reduces the level of surface expression of endothelial adhesion molecules by inhibiting their transcription, mRNA level of ICAM-1 were determined by real-time PCR. A strong induction of ICAM-1 mRNA expression in TNF-α-exposed cells compared to untreated cells was observed, which could be significantly inhibited by pre-incubation with roscovitine in a concentration-dependent manner. Treatment of HUVECs with roscovitine only did not influence the basal-level of mRNA expression of ICAM-1 (Figure III-6).

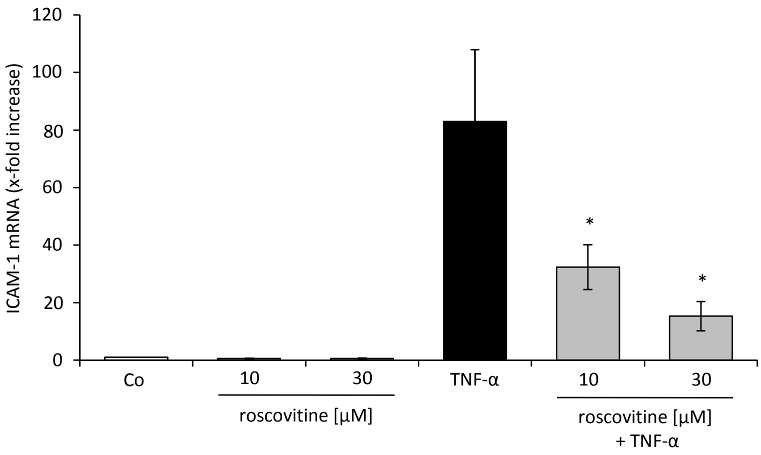

Figure III-6 Concentration-dependent inhibition of ICAM-1 mRNA expression by roscovitine.
Cells were treated as indicates and mRNA levels of ICAM-1 were analyzed. TNF-α treatment strongly increases mRNA levels, which are significantly reduced by pre-treatment with roscovitine for 30 min. Co was defined as 1. (n = 3 independent experiments; mean ± SEM. *, p<0.05, compared with TNF-α treated cells)

2 EFFECTS OF ROSCOVITINE ON THE NF-κB PATHWAY

2.1 CYTOTOXICITY OF ROSCOVITINE ON ENDOTHELIAL CELLS

To initially exclude that the shown effects are originated by roscovitine-induced apoptosis, DNA fragmentation according to the Nicoletti method[79] was measured, showing that roscovitine is well-tolerated by HUVECs in a range of 3 µM to 20 µM at the indicated times. Only at a concentration of 30 µM, roscovitine slightly induces apoptosis in HUVECs (Figure III-7).

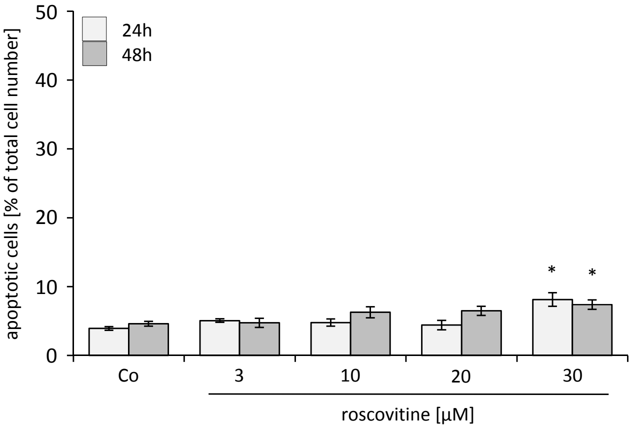

Figure III-7 Roscovitine does not induce apoptosis at concentrations up to 20 µM.
Confluent HUVECs were left untreated (Co) or were treated with increasing concentrations of roscovitine (3 µM - 30 µM) for 24 and 48 h. Afterwards apoptosis was determined according to the Nicoletti method. The sub-G1 population, obtained by flow cytometric measurement, is expressed as apoptotic cells in percent of the total cell number. (n = 3 independent experiments; mean ± SEM. *, p<0.05, compared with control cells)

2.2 ROSCOVITINE REDUCES TNF-α-EVOKED NF-κB PROMOTER ACTIVITY

NF-κB is the major transcription factor involved in the expression of CAMs. Therefore, we investigated whether roscovitine exerts its effects on ICAM-1 expression by affecting NF-κB promoter activity in a dual-luciferase™ reporter gene assay. Roscovitine concentration-dependently inhibited TNF-α-induced NF-κB promoter activity down to 20% residual activity (Figure III-8). Thus, roscovitine might reduce ICAM-1 mRNA level by interfering with NF-κB dependent gene expression.

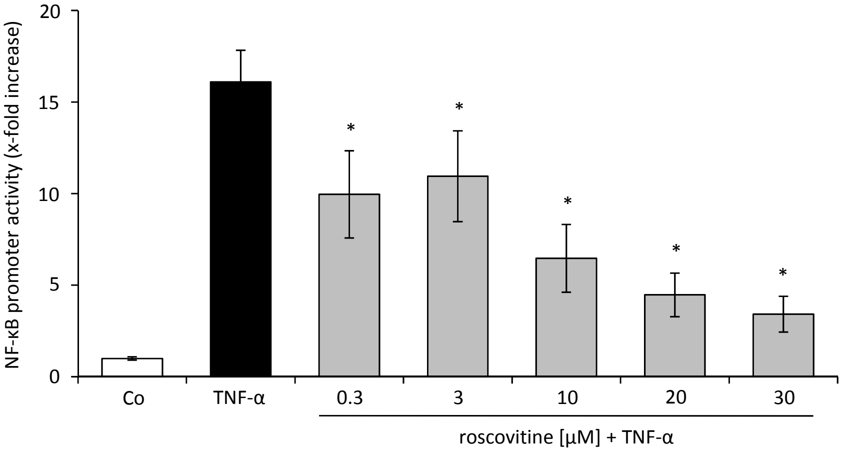

Figure III-8 NF-κB-dependent gene expression is inhibited by roscovitine in TNF-α-activated HUVECs. Confluent HUVECs were co-transfected with a reporter vector (firefly luciferase) and a control vector (*renilla* luciferase). 24 h after transfection, HUVECs were treated with various concentrations of roscovitine (0.3 µM - 30 µM) 30 min before TNF-α (6 h) or just treated with TNF-α for 6 h. Control cells were left untreated (Co). Afterwards, cells were lyzed and luciferase activity was measured. (n = 3 independent experiments; mean ± SEM. *, $p<0.05$, compared with TNF-α-treated cells)

2.3 ROSCOVITINE DOES NOT ALTER TNF-α-INDUCED NF-κB DNA-BINDING CAPACITY

Since NF-κB-dependent gene expression is inhibited by roscovitine, we investigated whether roscovitine affects the binding capacity of NF-κB to its DNA recognition site by electrophoretic mobility shift assay. Treatment with TNF-α increased NF-κB binding to its target sequence at the indicated times (Figure III-9). However, pre-treatment with roscovitine had no impact on this TNF-α-induced increase of DNA-binding of NF-κB (Figure III-9).

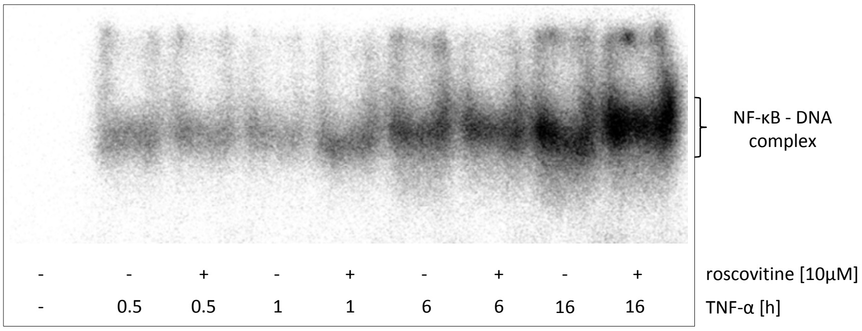
NF-κB - DNA complex
- - + - + - + - + roscovitine [10µM]
- 0.5 0.5 1 1 6 6 16 16 TNF-α [h]

Figure III-9 Roscovitine has no impact on the NF-κB DNA-binding capacity.
NF-κB DNA-binding capacity was determined by electrophoretic mobility shift assay (EMSA). Nuclear cell extracts were isolated from HUVECs that were either pre-treated with roscovitine for 30 min or left untreated prior to TNF-α (10 ng/ml) exposure for the indicated times. Control cells were left untreated. One representative image (out of three) is shown.

2.4 ROSCOVITINE HAS NO INFLUENCE ON THE TNF-*α*-INDUCED TRANSLOCATION OF p65

Further, we analyzed the translocation of p65, a subunit of NF-κB into the nucleus. NF-κB is usually localized in the cytosol (Figure III-10, Co) but translocates into the nucleus after it is released from its inhibitor IκBα. Our confocal analysis shows that TNF-α promotes the translocation of NF-κB into the nucleus (Figure III-10, TNF-α). This TNF-α-induced translocation was not inhibited by pre-treatment of the cells with roscovitine (Figure III-10, roscovitine + TNF-α). Cells that were treated with roscovitine only are comparable with control cells concerning the localization of p65 in the cytosol (Figure III-10, roscovitine 30 min).

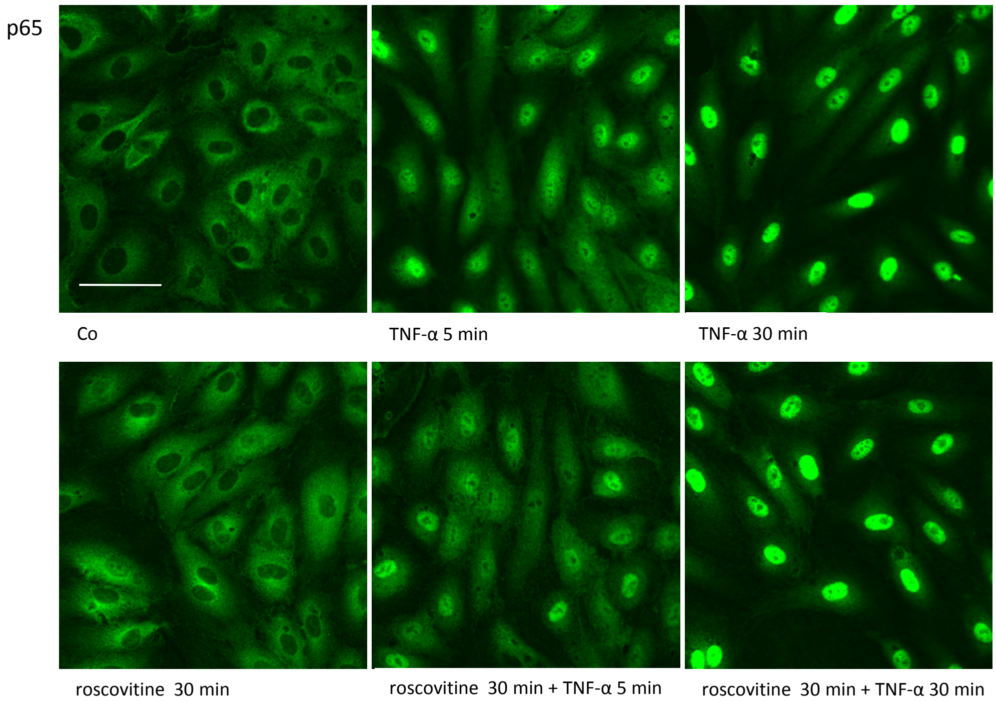
p65
Co
TNF-α 5 min
TNF-α 30 min
roscovitine 30 min
roscovitine 30 min + TNF-α 5 min
roscovitine 30 min + TNF-α 30 min

Figure III-10 Roscovitine does not interfere with TNF-α-induced nuclear translocation of p65 in HUVECs. p65 translocation upon treatment of cells with TNF-α alone, in combination with roscovitine or with roscovitine alone for the indicated times was assessed by immunocytochemistry. HUVECs were seeded, cultured until confluency was reached and left untreated or pretreated with roscovitine (10 µM) for 30min before TNF-α-treatment (10 ng/ml) for 5 and 30 min. Control cells were left untreated. p65 expression and cellular localization were detected by CLSM analysis. The results from one representative experiment out of three independently performed are shown. The white bar indicated in the upper panel corresponds to 20 µm.

2.5 ROSCOVITINE HAS NO EFFECTS ON IKK AND IκBα

As roscovitine neither interferes with TNF-α-induced translocation of NF-κB into the nucleus nor its binding to its DNA recognition site, we started to investigate effects of roscovitine on upstream kinases in the NF-κB pathway.

The activity of IKK was determined by Western blot analysis of the respective phosphorylation site (IKK: Ser$^{176/180}$) and by an *in vitro* kinase activity assay. Furthermore, total protein level of IκBα was assessed to quantify its degradation in response to TNF-α treatment.[30] TNF-α rapidly induces IKK phosphorylation which is not inhibited by roscovitine (Figure III-11, A). Also, degradation of IκBα can be observed rapidly, as IκBα can be barely detected after 15 min of treatment with TNF-α. After about 30 min incubation, IκBα is slowly recovered. 30 min pre-incubation of the cells with roscovitine before TNF-α did not affect IκBα degradation, but delayed the regeneration of IκB in comparison to TNF-α-treated cells (Figure III-11, B).

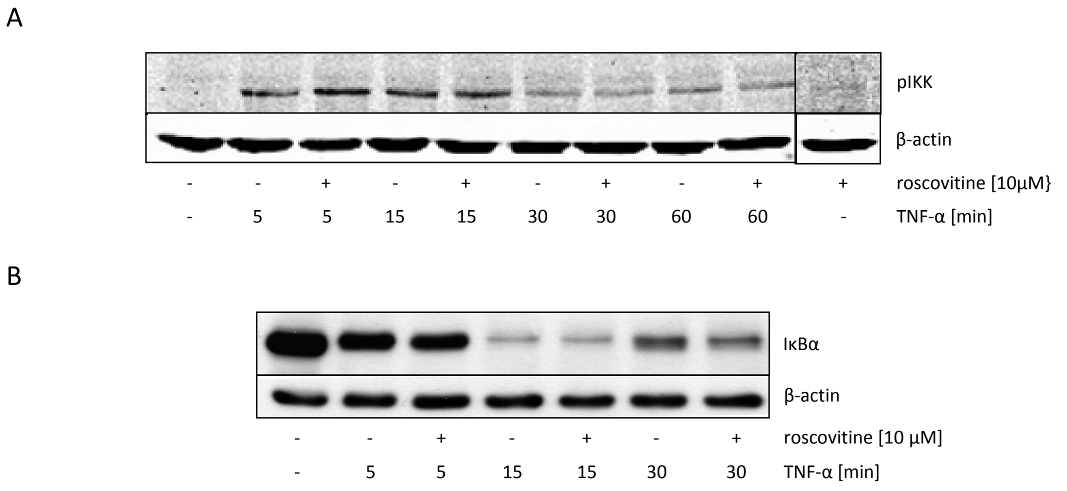
A
pIKK
β-actin
- - + - + - + - + + roscovitine [10µM}
- 5 5 15 15 30 30 60 60 - TNF-α [min]
B
IκBα
β-actin
- - + - + - + roscovitine [10 µM]
- 5 5 15 15 30 30 TNF-α [min]

Figure III-11 Roscovitine does not inhibit the TNF-α-evoked IKK phosphorylation and IκBα degradation.
Confluent HUVECs were pre-treated with roscovitine (10 µM) for 30 min before treatment with TNF-α (10 ng/ml) or were treated with TNF-α alone. All cells were additionally treated with calyculin in a concentration of 1 nM (in order to inhibit dephosphorylation of p-IKK). Phosphorylation-state of IKK and degradation of IκBα were analyzed by Western blot using the respective antibodies. The result from one representative experiment out of three independently performed is shown.

Furthermore, an IKKβ *in vitro* activity assay was performed to investigate whether IKKβ kinase activity is directly inhibited by roscovitine. The well-established kinase inhibitor staurosporine, which is known to inhibit IKKβ activity by binding to the ATP site, caused reduction of IKKβ phosphorylation, whereas roscovitine did not reduce activity of IKKβ (Figure III-12). Therefore, roscovitine seems not to interfere with signaling pathways that activate IKKβ.

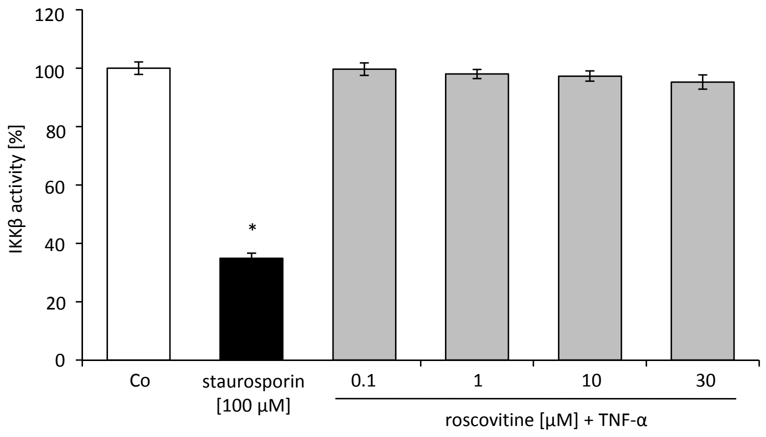

Figure III-12 Roscovitine does not directly inhibit the activity of IKK.
In the IKKβ kinase activity *in vitro* assay (HT-Scan® IKKβ kinase assay), increasing concentrations of roscovitine (0.1 µM – 30 µM) were tested. 100 µM staurosporin served as positive control and 1x kinase buffer was used as blind value (Co). The figure shows three independent experiments, control (Co) was defined as 100% (mean ± SEM. *, $p<0.05$, compared with 1x kinase buffer [Co])

3 THE INFLUENCE OF ROSCOVITINE ON KINASES

To identify kinases that are inhibited by roscovitine in TNF-α-treated HUVECs and might therewith be involved in NF-κB inhibiting action of roscovitine, a kinome array and a CDK activity assay were performed.

3.1 PEPCHIP ASSAY / KINASE PANEL

The kinome array (PepChip) presents a powerful tool to investigate the overall impact of a kinase inhibitor like roscovitine on specific kinases in a cellular context and to identify signaling networks that are affected by the tested agent in particular. Again, HUVECs were pre-treated for 30 min with roscovitine or were left untreated before cells were exposed to TNF-α.

The array revealed that the kinases CDK5, cAMP-dependent protein kinase (PKA) and ribosomal S6 kinase (RS6K) were reduced most in their activity in roscovitine/TNF-α-treated cells compared to control cells (Table 10). The activities of kinases that were affected by roscovitine were expressed as residual activity, whereas the kinase activities in TNF-α-treated cells were defined as 1.

Table 10 Kinome array data showing kinases that were reduced most in their activity in roscovitine/TNF-α-treated HUVECs compared to TNF-α-treated HUVECs. R.A. = residual activity.

Peptide	Kinase	R.A.
KSEPISPPRDR	CDK5	0.39
KKKKGSLDSDN	PKA	0.17
DDRHDSGLDSM	RS6K	0.56

3.2 EC50 PROFILING OF ROSCOVITINE

Since roscovitine is per definition a CDK inhibitor and the kinome panel of the PepChip did not included all CDKs, an additional CDK activity assay, including the indicated CDKs in Table 10, was performed (ProQinase).

This CDK activity assay revealed CDK2, CDK7 and CDK9 to be inhibited by roscovitine the strongest, as judged by EC50 values of roscovitine towards the indicated CDKs (Table 11).

Table 11 ***In vitro*** **CDK activity assay. The EC50 values of roscovitine towards the indicated CDKs are displayed.**

CDKs	roscovitine EC50 [µM]
CDK1	4.472
CDK2	0.441
CDK4	9.173
CDK7	0.916
CDK9	1.431

4 INVOLVEMENT OF PKA, RS6K AND CDKs ON THE EXPRESSION OF ICAM-1

The results gained in both kinase assays (PepChip and ProQinase) indicate that roscovitine potentially inhibits PKA, RS6K, CDK5, CDK2, CDK7 and CDK9. However, literature does not state an involvement of these kinases in ICAM-1 expression on endothelial cells. Therefore, we employed specific small molecule inhibitors and si-/sh-RNA targeting the respective kinase in HUVECs and determined the cell surface expression of ICAM-1 by flow cytometry analysis.

4.1 INHIBITION OF PKA OR RS6K HAS NO INFLUENCE OF ICAM-1 EXPRESSION

To specifically inhibit the activity of PKA, the peptide inhibitor PKA inhibitor fragment (6-22) amide and the cAMP-analog cAMPS-RP were used in this experiment. The activity of RS6K was blocked by rapamycin, a small molecule that inhibits mTOR and thereby interferes with RS6K activation.[83]

Our data show that ICAM-1 expression is not affected by the inhibition of PKA (Figure III-13, A), whereas the treatment of TNF-α-activated cell with rapamycin slightly reduced the ICAM-1 expression (Figure III-13, B). However, we cannot exclude that this effect is rather unspecific due to the impact of mTOR on overall protein biosynthesis.[84] Considering the fact that roscovitine had no effect on RS6K phosphorylation site, involved in its activation (Figure III-13, C), it seems not very likely that roscovitine specifically reduces ICAM-1 expression by inhibiting RS6K activation.

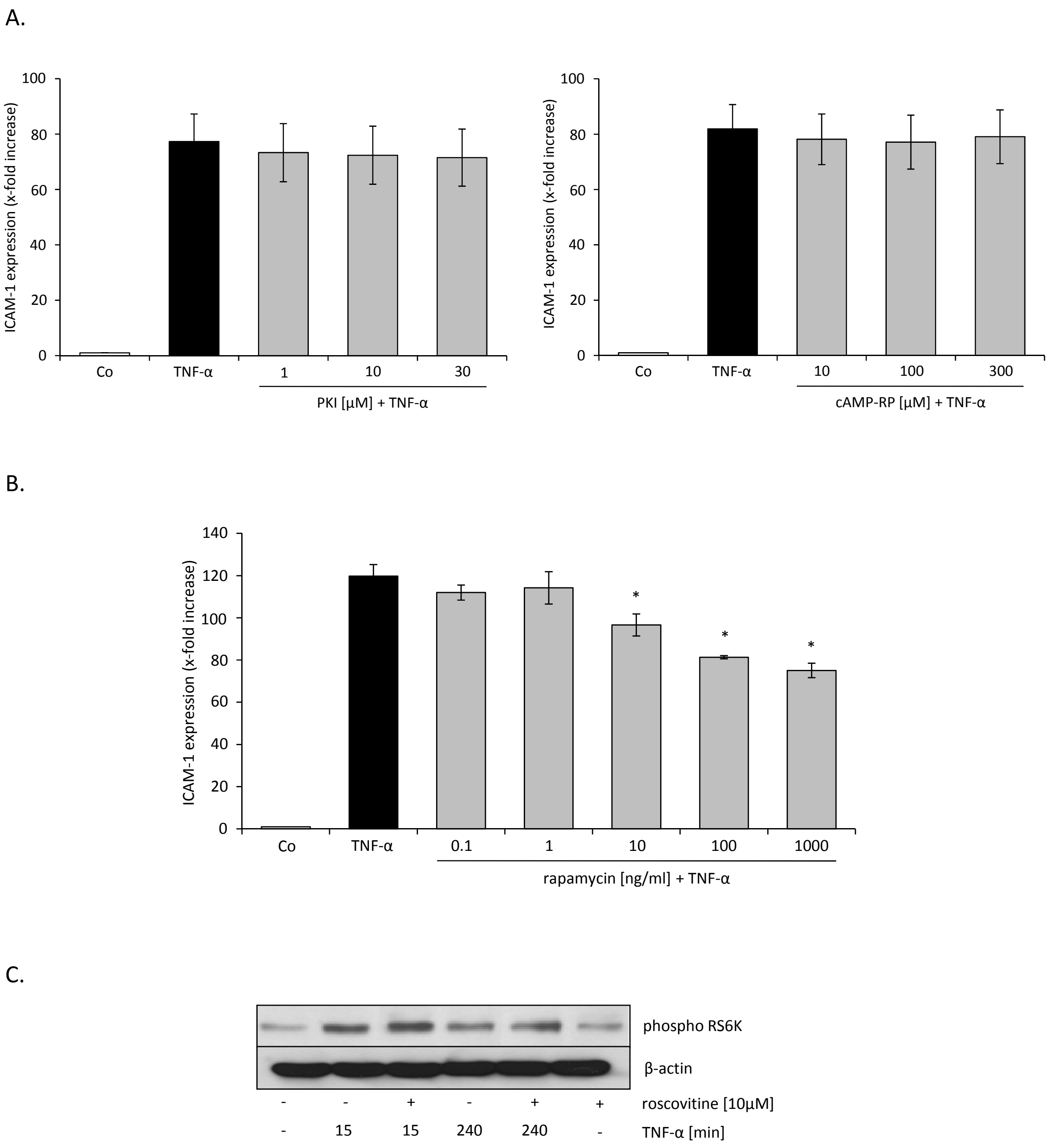

Figure III-13 Inhibition of PKA and RS6K kinase has no impact on TNF-α-induced ICAM-1 expression.

A. HUVECs were left untreated or treated with different concentrations of the specific PKA inhibitors cAMP-RP or PKI 30 min before TNF-α-treatment. Control cells were left untreated. Afterwards, the expression of ICAM-1 was determined by flow cytometric analysis. Co was defined as 1 (n = 3 independent experiments; mean ± SEM. *, p<0.05, compared with TNF-α treated cells)

B. HUVECs were left untreated or treated with different concentration of rapamycin 30 min before TNF-α. Control cells were left untreated. Afterwards the expression of ICAM-1 was determined by flow cytometric analysis. Co was defined as 1 (n = 3 independent experiments; mean ± SEM. *, p<0.05, compared with TNF-α-treated cells).

C. Western blot analysis of the two phosphorylation sites Thr^{421}/Ser^{424} of the RS6K. HUVECs were seeded, pre-treated with 10 µM roscovitine for 30 min before stimulation with TNF-α. After the indicated times, cells were harvested and Western blot analysis was performed. The result from one representative experiment out of three independently performed are shown.

4.2 THE IMPACT OF CDKs ON THE EXPRESSION OF ICAM-1

To analyze the impact of CDKs on the TNF-α-induced ICAM-1 expression, CDK2, CDK5, CDK7 and CDK9 were silenced and the ICAM-1 expression was determined. Short interference (si-) RNA (CDK2, CDK7) or short hairpin (sh-) RNA (CDK5, CDK9) targeting the respective mRNA was used. Non-targeting RNA was used as a control. Downregulation of neither CDK2 nor CDK7 seemed to affect the TNF-α-induced ICAM-1 expression (Figure III-14, A). The efficiency of the downregulation of CDK2 as well as CDK7 was analyzed by Western blot analysis (Figure III-14, B).

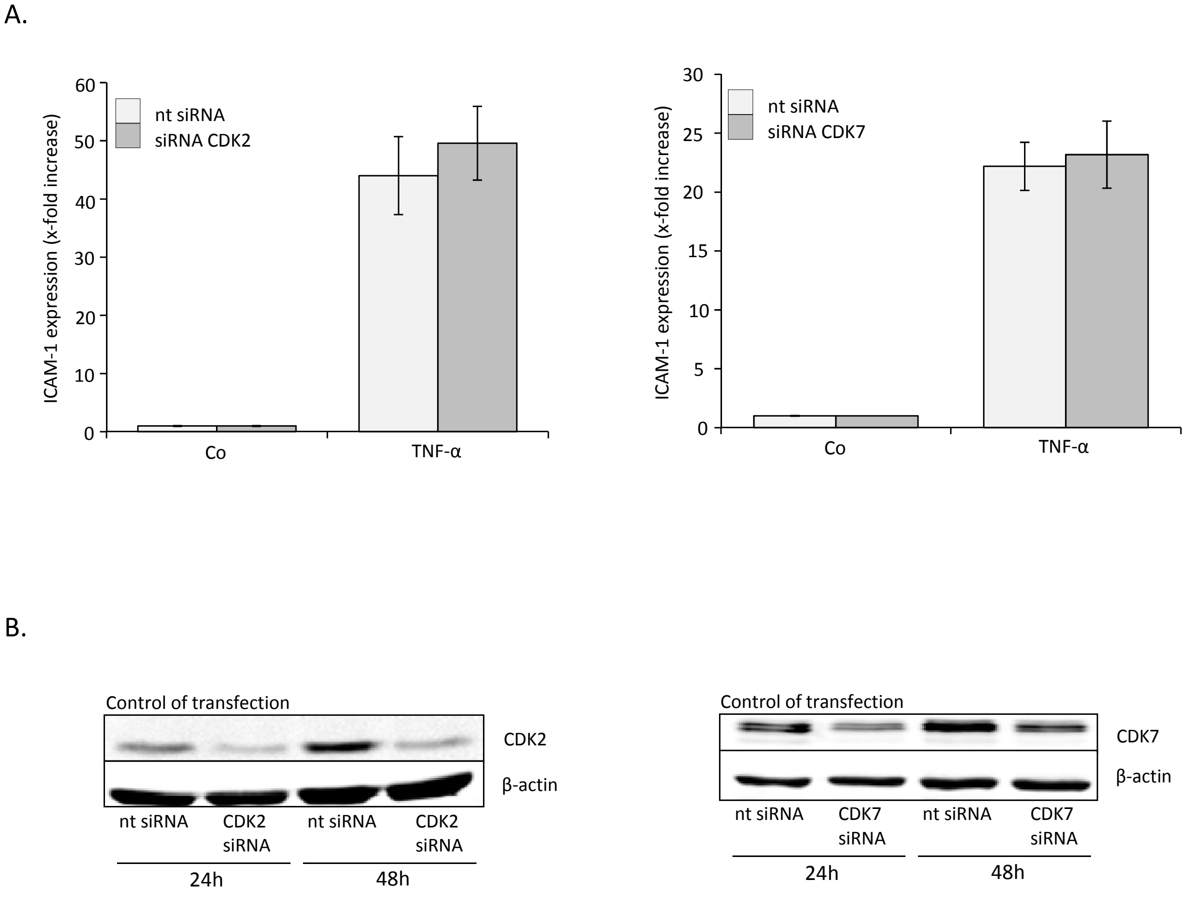

Figure III-14 The impact of CDK2 and CDK7 on the TNF-α-induced ICAM-1 expression in HUVECs.
A. The expression of the respective CDK was knocked down via siRNA towards the mRNA. 24 h after transfection with siRNA HUVECs were treated with TNF-α (10 ng/ml) for further 24h and ICAM-1 expression was measured using flow cytometric analysis. nt-siRNA transfected cells served as control (Co). Co was defined as 1 (n = 3 independent experiments; mean ± SEM. *, $p<0.05$ compared with control).
B. The performed Western blot analysis shows the efficiency of the downregulation of CDK2 and CDK7.

In contrast, knockdown of CDK5 and CDK9, respectively, reduced TNF-α-induced ICAM-1 expression compared to cells transfected with nt-siRNA. CDK5 knockdown leads to 60% reduction in ICAM-1 expression, knockdown of CDK9 reduced ICAM-1 expression by 70% (Figure III-15, A). The efficiency of the downregulation of CDK5 as well as CDK9 is shown in Figure III-15, B. The significant inhibition of CDK5 and CDK9 by roscovitine in the kinase assays and the impressive impact of CDK5 and CDK9 down-regulation on TNF-α-induced ICAM-1 expression, indicates that these two kinases are targets of roscovitine in activated HUVECs and may therefore be involved in the roscovitine-mediated inhibition of ICAM-1 expression.

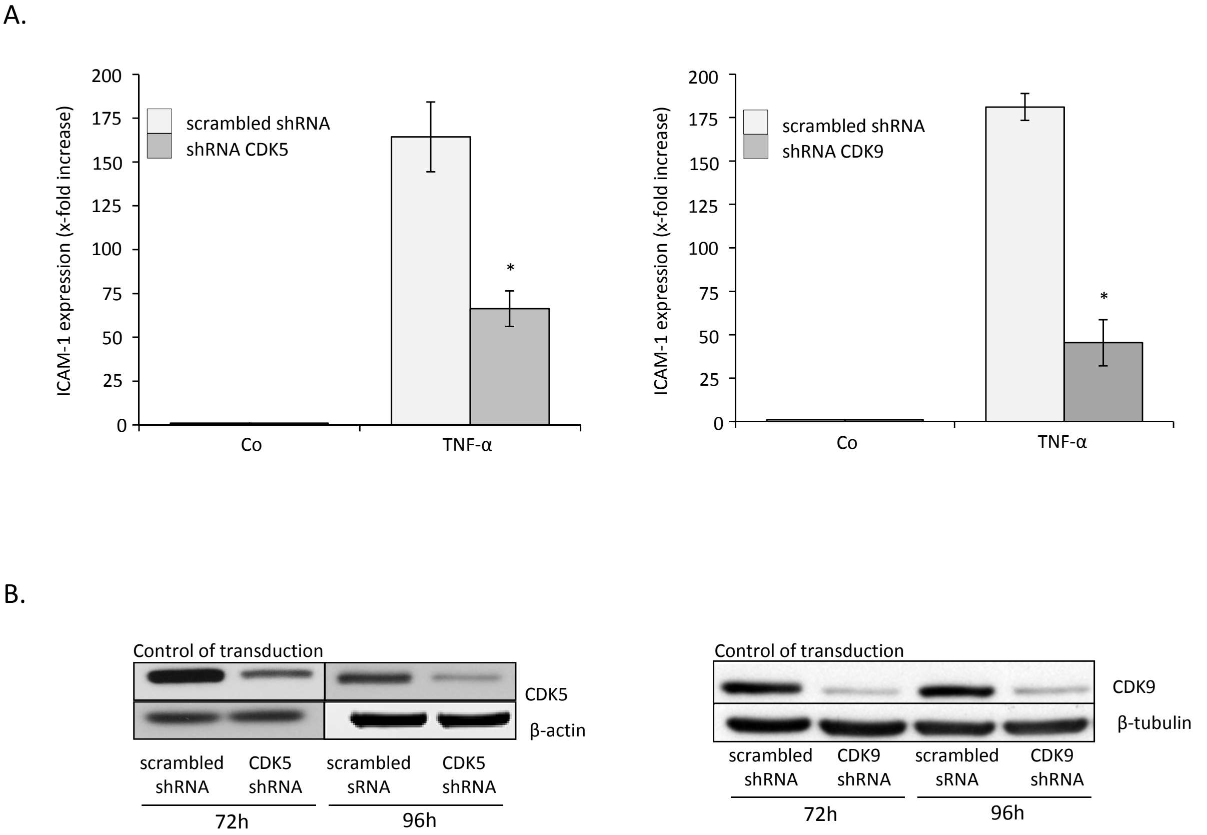

Figure III-15 The impact of CDK5 and CDK9 on the TNF-α-induced ICAM-1 expression in HUVECs.
A. The gene expression of the respective CDK was knocked down via target shRNA using adenoviral gene transfer. After gene transfer, HUVECs were directly seeded and cultivated for 72 h before TNF-α. 24 h after TNF-α treatment ICAM-1 expression was measured using flow cytometric analysis. Scrambled shRNA treated cells served as control (Co). Co was defined as 1 (n = 3 independent experiments; ± SEM. *, $p<0.05$ compared with control).
B. The performed Western blot analysis shows the efficiency of the downregulation of CDK5 as well as CDK9.

DISCUSSION

IV DISCUSSION

1 INFLAMMATION AND CDK INHIBITORS

1.1 IN GENERAL

Although CDK inhibitors were initially known as anti-cancer drugs, in the last years they have emerged as potential anti-inflammatory compounds, which enhance the resolution of inflammation. Resolution of inflammation manifests itself by apoptosis of inflammatory cells, subsequent clearance by macrophages and restoring of the tissue homeostasis. In this context, CDK inhibitors, such as roscovitine, have been found to promote the apoptosis of immune cells, although immune cells like neutrophils and eosinophils are terminally differentiated and do not undergo cell cycle progression. The induction of apoptosis by CDK inhibitors seems to be mediated by the modulation of Bcl-2 family members and to be executed in a caspase-dependent manner.[85] A panel of CDK inhibitor drugs has been shown to promote neutrophil apoptosis in a concentration- and time-dependent manner and the CDK inhibitor roscovitine overrides the anti-apoptotic effects of powerful survival factors, such as LPS and granulocyte macrophage-colony stimulating factor (GM-CSF). Apoptosis of neutrophils ensures that toxic neutrophil granule contents are securely packed in apoptotic bodies and expedites phagocytosis by professional phagocytes such as macrophages.[86] CDK inhibitors as anti-inflammatory pro-resolution drugs were established in some *in vivo* models for eosinophil- and neutrophil-driven inflammatory diseases such as glomerulonephritis,[87-89] carrageenan-induced acute pleurisy,[90] bleomycin-induced lung inflammation[90] and passively induced arthritis.[91]

In the current study, we could show for the first time that roscovitine effectively inhibits both *in vivo* and *in vitro* leukocyte-endothelial cell interaction, which is essential in inflammatory processes to permit the leukocyte emigration from the blood into the inflamed tissue. The inhibition of this important inflammatory step presents a new anti-inflammatory mode of action of CDK inhibitors.

1.2 THE IMPACT OF ROSCOVITINE ON LEUKOCYTE-ENDOTHELIUM INTERACTION *IN VIVO* AND *IN VITRO*

Although leukocyte infiltration into sites of infection is an important part of the host defense, this infiltration, when excessive, can cause free radical-, enzymatic, or cytokine-mediated tissue damage.[92] To prevent tissue damage, the leukocyte infiltration has to be stopped and this can be achieved by the inhibition of the interaction between leukocytes and endothelium. There is a hint that roscovitine reduces leukocyte infiltration established in an *in vivo* model of ischemia-reperfusion in rat livers.[93] However, the question remains how roscovitine attenuates the infiltration of leukocytes.

The focus of this study was on the anti-inflammatory role of roscovitine in regard to leukocyte-endothelium interaction and therefore we initially analyzed the key steps of the leukocyte extravasation in postcapillary venules of cremaster muscles of TNF-α/roscovitine-treated mice using intravital microcopy. In this experiment, we could observe that TNF-α-induced leukocyte adherence on the endothelium and TNF-α-induced transmigration of leukocytes were strongly inhibited by roscovitine. Further, an *in vitro* assay in HUVECs showed that the number of adherent leukocytes on TNF-α-activated endothelial cells is reduced by roscovitine. These results revealed that the transmigration of the leukocytes through the endothelium and the leukocytes adhesion on the endothelium is affected by roscovitine.

1.2.1 Roscovitine has no direct influence on the leukocytes

To exclude that these effects of roscovitine are caused by induction of apoptosis in leukocytes as it has been described in several publications[90] we determined the systemic leukocyte count during our *in vivo* experiment with the result of consistent leukocyte count in roscovitine- and drug vehicle-treated mice. Therefore, apoptosis of leukocytes caused by roscovitine can be excluded.

Of further interest was the influence of roscovitine on the activation of leukocytes which is induced during inflammation and accompanies increased integrin expression on the surface of leukocytes, namely VLA-a (α4β1), Mac-1 (CD11b/CD18; αMβ2) and LFA-1 (CD11a/CD18; αLβ2).[92] Activated leukocytes, arrived in the inflamed tissue, sequester enzymes, cytokines and free radicals (ROS) such as NO.[92] Our experiments on isolated leukocytes, investigating the influence of roscovitine on their activation, showed that roscovitine did not affect their ROS release but slightly reduced their CD11b expression. We proposed that the effect of roscovitine on CD11b expression does not sufficiently explain the strong effect on leukocyte adhesion. Thus we proceeded with the analysis on endothelial cells as major target for roscovitine in inflammatory processes.

1.2.2 Reduction of endothelial cell adhesion molecule levels by roscovitine

Endothelial cell activation is accompanied by the upregulation of diverse adhesion molecules on the luminal site of endothelial cells, induced by cytokines (e.g. TNF-α) or other pro-inflammatory stimuli (e.g. LPS).[92] Endothelial adhesion molecules bind to leukocyte integrins and mediate the sequences of events during leukocyte extravasation. Particularly the endothelial adhesion molecules ICAM-1, VCAM-1 and E-selectin are hereby involved.

In this context, we proposed that roscovitine inhibits the leukocyte transmigration and leukocyte adherence by affecting the expression of diverse endothelial adhesion molecules. *Dey et al*. recently showed in lung carcinoma cells (A549= carcinomic human alveolar basal epithelial cells and H1299 = non-small cell lung carcinoma cell line) that roscovitine inhibits the expression of ICAM-1.[71] Therefore, we investigated roscovitine in regard to its influence on the ICAM-1 and additionaly on the E-selectin and VCAM-1 surface expression as well as on the ICAM-1 mRNA levels in TNF-α-activated endothelial cells. The results of these experiments, showing inhibition of both the TNF-α-induced surface expression and ICAM-1 mRNA levels, indicate that roscovitine affects the TNF-α-induced ICAM-1 expression, whereas apoptosis in HUVECs could be excluded by Nicoletti assay.[79]

Linking the present findings with the previous results from our *in vivo* and *in vitro* experiments, it can be assumed that a reduced number of adhesion molecules on the activated endothelium abolishes leukocyte adhesion, transmigration and subsequent infiltration as indicated by the findings of two groups: *Bullard et al.* could show that the basal adhesion of monocytes to ICAM-1 deficient endothelial cells was significantly lesser than to wild-type endothelial cells (MAEC).[94] *Kevil et al.* revealed the relevance of ICAM-1 in an *in vivo* model of collagen-induced arthritis. They describe that ICAM-1 deficient mice show a significant reduction in the incidence of arthritis compared with wildtype (WT)-mice.[95] These two studies indicate that an attenuated ICAM-1 expression leads to decreased emigration of inflammatory cells, which is beneficial in inflammatory diseases.

2 IMPACT OF ROSCOVITINE ON THE NF-κB SIGNALING

Based on this novel role of roscovitine, the underlying signaling mechanisms were of interest. TNF-α, one of the major initiators of inflammatory processes, mainly exerts its effects via activation of NF-κB signaling. Moreover, the genes of endothelial adhesion molecules have recognition sites for the transcription factor NF-κB, indicating that their gene expression is NF-κB-dependent.

Interestingly, *Dey et al.* have shown in lung carcinoma cells (A549, H1299) that roscovitine is able to inhibit the TNF-α-induced NF-κB pathway by targeting the IKK kinase activity as well as phosphorylation and degradation of IκBα.[71] Furthermore, in mouse macrophages, it was shown that roscovitine attenuated LPS-induced phosphorylation of IKKβ and IκBα.[96] With this background, we postulated that roscovitine targets the NF-κB signaling in endothelial cell, as well.

First evidence was obtained in a NF-κB reporter gene assay. In this assay we could clearly show that transcription activation by NF-κB is inhibited by roscovitine in TNF-α-treated HUVECs. However, the findings of *Dey et al.* and *Du et al.* could not be confirmed in endothelial cells. In HUVECs, roscovitine did not target events upstream the NF-κB-dependent gene expression, suggesting that the transcription is inhibited by roscovitine. Of further relevance for the TNF-α-induced ICAM-1 inhibition by roscovitine might be other signaling pathways including other kinases.

3 ROSCOVITINE INHIBITS RS6K, PKA, AND DIVERSE CDKs

Aiming to identify potential signaling pathways responsible for the anti-inflammatory action of roscovitine, we screened kinases using a kinome array (PepChip) to detect which kinases are inhibited by roscovitine in TNF-α-treated HUVECs. In addition, a CDK activity assay was performed to achieve information about the influence of roscovitine on CDKs not included in the kinome array. By these two approaches we could narrow down the kinases affected by roscovitine to six candidates: R6SK, PKA, CDK2, CDK5, CDK7 and CDK9. This identified kinase-profiling of roscovitine largely accords with previous performed kinase profiling panels by which about 151 kinases were tested, and with data, achieved by affinity chromatography on immobilized roscovitine.[97-98] Further studies revealed that beside the previously mentioned CDKs, ERK1, ERK2 and casein kinase 1 (CK1) were also described to be inhibited by roscovitine, however in HUVECs, roscovitine neither alters the activation state of ERK1/2[99] nor the TNF-α-induced ICAM-1 expression is reduced by specific CK1 inhibitors (data not shown) allowing us to conclude that CK1 is not involved in the roscovitine-evoked reduction of the ICAM-1 expression.

4 IMPACT OF THE IDENTIFIED KINASES ON THE TNF-α-INDUCED ICAM-1 EXPRESSION

4.1 PKA

The impact of PKA on TNF-α-induced ICAM-1 expression was investigated, according to the findings of *Brasier et al.* which shown that the phosphorylation of the NF-κB subunit p65 on Ser^{276} is necessary for the transcription of some genes whose expression is NF-κB-dependent.[100] Because ICAM-1 gene expression is NF-κB-dependent and Ser^{276} is phosphorylated by PKA, we proposed that PKA is responsible for the reduction of the TNF-α-induced ICAM-1 expression by roscovitine. Contrary to this proposal, inhibition of PKA by specific PKA inhibitors did not reduced the TNF-α-induced ICAM-1 expression in HUVECs. This reveals that PKA has no impact in the reduction of the TNF-α-induced ICAM-1 expression concluding that PKA is no target of roscovitine.

4.2 CDK5 AND RS6K

CDK5 is known as an important player in the regulation of neuronal architecture and migration, and in the recent years increasing evidences emerged for its extra-neuronal effects. CDK5 is described to be involved in apoptosis, transcription, differentiation and endocytosis.[51] However, little is known about the role of CDK5 in inflammatory processes. Our study reveals that the absence of CDK5 results in a strong repression of the TNF-α-induced ICAM-1 expression.

RS6K is a key regulator of mRNA translation as it catalyzes ribosomal protein S6 phosphorylation to initiate the selective translation of mRNA. Thus, inactive RS6K cannot initiate the translation which results in incomplete gene expression. Activation of RS6K involves the phosphorylation of multiple Ser/Thr residues, including the proline-directed sites (Ser^{411} ,Ser^{418} ,Thr^{421} and Ser^{424}) in the auto-inhibitory domain near the C-terminus. Phosphorylation of Thr^{389}, which is rapamycin-sensitive and is mediated by mTOR, is also a crucial event in RS6K activation. Interestingly, we could show that rapamycin-mediated inhibition of RS6K slightly reduces the TNF-α-induced ICAM-1 expression, but Western blot analysis revealed that the important phorphorylation sites Thr^{421} and Ser^{424} for RS6K activation remain unaffected by roscovitine in TNF-α-treated HUVECs. This result might be explained by observations of *Hou et al.* in neurons and COS-7 cells. They have found that CDK5/p35 physically associates with RS6K and catalyzes RS6K phoshphorylation at Ser^{411}. This phosphorylation site is critical for regulating RS6K catalytic activity through the control of Thr^{389}. CDK5 inhibition or depletion strongly inhibits RS6K phosphorylation on Ser^{411} and Thr^{389}, whereas Thr^{421} and Ser^{424} remain unaffected. According to these results, we hypothesized that roscovitine inhibits the TNF-α-induced ICAM-1 expression via CDK5 inhibition, leading to inhibition of RS6K and this, in turn, abolishes the translation of mRNA coding for ICAM-1.

This hypothesis could explain the attenuated ICAM-1 expression on the surface of endothelial cells but does not explain the results of the diminished ICAM-1 mRNA level and the NF-κB-dependent gene expression by roscovitine.

4.3 CDK9

Also CDK9 plays an essential role in the TNF-α-induced ICAM-1 expression, as shown by attenuated TNF-α-induced ICAM-1 expression in CDK9-silenced HUVECs. Therefore, we presumed that roscovitine cause its effects by abolishing of transcriptional elongation of ICAM-1 mRNA according to inhibition of CDK9, the catalytic subunit of pTEFb.[101-103]

Previous studies on multiple myeloma cells already demonstrated that roscovitine induces rapid deposphorylation of the carboxyl-terminal domain of the large subunit of RNA polymerase II.[69] This suggests that roscovitine might suppress the gene transcription via inhibition of CDK9, which, in turn, leads to the deactivation of pTEFb. In the following pTEFb does not phosphorylate the RNA-polymerase II and thus the transcriptional elongation fails.

5 CONCLUSION

Hitherto, CDK inhibitors have been considered to exert anti-inflammatory properties only by promoting apoptosis in inflammatory cells and thereby enhancing the clearing of inflammation.

In this study we present a novel mode of action of the CDK inhibitor roscovitine in the inflammatory process. It became manifest that roscovitine also protects against inflammation as it abolishes the leukocyte extravasation from the blood flow into the inflamed tissue.

For the first time, we could show that roscovitine inhibits the leukocyte adhesion and transmigration on the endothelium by the expression of endothelial adhesion molecules as a consequence of inhibition of CDK5 and CDK9.

In conclusion, this study highlights roscovitine as promising anti-inflammatory drug, which might reach clinical relevance for the treatment of inflammatory diseases.

SUMMARY

V SUMMARY

In the recent years, the CDK inhibitor roscovitine has emerged as an anti-inflammatory agent. Hitherto, its anti-inflammatory effect was ascribed to the promotion of apoptosis of inflammatory cells thus enhancing the resolution of inflammation.

This study shows for the first time that roscovitine directly affects the leukocyte-endothelial cell interaction, which reduces the extravasation of leukocytes in the inflamed tissue.

First and important evidence for an attenuated leukocyte emigration into inflamed tissue by roscovitine was gained in an *in vivo* cremaster model in which the leukocyte-endothelial cell interaction in postcapillary venules of TNF-α-treated mice was investigated using intravital microscopy. Both readout parameters, leukocyte adhesion and leukocyte transmigration, were reduced by roscovitine. These *in vivo* results were confirmed *in vitro* through *s*trongly diminished leukocyte adhesion on roscovitine-treated HUVECs. Marginal alterations of leukocyte activation markers (CD11b and oxidative burst) by roscovitine indicated that leukocytes are not the major target of roscovitine. Therefore, we focused our investigations on the activation of the endothelial markers E-selectin, ICAM-1 and VCAM-1. The expression of these markers is induced by pro-inflammatory stimuli (e.g. TNF-α) and is crucial to facilitate extravasation of leukocytes. In our studies, pre-treatment of HUVECs with roscovitine and subsequent treatment with TNF-α significantly reduced the surface expression of E-selectin, ICAM-1 and VCAM-1. Furthermore, mRNA levels of ICAM-1 were strongly decreased in this model and in cremaster muscles of roscovitine/TNF-α-treated mice compared to drug vehicle/TNF-α-treated mice.

To identify the underlying signaling mechanism, we first analyzed the impact of roscovitine on NF-κB signaling, which is the major pathway in TNF-α-triggered inflammation. Although NF-κB-dependent gene transcription is inhibited by roscovitine in a concentration-dependent manner, the cascade leading to the activation of NF-κB remains unaffected (Figure V-1), raising the question which roscovitine-targeted kinases might be responsible for the reduction of the endothelial activation markers. Therefore, a kinome array as well as a CDK activity assay was performed to identify kinases that are inhibited by roscovitine in TNF-α-treated HUVECs. Among the six identified kinases (PKA, RS6K, CDK2, CDK5, CDK7 and CDK9), CDK5 and CDK9 were considerably implicated in the TNF-α-induced ICAM-1 expression. Their respective absence in TNF-α-treated endothelial cells caused enormous reduction of the ICAM-1 expression. It is not yet clear how the roscovitine-evoked inhibition of CDK5 and CDK9 is linked with the diminished ICAM-1 expression and the attenuation of the NF-κB-dependent gene expression. We presume that the mRNA elongation during transcription is abolished by inactive pTEFb due to the inhibition of CDK9 (Figure V-1) and that CDK5 inhibition might lead to inactive RS6K and thus the translation of mRNA by the ribosomes fails.

Taken together, the CDK inhibitor roscovitine directly affects endothelial activation, regulating the transmigration of leukocytes in the inflamed tissue, by inhibition of CDK9 and CDK5 which leads to strongly diminished expression of endothelial adhesion molecules.

In conclusion, this study presents a novel mode of action underlying the anti-inflammatory effect of the CDK inhibitor roscovitine, which might be reach clinical relevance in the treatment of inflammatory diseases.

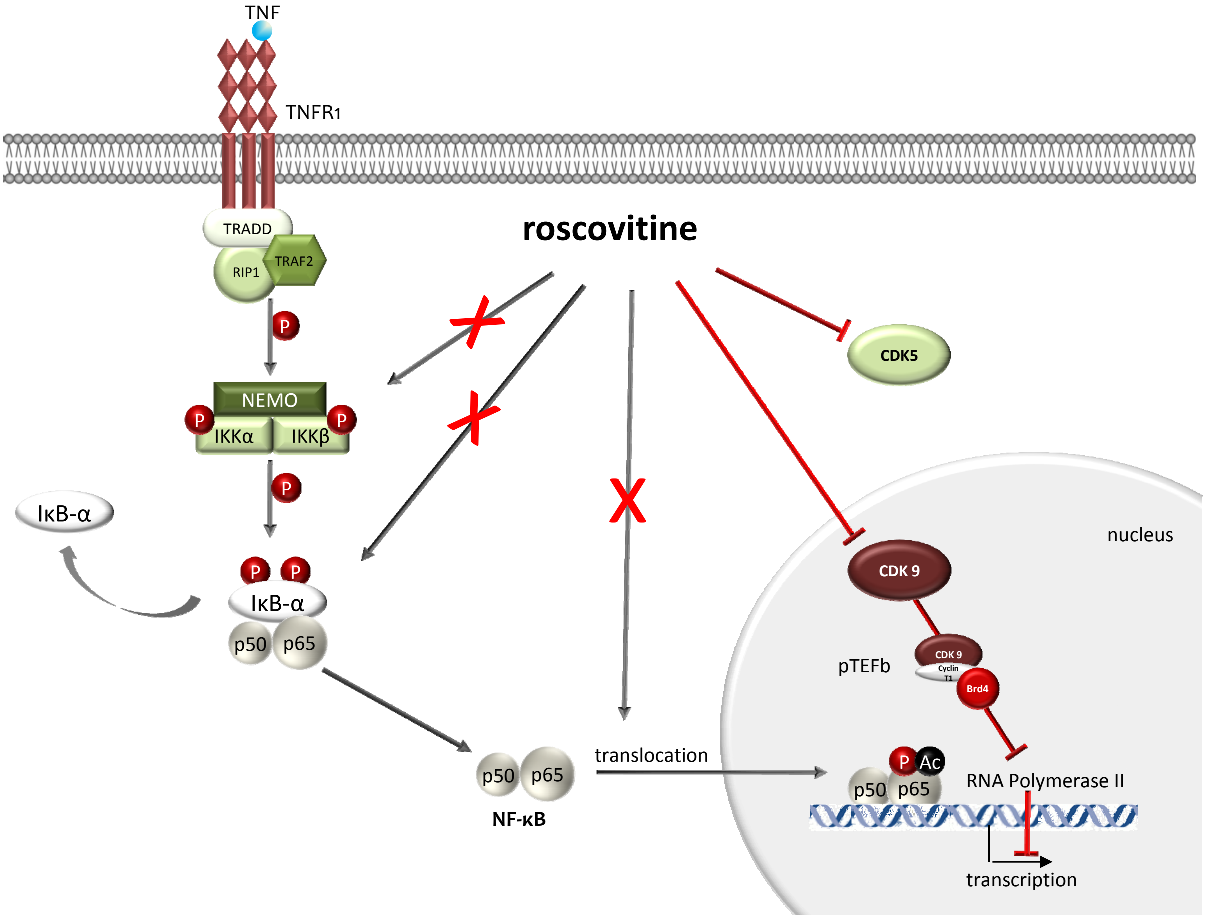
TNF
TNFR1
TRADD
TRAF2
RIP1
P
NEMO
IKKα
IKKβ
IκB-α
IκB-α
p50
p65
roscovitine
CDK5
nucleus
CDK 9
pTEFb
CDK 9
Cyclin T1
Brd4
translocation
p50
p65
NF-κB
P
Ac
RNA Polymerase II
transcription

Figure V-1 The effects of roscovitine on the inflammatory signaling in endothelial cells
Roscovitine inhibits the NF-κB-dependent gene transcription by inhibition of CDK9 and CDK5, thereby the NF-κB activation cascade remains unaffected.

REFERENCES

VI REFERENCES

1. Nathan C, Ding A. Nonresolving inflammation. Cell. 2010;140:871-882.

2. Rossi AG, Hallett JM, Sawatzky DA, Teixeira MM, Haslett C. Modulation of granulocyte apoptosis can influence the resolution of inflammation. Biochem Soc Trans. 2007;35:288-291.

3. Janeway C. Immunobiology : the immune system in health and disease (ed 6th). New York: Garland Science; 2005.

4. Parenti A, Morbidelli L, Cui XL, et al. Nitric oxide is an upstream signal of vascular endothelial growth factor-induced extracellular signal-regulated kinase1/2 activation in postcapillary endothelium. J Biol Chem. 1998;273:4220-4226.

5. Galley HF, Webster NR. Physiology of the endothelium. Br J Anaesth. 2004;93:105-113.

6. Downey GP, Worthen GS, Henson PM, Hyde DM. Neutrophil sequestration and migration in localized pulmonary inflammation. Capillary localization and migration across the interalveolar septum. Am Rev Respir Dis. 1993;147:168-176.

7. McIntyre TM, Prescott SM, Weyrich AS, Zimmerman GA. Cell-cell interactions: leukocyte-endothelial interactions. Curr Opin Hematol. 2003;10:150-158.

8. Lowe JB. Glycan-dependent leukocyte adhesion and recruitment in inflammation. Curr Opin Cell Biol. 2003;15:531-538.

9. Butcher EC. Leukocyte-endothelial cell recognition: three (or more) steps to specificity and diversity. Cell. 1991;67:1033-1036.

10. Barkalow FJ, Barkalow KL, Mayadas TN. Dimerization of P-selectin in platelets and endothelial cells. Blood. 2000;96:3070-3077.

11. Huber TS, Gaines GC, Welborn MB, 3rd, Rosenberg JJ, Seeger JM, Moldawer LL. Anticytokine therapies for acute inflammation and the systemic inflammatory response syndrome: IL-10 and ischemia/reperfusion injury as a new paradigm. Shock. 2000;13:425-434.

12. Radi ZA, Register KB, Lee EK, et al. In situ expression of intercellular adhesion molecule-1 (ICAM-1) mRNA in calves with acute Pasteurella haemolytica pneumonia. Vet Pathol. 1999;36:437-444.

13. Constantin G, Piccio L, Bussini S, et al. Induction of adhesion molecules on human schwann cells by proinflammatory cytokines, an immunofluorescence study. J Neurol Sci. 1999;170:124-130.

14. Lee E, Kang SG, Kehrli ME, Jr. Cloning, sequencing and analysis of cDNA encoding bovine intercellular adhesion molecule-1 (ICAM-1). Vet Immunol Immunopathol. 1997;59:121-129.

15. Staunton DE, Marlin SD, Stratowa C, Dustin ML, Springer TA. Primary structure of ICAM-1 demonstrates interaction between members of the immunoglobulin and integrin supergene families. Cell. 1988;52:925-933.

16. Elices MJ, Osborn L, Takada Y, et al. VCAM-1 on activated endothelium interacts with the leukocyte integrin VLA-4 at a site distinct from the VLA-4/fibronectin binding site. Cell. 1990;60:577-584.

17. Adams DH, Shaw S. Leucocyte-endothelial interactions and regulation of leucocyte migration. Lancet. 1994;343:831-836.

18. Muller WA. Leukocyte-endothelial-cell interactions in leukocyte transmigration and the inflammatory response. Trends Immunol. 2003;24:327-334.

19. Yadav R, Larbi KY, Young RE, Nourshargh S. Migration of leukocytes through the vessel wall and beyond. Thromb Haemost. 2003;90:598-606.

20. Parish CR. The role of heparan sulphate in inflammation. Nat Rev Immunol. 2006;6:633-643.

21. Rot A, von Andrian UH. Chemokines in innate and adaptive host defense: basic chemokinese grammar for immune cells. Annu Rev Immunol. 2004;22:891-928.

22. Granger DN, Kubes P. The microcirculation and inflammation: modulation of leukocyte-endothelial cell adhesion. J Leukoc Biol. 1994;55:662-675.

23. Campbell JJ, Qin S, Bacon KB, Mackay CR, Butcher EC. Biology of chemokine and classical chemoattractant receptors: differential requirements for adhesion-triggering versus chemotactic responses in lymphoid cells. J Cell Biol. 1996;134:255-266.

24. Campbell JJ, Hedrick J, Zlotnik A, Siani MA, Thompson DA, Butcher EC. Chemokines and the arrest of lymphocytes rolling under flow conditions. Science. 1998;279:381-384.

25. Nourshargh S, Marelli-Berg FM. Transmigration through venular walls: a key regulator of leukocyte phenotype and function. Trends Immunol. 2005;26:157-165.

26. Parish CR, Hindmarsh EJ, Bartlett MR, Staykova MA, Cowden WB, Willenborg DO. Treatment of central nervous system inflammation with inhibitors of basement membrane degradation. Immunol Cell Biol. 1998;76:104-113.

27. Cornelius LA, Taylor JT, Degitz K, Li LJ, Lawley TJ, Caughman SW. A 5' portion of the ICAM-1 gene confers tissue-specific differential expression levels and cytokine responsiveness. J Invest Dermatol. 1993;100:753-758.

28. Saha B, Jyothi Prasanna S, Chandrasekar B, Nandi D. Gene modulation and immunoregulatory roles of interferon gamma. Cytokine. 2010;50:1-14.

29. Shrikant P, Chung IY, Ballestas ME, Benveniste EN. Regulation of intercellular adhesion molecule-1 gene expression by tumor necrosis factor-alpha, interleukin-1 beta, and interferon-gamma in astrocytes. J Neuroimmunol. 1994;51:209-220.

30. Li Q, Verma IM. NF-kappaB regulation in the immune system. Nat Rev Immunol. 2002;2:725-734.

31. Ghosh S, May MJ, Kopp EB. NF-kappa B and Rel proteins: evolutionarily conserved mediators of immune responses. Annu Rev Immunol. 1998;16:225-260.

32. Lenardo MJ, Baltimore D. NF-kappa B: a pleiotropic mediator of inducible and tissue-specific gene control. Cell. 1989;58:227-229.

33. Bonizzi G, Karin M. The two NF-kappaB activation pathways and their role in innate and adaptive immunity. Trends Immunol. 2004;25:280-288.

34. Baeuerle PA, Baichwal VR. NF-kappa B as a frequent target for immunosuppressive and anti-inflammatory molecules. Adv Immunol. 1997;65:111-137.

35. Tak PP, Firestein GS. NF-kappaB: a key role in inflammatory diseases. J Clin Invest. 2001;107:7-11.

36. Nurse P. Genetic control of cell size at cell division in yeast. Nature. 1975;256:547-551.

37. Masui Y, Markert CL. Cytoplasmic control of nuclear behavior during meiotic maturation of frog oocytes. J Exp Zool. 1971;177:129-145.

38. Smith LD, Ecker RE. The interaction of steroids with Rana pipiens Oocytes in the induction of maturation. Dev Biol. 1971;25:232-247.

39. Morgan DO. Principles of CDK regulation. Nature. 1995;374:131-134.

40. Lolli G, Johnson LN. CAK-Cyclin-dependent Activating Kinase: a key kinase in cell cycle control and a target for drugs? Cell Cycle. 2005;4:572-577.

41. Ekholm SV, Reed SI. Regulation of G(1) cyclin-dependent kinases in the mammalian cell cycle. Curr Opin Cell Biol. 2000;12:676-684.

42. Malumbres M, Barbacid M. Mammalian cyclin-dependent kinases. Trends Biochem Sci. 2005;30:630-641.

43. Borgne A, Golsteyn RM. The role of cyclin-dependent kinases in apoptosis. Prog Cell Cycle Res. 2003;5:453-459.

44. Borgne A, Versteege I, Mahe M, et al. Analysis of cyclin B1 and CDK activity during apoptosis induced by camptothecin treatment. Oncogene. 2006;25:7361-7372.

45. Cruz JC, Tsai LH. A Jekyll and Hyde kinase: roles for Cdk5 in brain development and disease. Curr Opin Neurobiol. 2004;14:390-394.

46. Pareek TK, Keller J, Kesavapany S, et al. Cyclin-dependent kinase 5 activity regulates pain signaling. Proc Natl Acad Sci U S A. 2006;103:791-796.

47. Lilja L, Yang SN, Webb DL, Juntti-Berggren L, Berggren PO, Bark C. Cyclin-dependent kinase 5 promotes insulin exocytosis. J Biol Chem. 2001;276:34199-34205.

48. Garriga J, Grana X. Cellular control of gene expression by T-type cyclin/CDK9 complexes. Gene. 2004;337:15-23.

49. Loyer P, Trembley JH, Katona R, Kidd VJ, Lahti JM. Role of CDK/cyclin complexes in transcription and RNA splicing. Cell Signal. 2005;17:1033-1051.

50. Vermeulen K, Van Bockstaele DR, Berneman ZN. The cell cycle: a review of regulation, deregulation and therapeutic targets in cancer. Cell Prolif. 2003;36:131-149.

51. Dhavan R, Tsai LH. A decade of CDK5. Nat Rev Mol Cell Biol. 2001;2:749-759.

52. Pinhero R, Liaw P, Bertens K, Yankulov K. Three cyclin-dependent kinases preferentially phosphorylate different parts of the C-terminal domain of the large subunit of RNA polymerase II. Eur J Biochem. 2004;271:1004-1014.

53. Reddy GP. Cell cycle: regulatory events in G1-->S transition of mammalian cells. J Cell Biochem. 1994;54:379-386.

54. Norbury C, Nurse P. Animal cell cycles and their control. Annu Rev Biochem. 1992;61:441-470.

55. van den Heuvel S, Harlow E. Distinct roles for cyclin-dependent kinases in cell cycle control. Science. 1993;262:2050-2054.

56. Jacks T, Weinberg RA. The expanding role of cell cycle regulators. Science. 1998;280:1035-1036.

57. Nakayama KI, Nakayama K. Ubiquitin ligases: cell-cycle control and cancer. Nat Rev Cancer. 2006;6:369-381.

58. Fisher RP. Secrets of a double agent: CDK7 in cell-cycle control and transcription. J Cell Sci. 2005;118:5171-5180.

59. Spencer CA, Groudine M. Transcription elongation and eukaryotic gene regulation. Oncogene. 1990;5:777-785.

60. Fuda NJ, Ardehali MB, Lis JT. Defining mechanisms that regulate RNA polymerase II transcription in vivo. Nature. 2009;461:186-192.

61. Price DH. P-TEFb, a cyclin-dependent kinase controlling elongation by RNA polymerase II. Mol Cell Biol. 2000;20:2629-2634.

62. Devault A, Martinez AM, Fesquet D, et al. MAT1 ('menage a trois') a new RING finger protein subunit stabilizing cyclin H-cdk7 complexes in starfish and Xenopus CAK. EMBO J. 1995;14:5027-5036.

63. Shiekhattar R, Mermelstein F, Fisher RP, et al. Cdk-activating kinase complex is a component of human transcription factor TFIIH. Nature. 1995;374:283-287.

64. Li Q, Price JP, Byers SA, Cheng D, Peng J, Price DH. Analysis of the large inactive P-TEFb complex indicates that it contains one 7SK molecule, a dimer of HEXIM1 or HEXIM2, and two P-TEFb molecules containing Cdk9 phosphorylated at threonine 186. J Biol Chem. 2005;280:28819-28826.

65. Jang MK, Mochizuki K, Zhou M, Jeong HS, Brady JN, Ozato K. The bromodomain protein Brd4 is a positive regulatory component of P-TEFb and stimulates RNA polymerase II-dependent transcription. Mol Cell. 2005;19:523-534.

66. Soos TJ, Meijer L, Nelson PJ. CDK/GSK-3 inhibitors as a new approach for the treatment of proliferative renal diseases. Drug News Perspect. 2006;19:325-328.

67. Ubeda M, Rukstalis JM, Habener JF. Inhibition of cyclin-dependent kinase 5 activity protects pancreatic beta cells from glucotoxicity. J Biol Chem. 2006;281:28858-28864.

68. Schang LM. Cyclin-dependent kinases as cellular targets for antiviral drugs. J Antimicrob Chemother. 2002;50:779-792.

69. MacCallum DE, Melville J, Frame S, et al. Seliciclib (CYC202, R-Roscovitine) induces cell death in multiple myeloma cells by inhibition of RNA polymerase II-dependent transcription and down-regulation of Mcl-1. Cancer Res. 2005;65:5399-5407.

70. Lu W, Chen L, Peng Y, Chen J. Activation of p53 by roscovitine-mediated suppression of MDM2 expression. Oncogene. 2001;20:3206-3216.

71. Dey A, Wong ET, Cheok CF, Tergaonkar V, Lane DP. R-Roscovitine simultaneously targets both the p53 and NF-kappaB pathways and causes potentiation of apoptosis: implications in cancer therapy. Cell Death Differ. 2008;15:263-273.

72. http://www.cyclacel.com/cyc/rd/trials/seliciclib/.

73. Laemmli UK. Cleavage of structural proteins during the assembly of the head of bacteriophage T4. Nature. 1970;227:680-685.

74. Kurien BT, Scofield RH. Protein blotting: a review. J Immunol Methods. 2003;274:1-15.

75. Smith PK, Krohn RI, Hermanson GT, et al. Measurement of protein using bicinchoninic acid. Anal Biochem. 1985;150:76-85.

76. Bradford MM. A rapid and sensitive method for the quantitation of microgram quantities of protein utilizing the principle of protein-dye binding. Anal Biochem. 1976;72:248-254.

77. Baez S. An open cremaster muscle preparation for the study of blood vessels by in vivo microscopy. Microvasc Res. 1973;5:384-394.

78. Mempel TR, Moser C, Hutter J, Kuebler WM, Krombach F. Visualization of leukocyte transendothelial and interstitial migration using reflected light oblique transillumination in intravital video microscopy. J Vasc Res. 2003;40:435-441.

79. Nicoletti I, Migliorati G, Pagliacci MC, Grignani F, Riccardi C. A rapid and simple method for measuring thymocyte apoptosis by propidium iodide staining and flow cytometry. J Immunol Methods. 1991;139:271-279.

80. Bergelson JM, Cunningham JA, Droguett G, et al. Isolation of a common receptor for Coxsackie B viruses and adenoviruses 2 and 5. Science. 1997;275:1320-1323.

81. http://www.zeiss.de/C1256D18002CC306/0/99C3B5F289AFDB5CC125725F0027D28F/$file/45-0066_e.pdf

82. Pfaffl MW. A new mathematical model for relative quantification in real-time RT-PCR. Nucleic Acids Res. 2001;29:e45.

83. Hornberger TA, Sukhija KB, Wang XR, Chien S. mTOR is the rapamycin-sensitive kinase that confers mechanically-induced phosphorylation of the hydrophobic motif site Thr(389) in p70(S6k). FEBS Lett. 2007;581:4562-4566.

84. Hay N, Sonenberg N. Upstream and downstream of mTOR. Genes Dev. 2004;18:1926-1945.

85. Hallett JM, Leitch AE, Riley NA, Duffin R, Haslett C, Rossi AG. Novel pharmacological strategies for driving inflammatory cell apoptosis and enhancing the resolution of inflammation. Trends Pharmacol Sci. 2008;29:250-257.

86. Leitch AE, Haslett C, Rossi AG. Cyclin-dependent kinase inhibitor drugs as potential novel anti-inflammatory and pro-resolution agents. Br J Pharmacol. 2009;158:1004-1016.

87. Gherardi D, D'Agati V, Chu TH, et al. Reversal of collapsing glomerulopathy in mice with the cyclin-dependent kinase inhibitor CYC202. J Am Soc Nephrol. 2004;15:1212-1222.

88. Milovanceva-Popovska M, Kunter U, Ostendorf T, et al. R-roscovitine (CYC202) alleviates renal cell proliferation in nephritis without aggravating podocyte injury. Kidney Int. 2005;67:1362-1370.

89. Zoja C, Casiraghi F, Conti S, et al. Cyclin-dependent kinase inhibition limits glomerulonephritis and extends lifespan of mice with systemic lupus. Arthritis Rheum. 2007;56:1629-1637.

90. Rossi AG, Sawatzky DA, Walker A, et al. Cyclin-dependent kinase inhibitors enhance the resolution of inflammation by promoting inflammatory cell apoptosis. Nat Med. 2006;12:1056-1064.

91. Sekine C, Sugihara T, Miyake S, et al. Successful treatment of animal models of rheumatoid arthritis with small-molecule cyclin-dependent kinase inhibitors. J Immunol. 2008;180:1954-1961.

92. Radi ZA, Kehrli ME, Jr., Ackermann MR. Cell adhesion molecules, leukocyte trafficking, and strategies to reduce leukocyte infiltration. J Vet Intern Med. 2001;15:516-529.

93. Topaloglu S, Abbasoglu O, Ayhan A, Sokmensuer C, Kilinc K. Antiapoptotic and protective effects of roscovitine on ischemia-reperfusion injury of the rat liver. Liver Int. 2003;23:300-307.

94. Bullard DC, Hurley LA, Lorenzo I, Sly LM, Beaudet AL, Staite ND. Reduced susceptibility to collagen-induced arthritis in mice deficient in intercellular adhesion molecule-1. J Immunol. 1996;157:3153-3158.

95. Kevil CG, Patel RP, Bullard DC. Essential role of ICAM-1 in mediating monocyte adhesion to aortic endothelial cells. Am J Physiol Cell Physiol. 2001;281:C1442-1447.

96. Du J, Wei N, Guan T, et al. Inhibition of CDKS by roscovitine suppressed LPS-induced *NO production through inhibiting NFkappaB activation and BH4 biosynthesis in macrophages. Am J Physiol Cell Physiol. 2009;297:C742-749.

97. Bach S, Knockaert M, Reinhardt J, et al. Roscovitine targets, protein kinases and pyridoxal kinase. J Biol Chem. 2005;280:31208-31219.

98. Meijer L, Borgne A, Mulner O, et al. Biochemical and cellular effects of roscovitine, a potent and selective inhibitor of the cyclin-dependent kinases cdc2, cdk2 and cdk5. Eur J Biochem. 1997;243:527-536.

99. Liebl J. Anti-angiogenic effects of Cyclin dependent kinase inhibitors - Novel function of Cyclin dependent kinase 5 in endothelial cell migration. Department of chemistry and pharmacy. Munich: LMU Munich; 2008.

100. Brasier AR. Expanding role of cyclin dependent kinases in cytokine inducible gene expression. Cell Cycle. 2008;7:2661-2666.

101. Palancade B, Bensaude O. Investigating RNA polymerase II carboxyl-terminal domain (CTD) phosphorylation. Eur J Biochem. 2003;270:3859-3870.

102. Meinhart A, Kamenski T, Hoeppner S, Baumli S, Cramer P. A structural perspective of CTD function. Genes Dev. 2005;19:1401-1415.

103. Marshall RM, Grana X. Mechanisms controlling CDK9 activity. Front Biosci. 2006;11:2598-2613.

ANP

VII ATRIAL NATRIURETIC PEPTID (ANP)

To investigate *in vivo* the prevention of LPS-induced inflammation by ANP, we performed survival experiments.

1 SURVIVAL EXPERIMENTS

1.1 DETERMINATION OF THE APPROPRIATE LPS (*E.coli* and *Salmonella enterica*) DOSIS FOR SURVIVAL EXPERIMENTS

A.

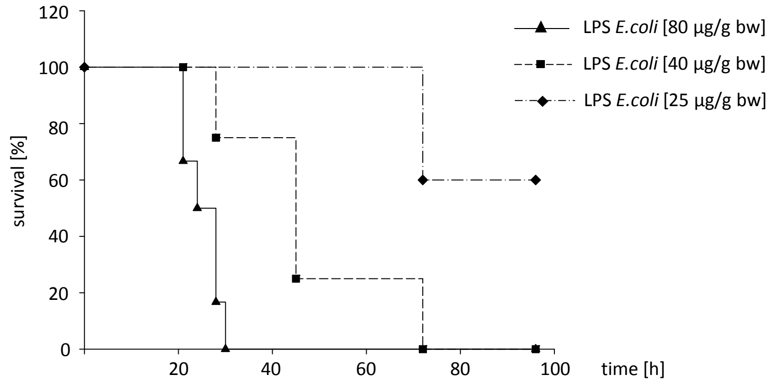

B.

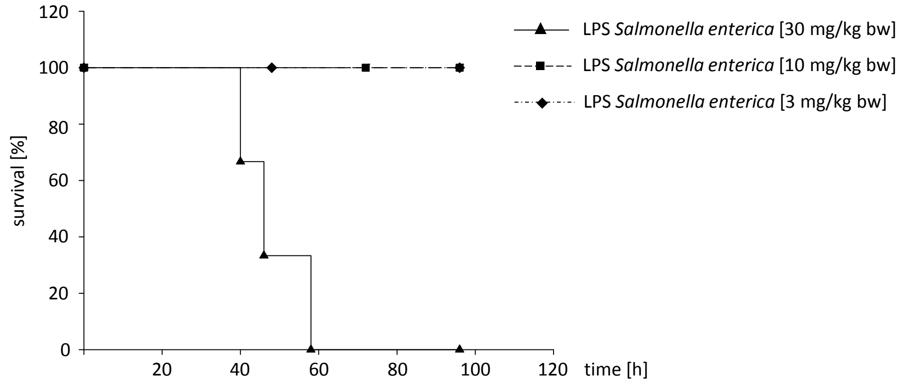

Figure VII-1 Determination of the appropriate LPS dosis for survival experiments.
Mice (male, C57BL/6) were intraperitonally injected either with LPS from *E.coli* or *Salmonella enterica serotype abortus equi* as indicated (bw: body weight). The animal state of health was continuously observed for 96 h. At least four and not more than six LPS (*E.coli*)-challenged mice and three LPS (*Salmonella enterica serotype abortus equi*)-challenged mice were analyzed for each treatment group. Graph displays survival rate in percentage of respective LPS-challenged mice.

1.2 ANP PRE-TREATMENT HAS NO INFLUENCE ON THE SURVIVAL OF LPS (*E.coli*)-CHALLENGED MICE

A.

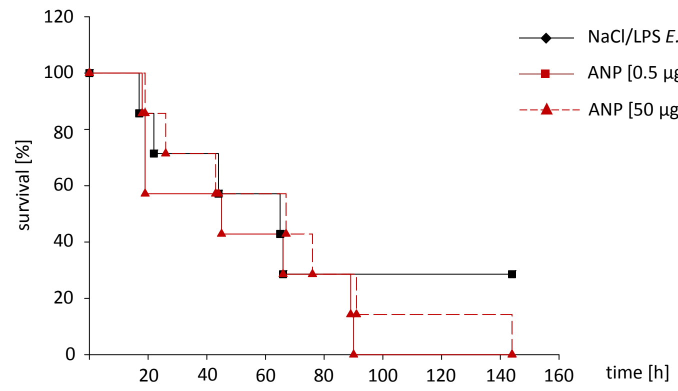

B.

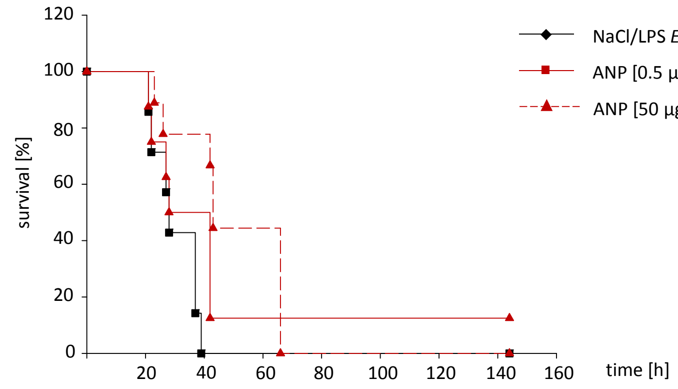

Figure VII-2 ANP pre-treatment has no influence on the survival of LPS (*E.coli*)-challenged mice.
Mice (male C57BL/6) were pre-treated with ANP (intravenous injection in the tail vein, 0.5 µg and 50 µg/kg bw) for 15 min before LPS (40 µg/g bw) injection. NaCl administration was used for control. The animal state of health was continuously observed for 144 h. At least nine and not more than eleven mice were analyzed for each treatment group. Graph displays survival rate in percentage of control mice, ANP (0.5 µM/kg bw)/LPS-treated mice and ANP (50 µM/kg bw)/LPS-treated mice. ANP does not protect against LPS-induced inflammation.

1.3 ANP PRE-TREATMENT HAS NO INFLUENCE ON THE SURVIVAL OF LPS (*Salmonella enterica*)-CHALLENGED MICE

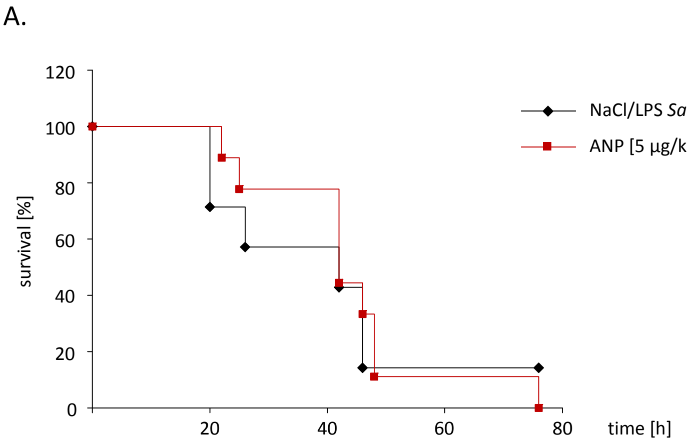

Figure VII-3 ANP pre-treatment has no influence on the survival of LPS (*Salmonella enterica serotype abortus equi*)- challenged mice.
Mice (male, C57BL/6) were pre-treated with ANP (intravenous injection in the tail vein, 5 µg/kg bw) for 15 min before intraperitonal LPS (30 mg/kg bw) injection. NaCl administration was used for control. The animal state of health was continuously observed for 76 h. At least seven and not more than nine mice were analyzed for each treatment group. Graph displays survival rate in percentage of control mice and ANP (5 µM/kg bw)/LPS-challenged mice. ANP does not protect against LPS-induced inflammation.

2 CYTOKINE MEASUREMENT

Further, we determined the influence of ANP on the cytokine levels in plasma of LPS (*E.coli*)-challenged mice.

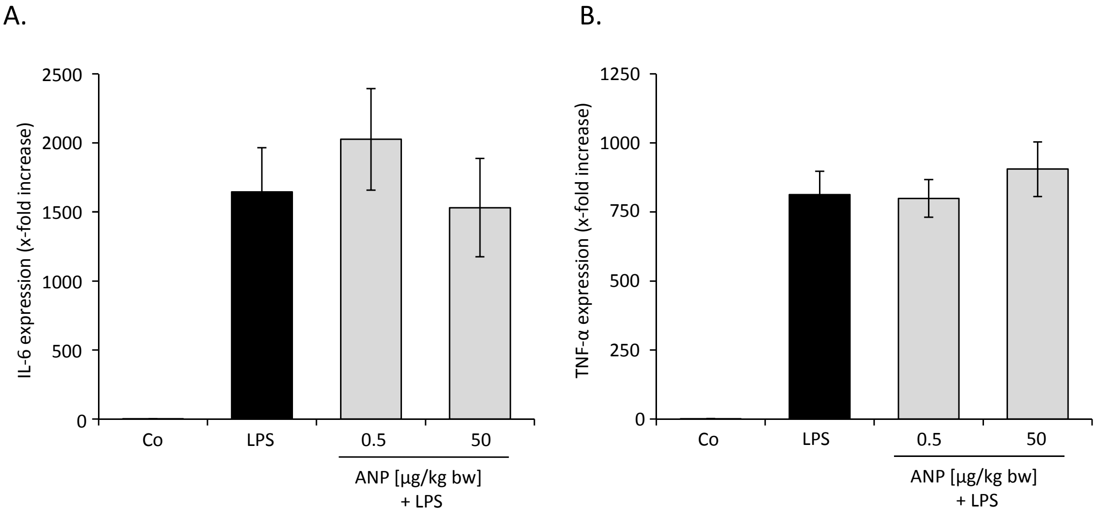

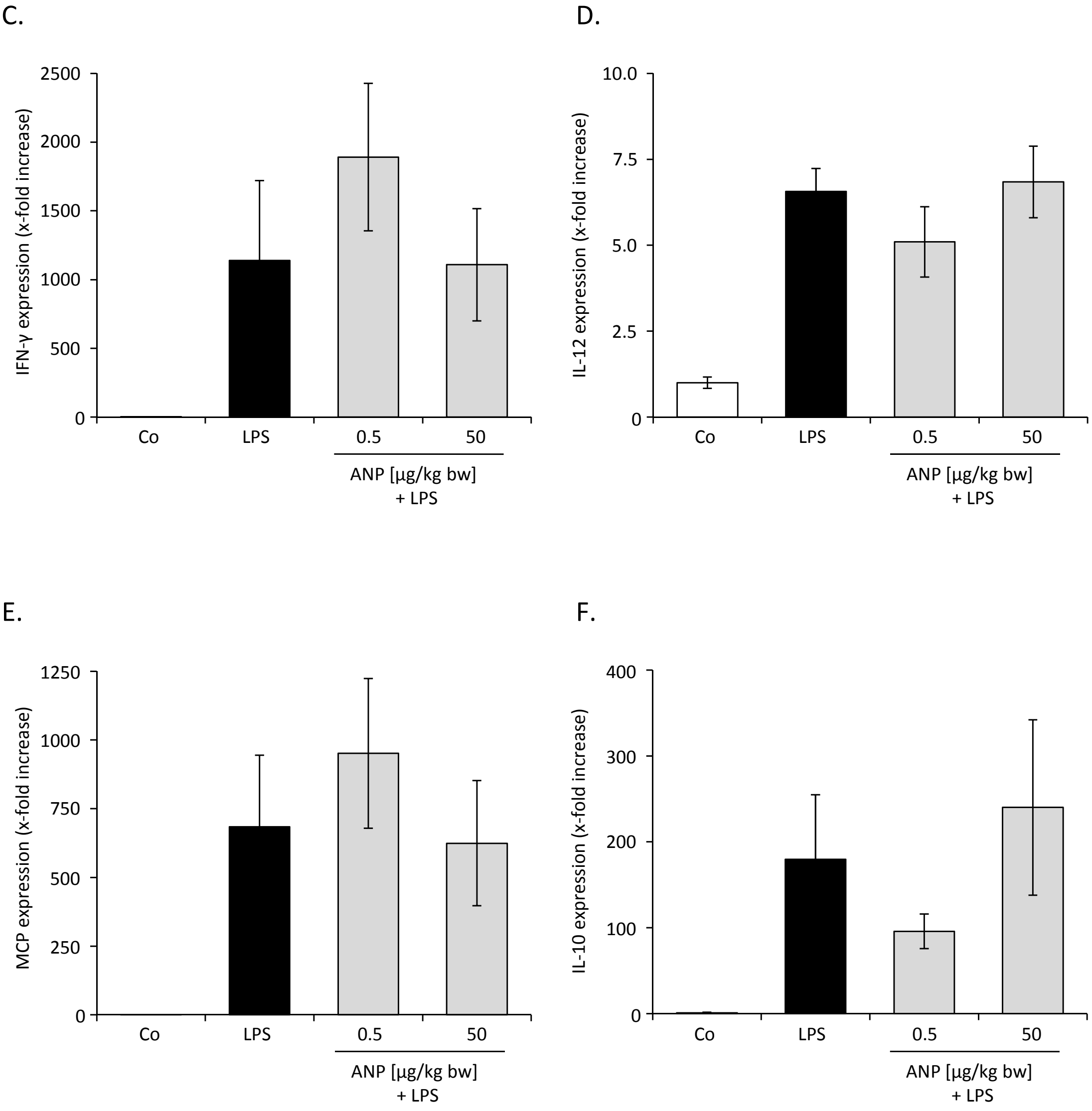

Figure VII-4 Protein levels of pro- and anti-inflammatory cytokines were determined in plasma of ANP/LPS-challengend mice.

Mice (male, C57BL/6) were pre-treated with ANP as indicated for 15 min (intravenous injection in the tail vein) before intraperitonal LPS (*E.coli*)-injection (80 µg/g bw). NaCl administration was used for control. After 6 h, mice were killed by cervical dislocation and blood samples were by heartpuncture. Plasma from whole blood was received by centrifugation (15 min at 10000 rpm). The plasma samples of eight mice were analyzed for each treatment group. Afterwards, cytokine levels were determined by flow cytometric analysis using BD™ Cytometric Bead Array according to the manufacturer`s instructions. This multiplexed bead-based immunoassay allows users to quantify multiple proteins simultaneously on the basis of ELISA (Enzyme-linked immunosorbent assay)-technology. Each capture bead in the array has a unique fluorescence intensity and is coated with a capture antibody specific for IL-6 (IL: interleukin), TNF-α, INF-γ, IL-12, MCP (monocyte chemotactic protein) and IL-10. A combination of the different beads, coupled with the specific antibody for the cytokines, is mixed with 50 µl of plasma, which was prior 1:5 diluted with ”Assay Diluent”, or standard and a mixture of detection antibodies that are conjugated to a reporter molecule (PE). Following incubation and subsequent washing, the samples were measured in the FL-2 channel of the flow cytometer. (Mice per group = 8, data show mean ± SEM; *, p>0.05, compared with NaCl/LPS treated mice)

APPENDIX

VIII APPENDIX

1 PUBLICATIONS

1.1 ORIGINAL PUBLICATIONS

Reichel CA, Rehberg M, Lerchenberger M, Berberich N, Bihari P, Khandoga AG, Zahler S, Krombach F.
Ccl2 and Ccl3 mediate neutrophil recruitment via induction of protein synthesis and generation of lipid mediators.
Arthereosclerosis, thrombosis and vascular biology (2009)

Reichel CA, Lerchenberger M, Rehberg M, Berberich N, Zahler S, Wymann M, Krombach F.
Plasmin antagonists prevent leukocyte accumulation and remodeling events in the postischemic microvasculature.
Submitted (2010)

Berberich N, Uhl B, Joore J, Schmerwitz UK, Mayer BA, Krombach F, Zahler S, Vollmar AM, Fürst R
Roscovitine inhibits the leukocyte-endothelial cell interaction via inhibition of CDK5 and CDK9
In preparation (2010)

Schmerwitz UK, Sass G, Khandoga AG, Joore J, Mayer BA, Berberich N, Totzke F, Krombach F, Tiegs G, Zahler S, Vollmar AM, Fürst R.
CDK9 inhibitor flavopiridol protects against inflammation in vivo and in vitro
In preparation (2010)

2 CURRICULUM VITAE

Personal data

Name	Nina Berberich
Date of birth	1980-05-03
Place of birth	Zweibrücken, Germany
Nationality	german
Marital status	unmarried

Education

Since 11/2006	PhD. student Institute of Pharmaceutical Biology, Prof. Dr. A. M. Vollmar Department of Pharmacy - Center of Drug Research, Ludwig-Maximilians-University, Munich, Germany
12/2005 – 10/2006	PhD. student Laboratory of Neurochemistry and Neurogenetics, PD. Dr. M. Riemenschneider Department of Psychiatry and Psychotherapy, TUM, Munich, Germany
05/2005	3rd State Examination, Licensure as Pharmacist
11/2004 – 05/2005	“First year resident“ as Pharmacist, HEXAL AG, Holzkirchen, Germany
05 - 11/2004	“First year resident“ as Pharmacist, Marien-Apotheke, Munich, Germany
04/2004	2rd State Examination
04 -10/2003	Internship as trainee in Pharmacology, Department of Pharmaceutical Bioscience Prof. Dr. Jarl Wikberg, BioMedicalCenter, Uppsala University, Sweden
08/2002	1rd State Examination
04/2000 – 04/2004	Studies of Pharmacy, University des Saarlandes, Saarbrücken, Germany
1990 - 1999	Grammar School: Gymnasium Johanneum, Homburg, Germany
1987 - 1990	Primary School: Grundschule Homburg - Beeden
1986 -1987	Primary School: Grundschule Saarbrücken - Eschberg

Work experience

Since 2005	Pharmacist, Reichenbach Apotheke, Munich, Germany
Since 04/2009	Pharmacist, Apotheke im WEP, Erding and St.-Silvester Apotheke, Forstinning, Germany
12/2007 – 06/2009	Pharmacist, Karwendel-Apotheke, Weilheim in Oberbayern, Germany
10- 12/2005	Pharmacist, Petuel-Apotheke, Munich, Germany

3 ACKNOWLEDGEMENTS

First and above all, I am very grateful to Prof. Dr. Angelika M. Vollmar for giving me the chance to carry out this thesis in her working group. I appreciate the fact that she was available for questions and advice. Her commitment to supervise and motivate me let this project turn out to be successful. I further would like to express my gratitude to Dr. Robert Fürst for great mentoring, discussions and helpful suggestions.
Sincere thanks to PD Dr. Stefan Zahler for technical advice, especially in small animal “surgery” and for adding his input so we would make good progress.

I am indebted to all members of my thesis committee: Prof. Dr. Carsten Culmsee, Prof. Dr. Christian Wahl-Schott, PD Dr. Manfred Ogris, Prof. Dr. Franz Paintner and Prof. Dr. Wolfgang Frieß. Special attention belongs to Prof. Dr. Carsten Culmsee (Philipps-University Marburg) for his extra effort to appraise this thesis and to participate in the event of my thesis defense.

Special thanks go to Dr. Christian Reichel and Bernd Uhl from the group of Prof. Dr Fritz Krombach for their collaboration in the mouse cremaster muscle studies and to Dr. Jos Joore for performing PepChip analysis.

I would like to thank all of my former and present members of the working group. It has been a pleasure to work among such friendly and encouraging colleagues, out of which I would distinguish Jana for her great help, Bianca for a nice time in the “mousehouse” and supporting me in the *in vivo* experiments, and Bettina for our shared time that each of us spent writing.
Several friendships have formed and turned out to be of great value for me, which I would not want to miss any more. My “Boxenluder” Ulla, Andrea and Uta deserve extra credit for supporting me even beyond life on campus.

Special gratitude to all my friends - thanks!

Finally, I deeply thank my family which suffered and laughed with me, which encouraged and advised me in all the steps on the way, no matter of what concern. Papa and Eric, you gave me the strength to keep going. Mama, you will always be with me.